



Total evidence analysis elucidates the tangled systematic scenario within Fidicinini (Hemiptera: Auchenorrhyncha, Cicadidae)

Tatiana Petersen Ruschel^{1,2,3,4}, Filipe Michels Bianchi¹, Luiz Alexandre Campos¹, Gervásio Silva Carvalho²

1 Departamento de Zoologia, Universidade Federal do Rio Grande do Sul (UFRGS), Av. Bento Gonçalves 9500, Prédio 43435, 91501-970, Porto Alegre, RS, Brazil

2 Programa de Pós-Graduação em Ecologia e Evolução da Biodiversidade, Escola de Ciências da Saúde e da Vida, Pontifícia Universidade Católica do Rio Grande do Sul (PUCRS), Av. Ipiranga, 6681, Prédio 11, Sala 921, 90619-900, Porto Alegre, RS, Brazil

3 Universidade Federal de Santa Maria, Rio Grande do Sul, Departamento de Ecologia e Evolução, Av. Roraima, 1000, Camobi, Santa Maria, 97105-900 RS, Brazil

4 Plazi, Porto Alegre, Rio Grande do Sul, Brazil

<http://zoobank.org/67A7EC9A-9E05-4C74-901E-E2735085C924>

Corresponding author: Tatiana Petersen Ruschel (tatiana.ruschel@gmail.com)

Received 25 April 2022

Accepted 22 November 2022

Published 20 January 2023

Academic Editors Christiane Weirauch, Martin Wiemers

Citation: Ruschel TP, Bianchi FM, Campos LA, Carvalho GS (2023) Total evidence analysis elucidates the tangled systematic scenario within Fidicinini (Hemiptera, Auchenorrhyncha, Cicadidae). *Arthropod Systematics & Phylogeny* 81: 35–77. <https://doi.org/10.3897/asp.81.e85755>

Abstract

The Linnean, Wallacean, and Darwinian shortfalls are knowledge gaps about species taxonomy, distribution, and evolution, respectively. Fidicinini is a tribe of cicadas that suffers from these gaps. We assessed specimens of the tribe sharing similar male genital shape (uncus), but fitting the somatic morphology of either *Dorisiana* Metcalf, 1952 and *Guyalna* Boulard & Martinelli, 1996. We build a phylogenetic hypothesis by total evidence analysis and perform a character optimization of the uncus and timbal cover shapes, the last used as diagnostic for both genera. *Dorisiana* and *Guyalna* were recovered non-monophyletic. A new genus, *Acanthoventris* **gen. nov.**, and ten new species are proposed: *A. charrua* Ruschel **sp. nov.**, *A. claudiae* Ruschel **sp. nov.**, *A. faustopsaltrius* Ruschel **sp. nov.**, *A. iara* Ruschel **sp. nov.**, *A. igneus* Ruschel **sp. nov.**, *A. olivarius* Ruschel **sp. nov.**, *A. phoenix* Ruschel **sp. nov.**, *A. rubemi* Ruschel **sp. nov.**, *A. tumidus* Ruschel **sp. nov.**, and *A. viridinotatus* Ruschel **sp. nov.**; and three new combinations *A. densusus* (Boulard & Martinelli, 2011) **comb. nov.**, *A. drewseni* (Stål, 1854) **comb. nov.**, and *A. jauffreti* (Boulard & Martinelli, 2001) **comb. nov.** We provide illustrated identification keys, occurrence maps, and discuss the distribution of the species in the new genus.

Keywords

Dorisiana, evolution, *Guyalna*, genitalia, phylogeny, taxonomy, timbal cover, *Tympanoterpes*, uncus.

1. Introduction

The announcement of the current biological crisis warned biologists of the accelerated loss of biodiversity (Wilson 1985; Butchart et al. 2010). Intending to suppress what has been called the Linnean shortfall, taxonomists have

been trying to describe living organisms before their potential extinction. The Linnean shortfall refers to the discrepancy between formally described species and the number of extant species (Lomolino 2004). However,

naming species is just the first step to understanding biodiversity on a large scale. The other two cornerstones are basic knowledge about a species, including its distribution and evolution – whose knowledge gaps are called Wallacean (Lomolino 2004) and Darwinian shortfalls (Diniz-Filho et al. 2013), respectively. The formalization of any species (i.e., taxonomic description), the distribution in space (i.e., geographic records), and placement in the tree of life (i.e., phylogenetic hypothesis) improve research on conservation, ecology, and evolution (Hortal et al. 2015).

Cicadas are insects well known for their underground nymphal stage and the loud songs performed by the males to attract females to mating (Boulard 1965; Claridge 1985). Recent phylogenies provided new evolutionary hypotheses for Cicadidae and broadly altered the classification of the family (e.g., Moulds 2005; Marshall et al. 2018; Simon et al. 2019). However, for most infrafamilial taxa, the out-of-date delimitations (i.e., descriptions) and classification arrangements built without phylogenetic hypotheses worsen the Linnean, Wallacean, and Darwinian shortfalls.

Fidicinini Distant, 1905, is the second most diverse tribe of Cicadinae Latreille, 1802, containing 25 genera and 244 species widespread in Nearctic and Neotropical regions (Sanborn 2013; Marshall et al. 2018; Ruschel and Sanborn 2021). The current hypothesis for the relationships within Fidicinini lacks a phylogenetic background. Furthermore, only a few genera have recent taxonomic reviews with a detailed study on genital morphology, despite the long-recognized importance of insect genital structures for species identification (e.g., Snodgrass 1957; Song and Bucheli 2010).

The uncus (10th abdominal segment) plays a primary role in cicada copula (Ruschel et al. 2019), and slowly has been employed in phylogenies and improved generic delimitation. The uncus has a conserved general aspect in those genera in which genital structures were used to decide the taxa grouping [e.g., *Arunta* Distant, 1904; *Thopha* Amyot & Serville, 1843 (Moulds and Hill 2015); *Neotibicen* Hill & Moulds, 2015; *Hadoa* Moulds, 2015 (Hill et al. 2015)]. In Fidicinini, the regionalization of the uncus with the corresponding terminology was proposed only recently (Marshall et al. 2018), despite an initial attempt due to the great diversity of forms of this structure within the tribe.

The timbal cover, a fold projecting forwards one each side of the second male urotergite (Pringle 1954; Moulds 2005), has features used as the base of the taxonomic history of Cicadidae and the classification of its subfamilies (Moulds 2005). The timbal cover is often considered a relevant source of morphological information and valuable in the tribal and subfamilial classification of cicadas (Moulds 2005), for instance, in the differential diagnoses of genera in Fidicinini (Boulard and Martinelli 1996; Sanborn 2016). However, recent phylogenies hypothesize that the timbal cover shape is convergent between taxa (Marshall et al. 2018; Simon et al. 2019), challenging the appropriateness of using the timbal cover to delimit monophyletic groups.

Dorisiana Metcalf, 1952 and *Guyalna* Boulard & Martinelli, 1996 (Fidicinini) are morphologically similar genera and share taxonomic history with other genera in the tribe (Sanborn 2016a). The species classified in both genera differ by the shape of the timbal cover margins and have an uncus with a wide morphological heterogeneity. We have assessed specimens from several collections (see Methods), where we found putative groups of undescribed species showing similar uncus, and whose somatic morphology fit either with *Dorisiana* and *Guyalna*.

Here we investigate the relationships of these new species of Fidicinini and assess the evolution of the uncus and the timbal cover morphology within a phylogenetic perspective. We hypothesize that the uncus helps define monophyletic groups in Fidicinini while the timbal cover does not, i.e., the uncus morphology is less convergent than the timbal cover. Building a phylogenetic hypothesis, we intend to reduce the Darwinian shortfall in cicadas; while describing new species and discussing their distribution, we limit the Linnean and Wallacean shortfalls, respectively.

2. Methods

2.1. Morphological study

Dry pinned specimens of both sexes were studied in a stereoscopic microscope. The male genitalia were extracted with forceps, heated in a potassium hydroxide aqueous solution (10% KOH), and posteriorly washed in water. The genitalia were conserved in micro vials filled with glycerine and attached to the specimen's pin. The female reproductive system was not extracted due the distortion and decomposition observed in dried specimens (as reported by Moulds 2005).

Photographs of the major morphological structures were obtained with an AxioCam ERc 5s digital camera attached to a Stemi 2000 C P.06 stereoscopic microscope with Zen Lite 2011 software and with a Nikon AZ100M, followed by stacking with the Nikon NIS-Elements Ar Microscope Imaging Software. Vectorized drawings were made on the photographs. In addition, full-body images (dorsal view) were made with a digital camera. Terminologies adopted here follow Moulds (2005; 2012) for general and genital morphology, Marshall et al. (2018) and Ruschel et al. (2019) for genital morphology. Measurements were made using a digital caliper. For the syntype of *Dorisiana drewseni*, the measurements were made on photographs with IC Measure v.1.2.0.265 (2016).

2.2. Taxon sampling

While studying specimens of Fidicinini, we observed *Dorisiana drewseni* (Stål, 1854), *Guyalna densusa* Boulard & Martinelli, 2011, and *G. jauffreti* Boulard & Martinelli, 2011 along with ten putative new species, exhibit similar

characteristics of somatic morphology and male genitalia. These 13 species compose the ingroup. The outgroup comprises mainly *Dorisiana* (10) and *Guyalna* (16) species, including the type species of each genus, *Cicada semilata* Walker, 1850 and *Fidicina bonaerensis* Berg, 1879, respectively. We also sampled other four putative new species of *Dorisiana*, intending to reduce the Linnean shortfall.

Other genera were chosen based on the current classification of the Fidicinini and specimen availability for morphological and molecular analyses: *Ariasa* Distant, 1905 (5), *Beameria* Davis, 1934 (1), *Bergalna* Boulard & Martinelli, 1996 (1), *Diceroprocta* Stål, 1870 (1), *Fidicina* Amyot & Serville, 1843 (4), *Fidicinoidea* Boulard & Martinelli, 1996 (2), *Majeorona* Distant, 1905 (2), *Nosola* Stål, 1866 (1), *Orialella* Metcalf, 1952 (1), *Pompanonia* Boulard, 1982 (1), *Proarna* Stål, 1864 (1), *Tympanoterpes* Stål, 1861 (2), and one putative new species for the tribe (identified here as **sp. nov.** MOL08). The species *Zammara smaragdina* Walker, 1850 (Zammarini) was selected for character polarization and rooting of trees based on the most recent phylogeny of Cicadidae (Marshall et al. 2018), which recovered Zammarini as a sister group to Fidicinini. A list of the species sampled and the literature used to determine species is shown in Supplementary Material (Table S1). We used photographs of types for the identification of specimens sent by **AMNH** – American Museum of Natural History, New York, USA for *Dorisiana compostela* (Davis, 1934); **NHRS** – Swedish Museum of Natural History, Stockholm, Sweden for *Dorisiana drewseni* (Stål, 1854); **ZMD** – Ivan Franko National University of Lviv, Lviv, Ukraine for *Tympanoterpes serricosta* (Germer, 1834), and of specimens deposited in **MNHN** – Muséum national d'Histoire naturelle Paris, France, identified by M. Boulard.

The specimens examined in this study belong to the following collections: **DZRJ** – Coleção Entomológica Prof. José Alfredo Pinheiro Dutra da Universidade Federal do Rio de Janeiro, Rio de Janeiro, Brazil; **DZUP** – Coleção Entomológica Padre Jesus Santiago Moure da Universidade Federal do Paraná, Curitiba, Brazil; **INPA** – Instituto Nacional de Pesquisas da Amazônia, Manaus, Amazonas, Brazil; **MAPA** – Museu Anchieta de Ciências Naturais, Porto Alegre, Rio Grande do Sul, Brazil; **MCNZ** – Museu de Ciências Naturais da Fundação Zoológica de Porto Alegre, Rio Grande do Sul, Brazil; **MCTP** – Museu de Ciências e Tecnologia da PUCRS, Porto Alegre, Rio Grande do Sul, Brazil; **MNRJ** – Museu Nacional da Universidade Federal do Rio de Janeiro, Rio de Janeiro, Brazil; **MUSM** – Museo de Historia Natural de la Universidad Mayor de San Marcos, Lima, Peru; **NHMUK** – Natural History Museum, London, England; **ZMUC** – Zoological Museum University of Copenhagen, Denmark.

2.3. Morphological characters

The morphological characters were coded in Mesquite version 3.5.1 (Maddison and Maddison 2021). The characters and states were described as neomorphic or trans-

formational, following Sereno (2007). All characters were treated as discrete and non-additive and polarized following the outgroup method (Nixon and Carpenter 1993). The autapomorphies were not included in the analysis. The symbols “?” and “–” were used for missing and non-applicable data, respectively. Morphological characters analysed using probabilistic methods were treated under the Mkv evolutionary model (Lewis 2001).

2.4. DNA extraction, amplification and sequencing

DNA was extracted from ethanol-preserved and pinned specimens. We preferably removed the right foreleg from the coxal cavity to access the indicated amount of muscular tissue. Genomic DNA was extracted using DNeasy Blood and Tissue kit (Qiagen, Valencia, CA, U.S.A.) according to the manufacturer's instructions, eluting to a final volume of 100 µL when DNA was extracted from ethanol-preserved specimens or 50 µL from pinned specimens.

Two DNA markers were amplified, the nuclear elongation factor 1 alpha (EF-1α) and the mitochondrial gene region cytochrome oxidase subunit I (COI). DNA markers were amplified using polymerase chain reactions (PCRs). Primers and PCR annealing temperatures are listed in Supplementary Material (Table S3).

All PCR products were purified using Exonuclease I and shrimp alkaline phosphatase (Affymetrix, Inc. USB Products, Cleveland, OH, U.S.A.). Both DNA strands for all PCR products were sequenced by Macrogen, Inc. (Seoul, South Korea). Sequence chromatograms were visually inspected, verified, and manually edited using the Staden package (Staden et al. 2000). Sequences were verified using BLAST (<http://blast.ncbi.nlm.nih.gov/Blast.cgi>), confirming the high similarity of our submitted sequences to cicada species.

2.5. Multiple sequence alignments and analyses

Additional DNA sequences of Fidicinini were obtained from Genbank, whose access numbers are provided in Supplementary Material (Table S4). Alignments of individual gene regions were performed using Mafft 7 (Kato and Standley 2013), online version (<http://mafft.cbrc.jp/alignment/server/index.html>), applying the strategy “Auto”. Alignments were concatenated in a single matrix using Sequence Matrix 1.8 (Vaidya et al. 2011), recoding external gaps as “?”, and the final matrix was exported in both Phylib (for raxml analyses on CIPRES) and NEXUS (for mrbayes analyses) formats. Molecular and morphological datasets were merged using Mesquite 3.5.1 (Maddison and Maddison 2021).

Two probabilistic methods were used to build the phylogenetic trees, Maximum-Likelihood (ML) and Bayesian inference (BI). The ML analysis was performed on the matrix using RAXML-HPC2 at CIPRES Science

Gateway (Miller et al. 2011) (www.phylo.org/portal2). The GTR-CAT model optimized site-specific evolutionary rates and was employed for each molecular marker, while the Multi-state-CAT+MK was used for the morphological partition. Nodal support was assessed with automatic Stop Bootstrapping Automatically with Majority Rule Criterion (autoMRE). BI of the total evidence matrix was performed in the multithreading version of the program MrBayes 3.2.0 (Ronquist and Huelsenbeck 2003), setting $nst = 6$ rates = $invgamma$ for the marker; 5 million of generation ($nruns = 2$ $nchains = 4$) with trees sampled every 1000 generations. Tracer v.1.6.0 (Rambaut et al. 2014) was used to inspect the convergence to the stationary distribution of the chains. The first 25% of the generations were discarded as “burn-in” and the chains were combined. The combined ESS values for each parameter were higher than 200, and the posterior probability (PP) was estimated for the remaining generations. Nodes with PP lower than 0.5 were considered weak and then collapsed. Phylogenetic trees were visualized and edited using FigTree v1.4.0 (Rambaut et al. 2014) (<http://tree.bio.ed.ac.uk/software/figtree>).

Character states related to timbal cover and uncus shape (see results, characters 31–35, and 44) were optimized on the consensus resulting tree from the BI analysis. The optimizations were made under parsimony, considering unordered states using Mesquite 3.5.1 (Maddison and Maddison 2021). We opted for the parsimony model because the ancestral states minimize the number of steps of character change given the tree and observed character distribution, not considering branch lengths as parameters, such as likelihood and bayesian reconstruction.

2.6. Distribution map

The distribution map was made in Quantum Gis 3.16.4 (https://qgis.org/pt_BR/site) using the shapefile based on the Neotropical biogeographical regionalization proposed by Morrone et al. (2022). The species records were taken from the list of material examined and the bibliography. The collection sites were georeferenced using Global Gazetteer Version 2.3 (<http://www.fallingrain.com/world/index.html>) and Google Earth, and the coordinates were converted to decimal degrees with the Species Link converter tool (<http://splink.cria.org.br/conversor>). The records and coordinates of species of the new genus proposed here are listed in Supplementary Material (Table S5).

Some taxonomic studies have identified species as *Dorisiana drewseni* without robust morphological analysis (Martinelli and Zucchi 1989, 1997). Thus, these identifications may be erroneous due to the similar morphology of the species shown here. Therefore, we chose not to use the records of these coffee pest species identified in the literature as *D. drewseni*. The type species is registered for Minas Gerais State (no specific locality), and the only species found in a scientific collection is registered in Goiás State.

3. Results

A total of 50 morphological characters of male adults were coded and included in a matrix (Table S2 and File S1), 42 out of these were characters of general morphology, and eight were genital.

3.1. Character list

Head (characters 1–12)

1. Width relative to the pronotal width: (0) narrow (Fig. 1A); (1) wide (Fig. 1B, C).
2. Width relative to the width of mesonotum: (0) narrow (Fig. 1A); (1) wider (Fig. 1B, C).
3. Vertex, width relative to length: (0) narrow, width two or three times the length (Fig. 1A); (1) wide, width five or six times the length (Fig. 1B, C).
4. Vertex, median ocellus, in frontal view, height compared to lateral ocelli: (0) higher; (1) not higher.
5. Lateral ocelli, distance to each other compared to the distance between each lateral ocellus to the median one: (0) closely spaced, distance between any two ocelli equal; (1) widely separated, distance between the lateral ocelli greater than between each lateral to the median.
6. Supra-antennal plate, distance to the corresponding eye: (0) smaller than the plate length (Fig. 1A, D); (1) equal to or larger than the plate length (Fig. 1B, C, E).
7. Gena, lateral margin relative to lorum: (0) not prominent; (1) prominent.
8. Postclypeus, apex, relative to the anterior margin of head in dorsal view: (0) slightly prominent (Fig. 1A, B); (1) not prominent (Fig. 1C).
9. Postclypeus, shape in ventral view: (0) rectangular; (1) oval (Fig. 1D); (2) subcircular (Fig. 1E).
10. Postclypeus, apex, dorsal groove: (0) absent (Fig. 1A, C); (1) present (Fig. 1B).
11. Anteclypeus, dorsal surface: (0) tumid (Fig. 1D); (1) flat (Fig. 1E).
12. Anteclypeus, end flaps: (0) absent (Fig. 1D); (1) present (Fig. 1E).

Thorax (characters 13–30)

13. Pronotum, pronotal collar, dorsal midline, length relative to the eye diameter: (0) shorter (Fig. 1A, C); (1) longer (Fig. 1B).
14. Pronotum, paranota, dorsal, extent: (0) wide, exceeding the lateral margin of eyes; (1) wide, not exceeding the lateral margin of eyes; (2) narrow. (adapted from Moulds, 2012).
15. Pronotum, paranota, position relative to the eyes in lateral view: (0) medial; (1) ventral, exceeding the ventral limit of the eye (Fig. 1F); (2) ventro-posterior, not exceeding the ventral limit of the eye (Fig. 1G).

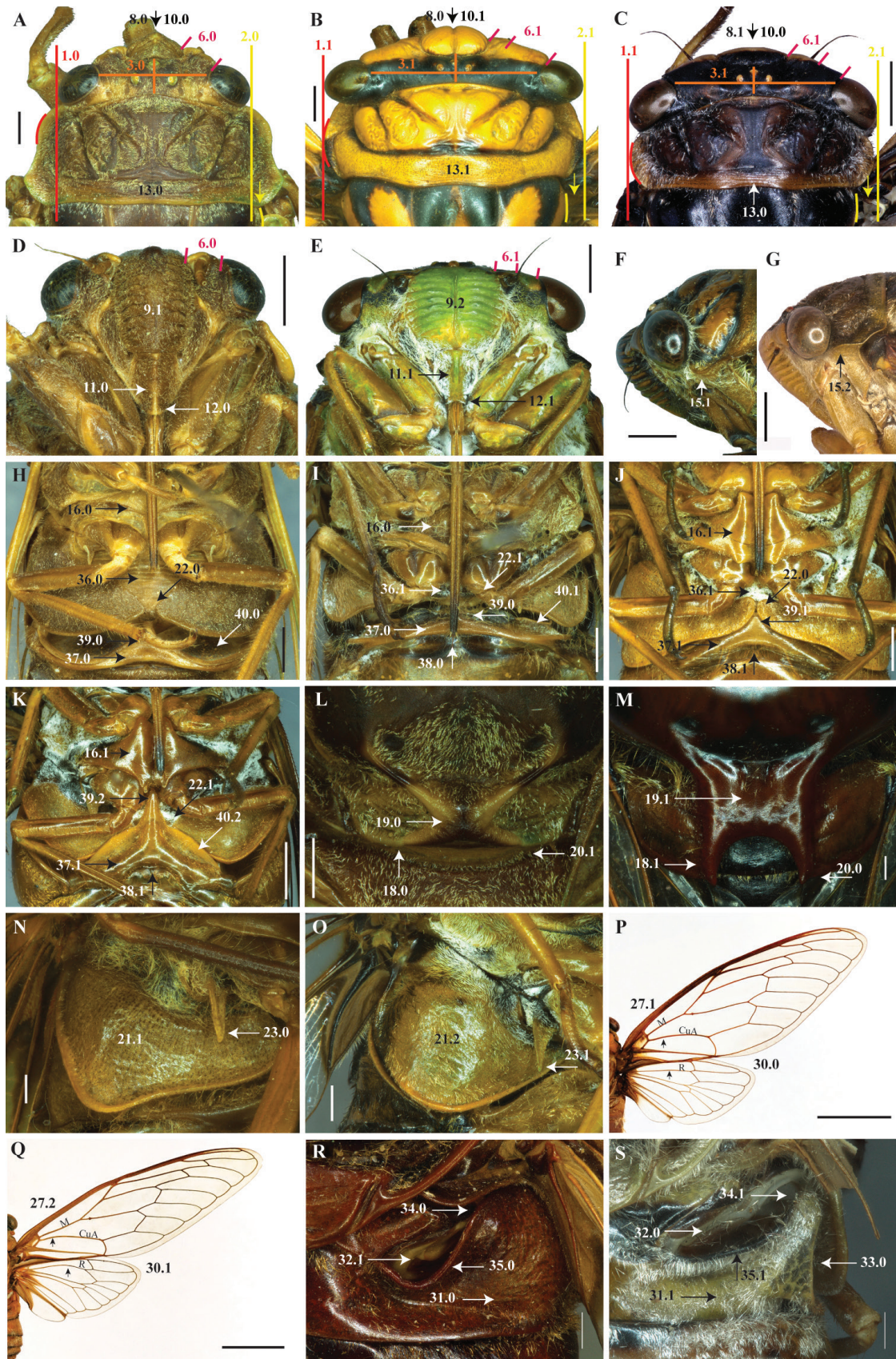


Figure 1. Characters. Head and pronotum in dorsal view: **A** *Proarna bufo*; **B** *Guyalna bonaerensis*; **C** *Acanthoventris drewseni* **comb. nov.** Head in ventral view: **D** *Proarna bufo*; **E** *Guyalna bicolor*. Pronotum in lateral view: **F** *Guyalna brisa*; **G** *Acanthoventris densusa* **comb. nov.** Thorax and abdomen in ventral view: **H** *Proarna bufo*; **I** *Ariasa albiplica*; **J** *Dorisiana amoena*; **K** *Acanthoventris tumidus* **sp. nov.** Cruciform elevation in dorsal view: **L** *Proarna bufo*; **M** *Fidicina toulgoeti*. Operculum in latero-ventral view: **N** *Guyalna bonaerensis*; **O** *Acanthoventris densusa* **comb. nov.** Wings in dorsal view: **P** *Guyalna bicolor*; **Q** *Dorisiana amoena*; Timbal cover in dorso-lateral view: **R** *Guyalna flavipronotum*; **S** *Dorisiana* sp. 2. The numbers indicate the character and the state after the point. Scale bars: (A–K) 2 mm; (L–O, R, S) 1 mm; (P, Q) 1 cm. Photographs P and Q by Laurent Favre (MNHN).

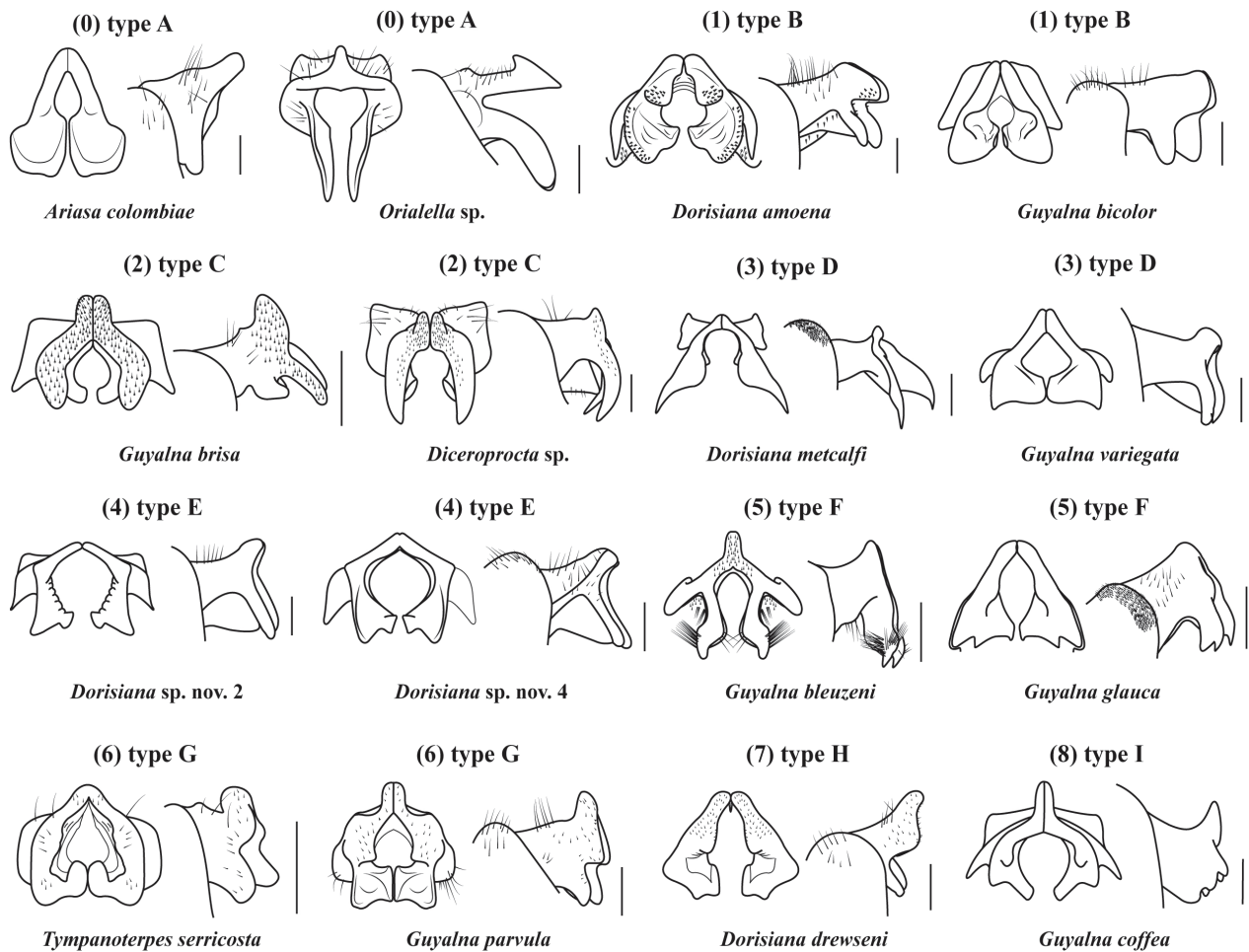


Figure 2. Types of uncus (character 44) in ventral and lateral views. The numbers indicate the character state. Scale bar: 1 mm.

16. Mesonotum, basisternum 3, shape relative to the mesocoxae: (0) obtuse, not prominent (Fig. 1H, I); (1) plane, prominent (Fig. 1J, K).
17. Mesonotum, basisternum 3, posterior angle, shape: (0) obtuse; (1) acute. (inapplicable to posterior margin straight).
18. Mesonotum, cruciform elevation, arc of posterior projections, apex, shape: (0) not acute (Fig. 1L); (1) acute (Fig. 1M).
19. Mesonotum, cruciform elevation, central area, surface: (0) swollen (Fig. 1L); (1) flat (Fig. 1M).
20. Mesonotum, cruciform elevation, length relative to tergite 1: (0) long, covering tergite 1 (Fig. 1M); (1) short, not covering tergite 1 (Fig. 1L).
21. Metapleura, operculum, shape (male): (0) semilunar; (1) triangular (Fig. 1N); (2) obtuse (Fig. 1O).
22. Metapleura, operculum, internal angles, distance between them (male): (0) closely spaced, touching each other or nearly touching each other (Fig. 1H, J); (1) widely spaced (Fig. 1I, K).
23. Metapleura, operculum, meracanthus, range relative to the posterior margin of operculum (male): (0) not reaching (Fig. 1N); (1) reaching (Fig. 1O).
24. Mesonotum, lateral metascutellar plate, development relative to timbal chamber: (0) not covering; (1) partially or completely covering.
25. Tarsus, tarsomeres, number: (0) 2; (1) 3.
26. Forewings, costal vein (C), base of expansion (shelf-like): (0) expanded; (1) not expanded.
27. Forewings, median and cubitus anterior veins, base, direction relative to each other: (0) joined; (1) divergent (Fig. 1P); (2) subparallel (Fig. 1Q).
28. Forewings, vein radius anterior (RA), direction relative to subcostal vein Sc: (0) parallel; (1) divergent.
29. Forewings, basal cell (bc), shape: (0) rectangular; (1) subpolygonal.
30. Hindwings, radius, shape: (0) straight (Fig. 1P); (1) arched (Fig. 1Q).

Male abdomen (characters 31–42)

31. Timbal cover, surface: (0) tumid (Fig. 1R); (1) flat (Fig. 1S).
32. Timbal, aperture relative to the timbal cover: (0) exposed (Fig. 1S); (1) partially exposed (Fig. 1R).
33. Timbal cover, ventral anterior margin, shape: (0) parallel to the long body axis (sensu Sanborn 2016a) (Fig. 1S); (1) angled dorsally (sensu Sanborn 2016a) (inapplicable for tumid timbal cover and *Beameria venosa*).
34. Timbal cover, dorsal and ventral margins, shape: (0) approximately parallel on the anterior extension above the lateral timbal (sensu Sanborn 2016a) (Fig. 1R); (1) not approximately parallel on the anterior

extension above the lateral timbal (Fig. 1S). (inapplicable for *Beameria venosa*).

35. Timbal cover, middle third of anteromedial margin, shape: (0) concave (Fig. 1R); (1) straight (Fig. 1S); (2) convex.
36. Sternite I, length relative to length of metacoxae: (0) longer (Fig. 1H); (1) shorter (Fig. 1I, J).
37. Sternite II, surface: (0) tumid (Fig. 1H, I); (1) flat (Fig. 1J, K).
38. Sternite II, posterior margin, shape: (0) slightly arched (Fig. 1I); (1) arched (Fig. 1J, K).
39. Sternite II, median projection: (0) obtuse (Fig. 1H, I); (1) acute (Fig. 1J); (2) very acute (Fig. 1K).
40. Sternite II, edge, expansion: (0) undeveloped (Fig. 1H); (1) developed (Fig. 1I); (2) well developed (Fig. 1K).
41. Sternite II, auditory capsule position in ventral view: (0) ventral; (1) lateral.
42. Sternite VII, shape: (0) sub-triangular; (1) sub-rectangular.

Male genitalia (characters 43–50)

43. Uncus, length relative to the distal shoulder in lateral view: (0) longer; (1) shorter.
44. Uncus, shape: (0) type A; (1) type B; (2) type C; (3) type D; (4) type E; (5) type F; (6) type G; (7) type H; (8) type I (Fig. 2).
45. Pygofer, basal lobe, length relative to lobes of uncus: (0) short, not reaching the imaginary line bisecting the pygofer at the apex of uncus lobes; (1) long, reaching or nearly reaching the imaginary line bisecting the pygofer at the apex of uncus lobes; (2) very long, surpassing the imaginary line bisecting the pygofer at the apex of uncus lobes or reaching the imaginary line at the apex of median uncus lobe.
46. Pygofer, lateral flaps, expansion: (0) absent; (1) present.
47. Aedeagus, theca, lateral thecal process: (0) absent; (1) present.
48. Aedeagus, theca, lateral left thecal process, shape: (0) serrated; (1) smooth. (inapplicable for lateral thecal process absent).
49. Aedeagus, theca, lateral right thecal process, position: (0) laterally to the theca; (1) bending ventrally.
50. Aedeagus, theca, ventral thecal process: (0) absent; (1) present.

3.2. Phylogeny

The phylogenetic reconstructions under BI and ML were congruent concerning the non-monophyly of most genera included in the analyses, such as *Dorisiana*, *Guyalna*, *Majeorona*, and *Tympanoterpes*. Both analyses recovered our ingroup, *Dorisiana drewseni*, *Guyalna densusa*, *G. jauffreti*, and the ten new species as a monophyletic group (clade A) with high support (PP = 1, BS = 97) (Fig. 3). *Acanthoventris* **gen. nov.** is proposed for this grouping based on the resulting phylogenetic analyses and diagnostic mor-

phological characters (see Taxonomy section). This clade presents seven shared exclusive morphological states, including the same type of uncus (Type H, Figs 2, 3).

Besides *D. drewseni*, the remaining *Dorisiana* species in our analyses were grouped (clade B) with *Guyalna variegata* and other four new species (PP = 0.79, BS = 74). Five species of *Guyalna* and *Tympanoterpes serri-costa* (type species of the genus) grouped (*Tympanoterpes* clade) with high support (PP = 0.91, BS = 84), sharing an exclusive uncus type G, and having **sp. nov.** MOL08 as sister taxon, composing the clade C (PP = 0.91, BS = 75). The other *Tympanoterpes* species sampled, *T. elegans*, was recovered in clade D with *Pompanonia buzien-sis* and *Proarna bufo* in BI and ML, both with high clade support (PP = 0.97, BS = 80). *Fidicina* was recovered monophyletic (clade F; PP = 1, BS = 98). *Guyalna flavipronotum* and *Majeorona ecuatoriana* were recovered as sister species with moderate to low support (PP = 76, BS = 68). The remaining nine *Guyalna* species sampled (including *Guyalna bonaerensis*, type species of the genus) were recovered in a polytomy with *Bergalna pullata*, *Fidicinoidea* species, *Majeorona bovilla*, *Orialella* sp. *G. flavipronotum* + *M. ecuatoriana*, and the clades A, B, C, and F as a highly supported clade (clade B; PP = 0.95, BS = 88). The clade G is sister to *Ariasa*, recovered monophyletic (clade E; PP = 1, BS = 98). The sister relationship between the clades E and G was highly supported (PP = 0.98, BS = 97), composing the clade H.

3.3. Characters optimization

The optimization of the timbal cover characters (32–35) showed the convergence of the states by multiple transitions and reversions across the evolutionary scenario, lacking shared exclusive states in the recovered clades (Fig. 4). Although the polytomy in clade G blurs a precise interpretation of state transformations, due to the uncertainty of the relationships, the shape of the timbal cover (31) presented at least one reversion from flat (31₀) to tumid (31₁). The uncus shape also showed high convergence but presented exclusive states in some clades (e.g., type H in clade A and type G in the *Tympanoterpes* clade). Within the clade B (grouping 11 species), the ancestor state is type B (present in 3 species), changing to type D (present in 5 species), and then to type E (present in 3 species). The *Ariasa* species (clade E) presented all the same uncus shape (type A), also present in clade D and three species within clade G.

3.4. Distribution

We georeferenced data for the 13 species of *Acanthoventris* **gen. nov.** totaling 30 records (Fig. 5 and Table S5). The species of *Acanthoventris* **gen. nov.** are distributed in three countries, two subregions, four dominions, and 11 provinces in the Neotropical region. Eleven species occur exclusively in Brazil, one in French Guiana, and one in Peru.

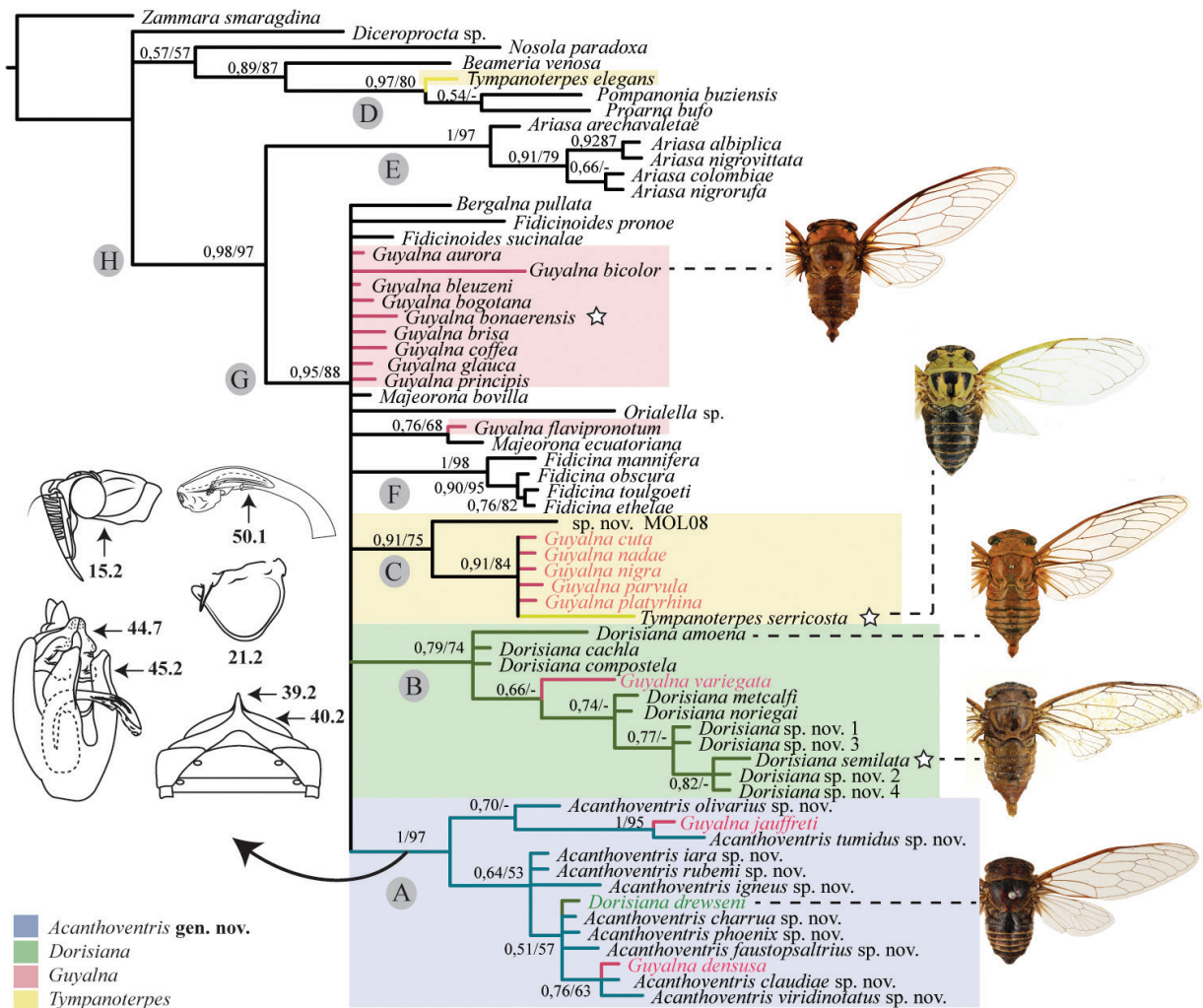


Figure 3. Bayesian inference consensus tree based on the analysis of two molecular markers and 50 morphological characters for 61 species of Fidicinini. Capital letters in circles above branches indicate the clades referred in discussion. Numbers close to nodes are Bayesian posterior probability (PP) and maximum likelihood bootstrap support (BS), respectively. Stars indicate the type species from the genera previously described. Figures indicated in clade A represent the seven shared exclusive morphological states. Photographs of *G. bicolor* and *D. amoena* by Laurent Favre (MNHN), and *D. drewseni* by Gunvi Lindberg (NHRS).

The Brazilian subregion is represented here by the Boreal Brazilian dominion (BBD) and the South Brazilian dominion (SBD). *Acanthoventris iara* sp. nov. and *A. jaffreti* comb. nov. occur in the BBD, in the Roraima and Guianan provinces (Brazil) and Guianan Lowlands province (French Guiana), respectively. *Acanthoventris tumidus* sp. nov. occur in the SBD (Peru), in Yungas and Rondonia provinces.

The remaining ten species are recorded in the Chacoan subregion, represented here by the Chacoan dominion (CD) and the Parana dominion (PD) in Brazil. The Parana dominion (PD) has the highest number of records, with 17 of the total.

Three species occur exclusively in CD, *A. igneus* sp. nov. and *A. drewseni* comb. nov. in the Cerrado province and *A. claudiae* sp. nov. in the Pampean province. Five species are exclusive in PD, *A. rubemi* sp. nov. in the Southern Espinhaco province, *A. viridinotatus* sp. nov. and *A. olivarius* sp. nov. in the Parana forest province, and *A. faustopsaltrius* sp. nov. and *A. phoenix* sp. nov. in the Atlantic province.

Acanthoventris charrua sp. nov. and *A. densus* com. nov. occur in CD and PD, both with records in the Araucaria forest, Parana forest, and Pampean provinces, but only the last including Atlantic and Cerrado provinces.

3.5. Taxonomy

Acanthoventris Ruschel gen. nov.

<http://zoobank.org/AC028B60-9754-482B-B225-5CFC-CE978EC1>

Type species. *Cicada drewseni* Stål, 1854: 242, here designated.

Included species. *Acanthoventris charrua* Ruschel sp. nov., *Acanthoventris viridinotatus* Ruschel sp. nov., *Acanthoventris claudiae* Ruschel sp. nov., *Acanthoventris densus* (Boulard & Martinelli, 2011) comb. nov., *Ac-*

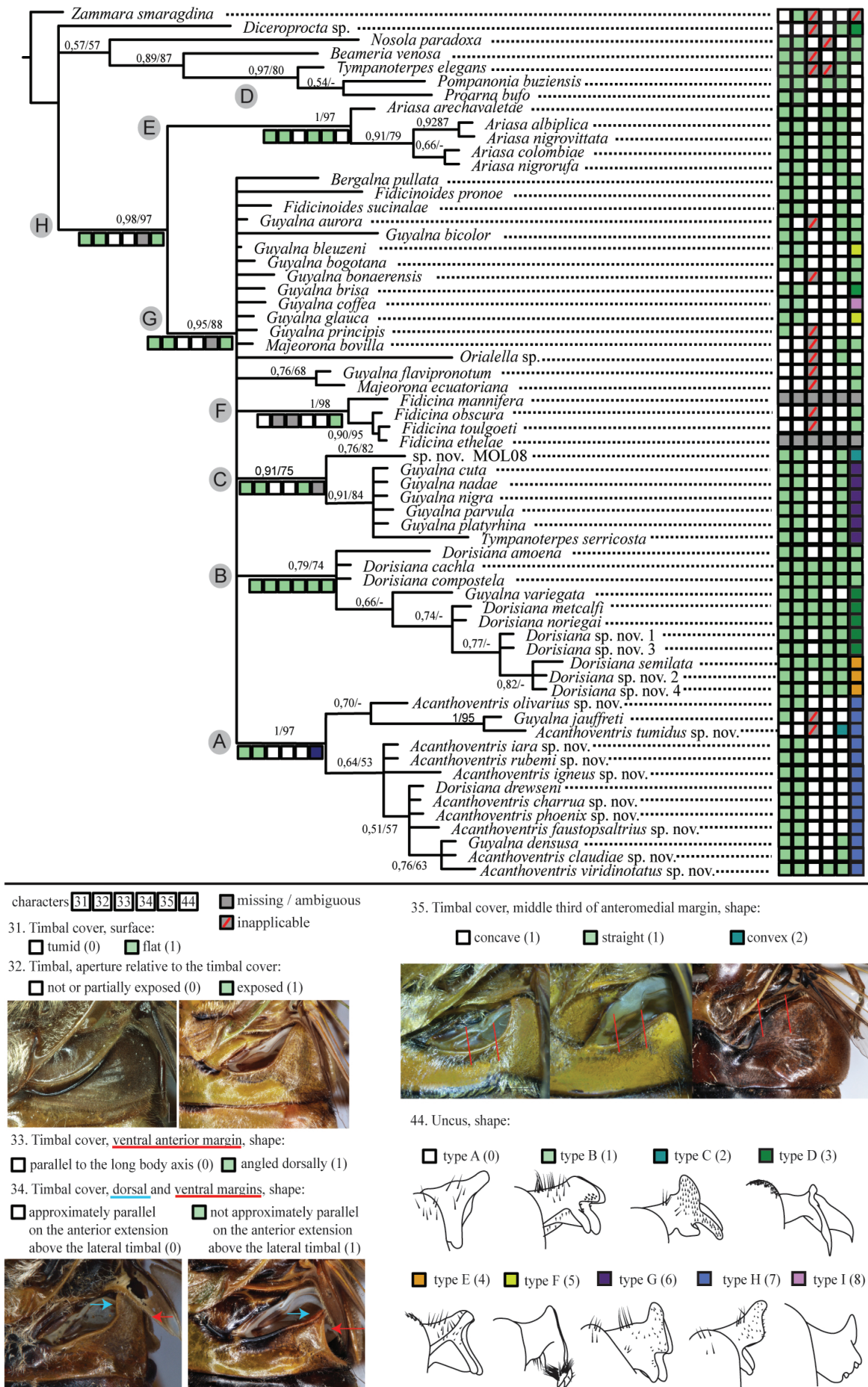


Figure 4. Characters optimization of timbal cover (31–35) and uncus shape (44) under parsimony based on Bayesian inference consensus tree. Capital letters in circles indicate the clades referred in discussion.

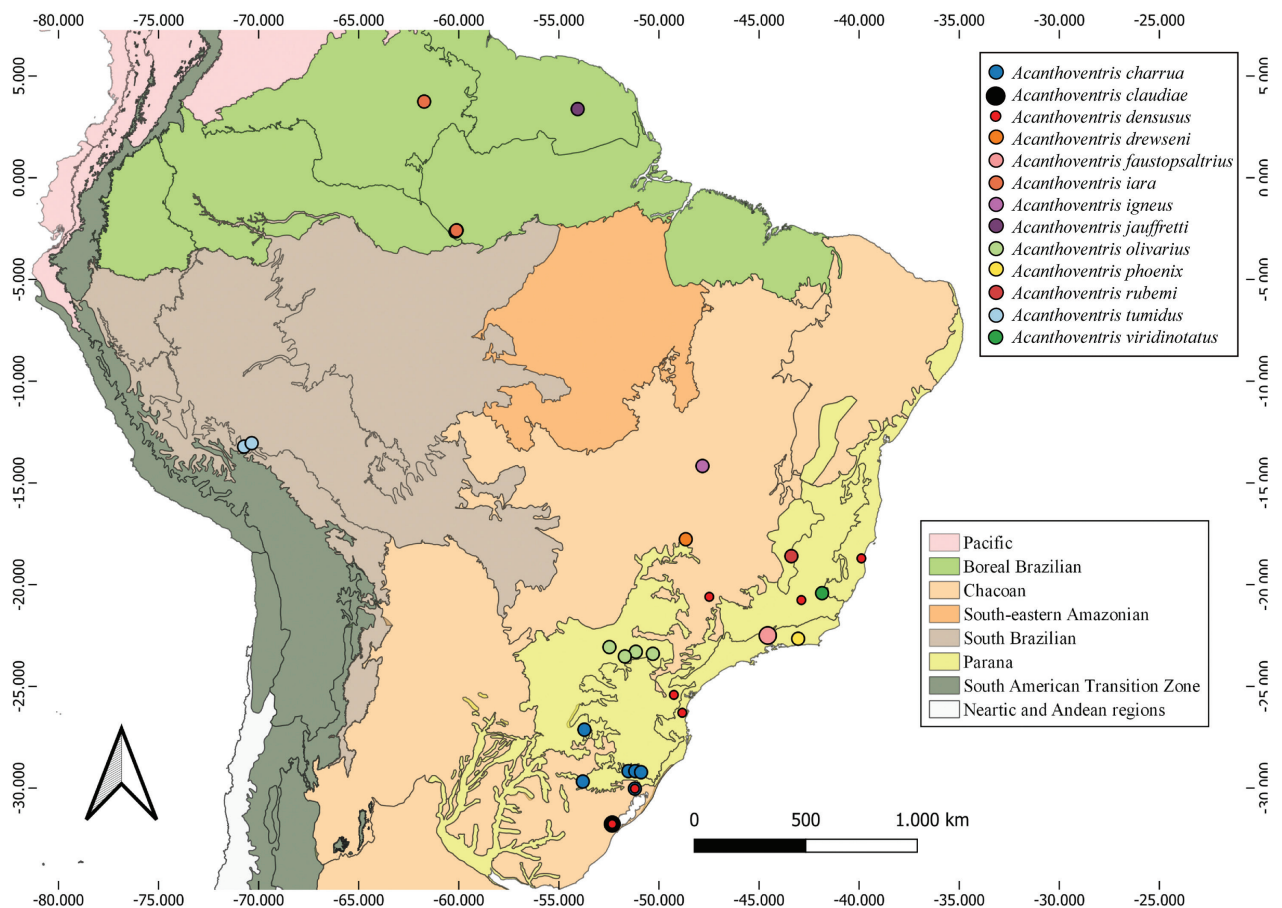


Figure 5. Distribution map of *Acanthoventris* species and dominions based on Neotropical biogeographical regionalization proposed by Morrone et al. (2022).

anthoventris drewseni (Stål, 1854) **comb. nov.**, *Acanthoventris faustopsaltrius* Ruschel **sp. nov.**, *Acanthoventris iara* Ruschel **sp. nov.**, *Acanthoventris igneus* Ruschel **sp. nov.**, *Acanthoventris jauffreti* (Boulard & Martinelli, 2001) **comb. nov.**, *Acanthoventris olivarius* Ruschel **sp. nov.**, *Acanthoventris phoenix* Ruschel **sp. nov.**, *Acanthoventris rubemi* Ruschel **sp. nov.**, *Acanthoventris tumidus* Ruschel **sp. nov.**

Etymology. The name refers to the long, acute median projection of sternite II, like a thorn. Latin, m.: *acanthus*, thorn; *ventris*, belly. The genus is masculine.

Diagnosis. The new genus differs from any other Fidicinini for the following combination of features: head (including eyes) broader than pronotum (except pronotal collar) and mesonotum; vertex short; supra-antennal plate not prominent relative to the anterior margin of head in dorsal view; pronotal collar wide, not exceeding the lateral margin of eyes; paranota posterior to eyes in lateral view; operculum obtuse with internal angles widely spaced (males); meracanthus reaching the posterior margin of operculum; forewings hyaline, veins not infuscated; vein RA divergent to Sc; anal lobe margin in hindwings slightly convex, slightly prominent relative to jugum margin; timbal cover flat (except in *A. jauffreti* **comb. nov.** and *A. tumidus* **sp. nov.**); median projection of sternite II acute, inserted between the metacoxae; ster-

nite II with the edge well developed; sternite III longer than IV; sternite VII sub-triangular (except in *A. igneus* **sp. nov.**, *A. jauffreti* **comb. nov.**, *A. tumidus* **sp. nov.**, and *A. olivarius* **sp. nov.**); uncus shorter than the basal lobe in lateral view; uncal dorsal crest fused and dorsally projected; lateral branches of uncus undeveloped, bud-like; ventral apophyses sub-rectangular and ventrally developed; basal lobe of pygofer very long, reaching or nearly reaching the apex of uncal dorsal crest, clearly delimited with the lateral margin of the pygofer; protuberance of the basal plate of pygofer distant to the apex of the basal lobe; basal curve of the aedeagus short, near to the lateral lobes. Theca dorsally developed with a ventral thecal process.

Description. Head: including eyes, broader than the pronotum (except pronotal collar) and mesonotum; vertex short, wide and slender, the lateral ocelli widely separated, supra-antennal plates not prominent relative to the anterior margin of the head in dorsal view, distant to the eyes; apex of postclypeus convex, without a groove; postclypeus oval in ventral view, flat or slightly salient in lateral view; anteclypeus flat, with a concave basal area. Thorax: pronotal collar wide, not exceeding the lateral margin of eyes; paranota in ventro-posterior position relative to the eyes in lateral view, not exceeding the ventral limit of the eye; cruciform elevation with the central and lateral areas flat, and the arc of the posterior projections obtuse; basisternum 3 flat and prominent relative to the

mesocoxae, with protuberances well developed and the posterior margin angled; three segmented tarsi; profemora armed with three spines: the proximal round, leaning forward at the apex, the median sharp and straight, and the distal shorter than the others; posterior tibiae with at least four spines: two dorsal, one of which is at the middle of the tibia and one of which is three-fifths the distance from the base to the apex of the tibia, and two ventral, one of which is three-quarters of the distance from the base to the apex of the tibia and one of which is sub-apical. Wings hyaline, veins not infuscated; forewings: vein RA divergent to Sc from the basal cell; basal vein of the second apical cell oblique (except in *A. claudiae* sp. nov.); hindwings with radius vein straight, anal lobe margin slightly convex, slightly prominent relative to jugum margin. — **Males:** Operculum obtuse with internal angles widely spaced; meracanthus reaching the posterior margin of operculum; lateral metascutellar plates do not cover the timbal chamber; timbal cover flat (except in *A. jauffreti* comb. nov. and *A. tumidus* sp. nov.), the medial margin concave; lateral margin tightly concave (near the posterior margin of the operculum) except in *A. charrua* sp. nov., *A. phoenix* sp. nov. and *A. densus* comb. nov. slightly concave (near the posterior margin of opercu-

lum); sternite I short, the space between sternites I and II smaller than metacoxae; sternite II flat, posterior margin arched; median projection of sternite II acute, inserted between the metacoxae; sternite II with the edge well developed, expanded to posterior margin of operculum; sternite III longer than the others; sternite VII sub-triangular; uncal dorsal crest fused and dorsally projected; lateral branches of uncus undeveloped, bud-like; ventral apophyses sub-rectangular and ventrally developed, originating from below the lateral branches of uncus; pygofer sub-cylindrical; basal lobe of pygofer very long, reaching or nearly reaching the apex of uncal dorsal crest; protuberance of the basal plate of pygofer distant to the apex of the basal lobe; basal curve of the aedeagus short, near to the lateral lobes. Theca dorsally developed with a ventral thecal process; lateral thecal process absent; vesica internally and externally bearing the cornuti. — **Females:** Operculum obtuse, meracanthus longer than the posterior margin; sternite VII wider than it is long, with a deep, triangular or obtuse groove; the dorsal beak of tergite 9 of the same length than the ovipositor sheath; ovipositor with six to nine teeth.

Distribution. French Guiana, Brazil and Peru.

Key to the males of *Acanthoventris* Ruschel gen. nov.

- 1 Timbal cover tumid (Fig. 20F).....2
- Timbal cover flat (Fig. 6F).....3
- 2 Middle third of the anteromedial margin of the timbal cover convex (Fig. 20F).....*A. tumidus* sp. nov.
- Middle third of the anteromedial margin of the timbal cover concave.....*A. jauffreti* comb. nov.
- 3 Labium reaching (Fig. 16D) or surpassing the middle of sternite II (Fig. 12D).....4
- Labium not reaching or surpassing the middle of sternite II (Figs 22D, 10D).....5
- 4 Anterior margin of head slightly concave (Fig. 12B); operculum not slightly reddish, short, the apex not reaching the auditory capsule (Fig. 12E); sternite VII sub-triangular (Fig. 12G).....*A. drewseni* comb. nov.
- Anterior margin of head tightly concave (Fig. 16B); operculum slightly reddish, long, the apex reaching the auditory capsule (Fig. 16E); sternite VII sub-rectangular (Fig. 16G).....*A. igneus* sp. nov.
- 5 Posterior margin of basisternum 3 straight (Fig. 8D); body totally yellow; basal vein of the second apical cell straight (Fig. 8A).....*A. claudiae* sp. nov.
- Posterior margin of basisternum 3 angled (Figs 22D, 13D); body not totally yellow; basal vein of the second apical cell oblique (Figs 22A, 13A).....6
- 6 Posterior margin of basisternum 3 forming an obtuse angle (Fig. 22D).....7
- Posterior margin of basisternum 3 in an acute angle (Fig. 14D).....10
- 7 Labium reaching or almost reaching the base of the basisternum (Fig. 18D).....8
- Labium reaching the apex of the median projection of sternite II (Fig. 13D).....9
- 8 Tergites 2 to 7 with pilus setae in both lateral margins (Fig. 18A); apex of timbal cover directed to the metascutellar plate (Fig. 18F); anterior margin of ventral sclerotized expansion of theca with a slender projection (Fig. 18M).....*A. phoenix* sp. nov.
- Tergites 2 to 7 without pilus setae in both lateral margins (Fig. 22A); apex of timbal cover directed to the base of hindwings (Fig. 22F); anterior margin of ventral sclerotized expansion of theca without a slender projection (Fig. 22M).....*A. viridinatatus* sp. nov.
- 9 Apex of timbal cover almost reaching the lateral metascutellar plate (Fig. 6F); basal lobe of pygofer almost reaching the apex of ventral apophyses (Fig. 6J).....*A. charrua* sp. nov.
- Apex of timbal cover distant from the lateral metascutellar plate (Fig. 13F); basal lobe of pygofer longer than the ventral apophyses (Fig. 13J).....*A. faustopsaltrius* sp. nov.
- 10 Anterior margin of head tightly concave (Fig. 14B); operculum not covering the timbal cavity and the apex not reaching the auditory capsule (Fig. 14E).....*A. iara* sp. nov.
- Anterior margin of head slightly concave (Fig. 19B); operculum covering the timbal cavity and the apex reaching the auditory capsule (Fig. 19E).....11

- 11 Timbal cover wide, almost covering the timbal cavity (Fig. 17F); sternite VII sub-rectangular (Fig. 17G).....*A. olivarius* sp. nov.
- Timbal cover not covering the timbal cavity (Fig. 19F); sternite VII sub-triangular (Fig. 19G).....12
- 12 Tergites with pilus setae in both lateral margins of tergites 2 and 3 and in the anterior margin of tergite 6 (Fig. 10A); gutter of operculum slender present in all margins (Fig. 10E).....*A. densusus* comb. nov.
- Tergites without pilus setae in both lateral margins of tergites 2 and 3 and in the anterior margin of tergite 6 (Fig. 19A); gutter of operculum broad present in all margin (Fig. 19E).....*A. rubemi* sp. nov.

Acanthoventris charrua Ruschel sp. nov.

<http://zoobank.org/76D053B4-84F8-4501-9E85-A106B5643B9D>

Figs 6, 7

Type locality. Bento Gonçalves, Rio Grande do Sul (Brazil).

Type material. Holotype: male (MCNZ) (Fig. 6A), B. Gonçalves, RS, 5.XI.1960, E. Viana leg., Col. MCN 19289. — **Paratypes** (1 male, 2 females): male (MCNZ), Caxias, 5.III.1928, Col. MCN 19916; female (MCNZ), Porto Alegre, RS, 25.III.1982, T. de Lema leg., Col. MCN 42.787 (Fig. 7A); female (MCNZ), Caxias do Sul, RS, IV.1926, Col. MCN 19918.

Genbank access number. OM937994 (COI); OP548614 (EF1-alpha).

Etymology. The specific name refers to the distribution of species. The charruas were indigenous people who inhabited southern South America.

Diagnosis. The species can be distinguished from all other species of *Acanthoventris* **gen. nov.** by the following combination of features: anterior margin of head slightly convex; timbal cover long, apex acute, almost reaching the lateral metascutellar plate; operculum long, covering the timbal cavity and the apex reaching the auditory capsule; basal lobe long, almost reaching the apex of ventral apophyses; lateral margin of uncus straight becoming convex in the ventral apophyses; ventral apophyses grooved, internal margin forming a sub-rectangular distally directed and posterior margin forming an acute angle posteriorly directed. This species has a similar morphology to *A. faustopsaltrius* sp. nov. and *A. rubemi* sp. nov. due to the body color and bands, but *A. charrua* sp. nov. can be distinguished by the longer timbal cover, the operculum slightly longer, covering the auditory capsule, the gutter at apex of the operculum slender, and the basal lobe of pygofer shorter.

Color. Body tawny with the head, thorax and abdomen marked in black.

Description. Head (Fig. 6B): with a transverse wide black band extended over the vertex, covering the region of ocellus and reaching the apex of the postclypeus; two black vittae in “V” at the posterior margin of the head (the base concealed by the pronotum); base of eyes

marked with black; anterior margin of head slightly convex; antenna with a tawny scape and flagellum, and the pedicel black; a black band below each antenna reaches the posterior margin of the eyes; postclypeus (Fig. 6C) unmarked, oval in ventral view and flat in lateral view, the apex not prominent in dorsal view relative to the supra-antennal plates; longitudinal groove slender and shallow; anteclypeus and carina tawny; lorum black; rostrum with a tawny mentum and labium; labium short, reaching the base of basisternum 3 black at the apex. Pronotum (Fig. 6B): with lateral and sub-lateral lobes with wrinkles; ambient fissure with a black band in the middle. Mesonotum (Fig. 6A): lateral and submedian sigillae marked with black; scutal depression marked with black; basisternum 3 (Fig. 6D) with very developed protuberances relative to the median insertion, closely spaced forming an acute angle; posterior margin in an obtuse angle; cruciform elevation not covering tergite 1; apex of the posterior projections of the cruciform elevation obtuse; operculum (Fig. 6E) obtuse and long, covering the timbal cavity and the apex reaching the auditory capsule, the internal angles short, and the apices obtuse and widely spaced, anteromedian margin concave anteriorly to internal angle, the lateral margin convex, posterior margin slightly concave; meracanthus reaches the posterior margin base of the meracanthus marked with black, gutter present in all margins; legs tawny; wings hyaline; forewings: basal cell opaque, basal vein of the second apical cell oblique; hindwings: radius vein straight. Abdomen subcylindrical, the length is equivalent to the combined length of the head and thorax in dorsal view (Fig. 6A); timbal cover (Fig. 6F) flat and long, apex acute, almost reaching the lateral metascutellar plate, middle third of anteromedial margin concave, ventral anterior margin slightly concave (near the posterior margin of the operculum); tergites 2 to 8 marked with black anteriorly; sternite VII (Fig. 6G) sub-triangular, the lateral margin concave, becoming convex, the posterior margin emarginate. Uncus (Fig. 6H, I): lateral margin straight becoming convex in the ventral apophyses; lateral branches of uncus undeveloped, convex bud-like, the internal margin slightly concave; ventral apophyses grooved, ventrally developed originating from below the lateral branches of uncus; internal margin forming a sub-rectangular distally directed; posterior margin forming an acute angle posteriorly directed. Pygofer (Fig. 6J) sub-cylindrical; the basal lobe long, almost reaches the apex of ventral apophyses. Theca (Fig. 6K–M) dorsally developed with a ventral thecal process; vesica originates in a fissure at the distal third of the theca; vesica extruded and ornamented with cornuti in both the inner and outer surfaces. — **Female (Fig. 7A–**

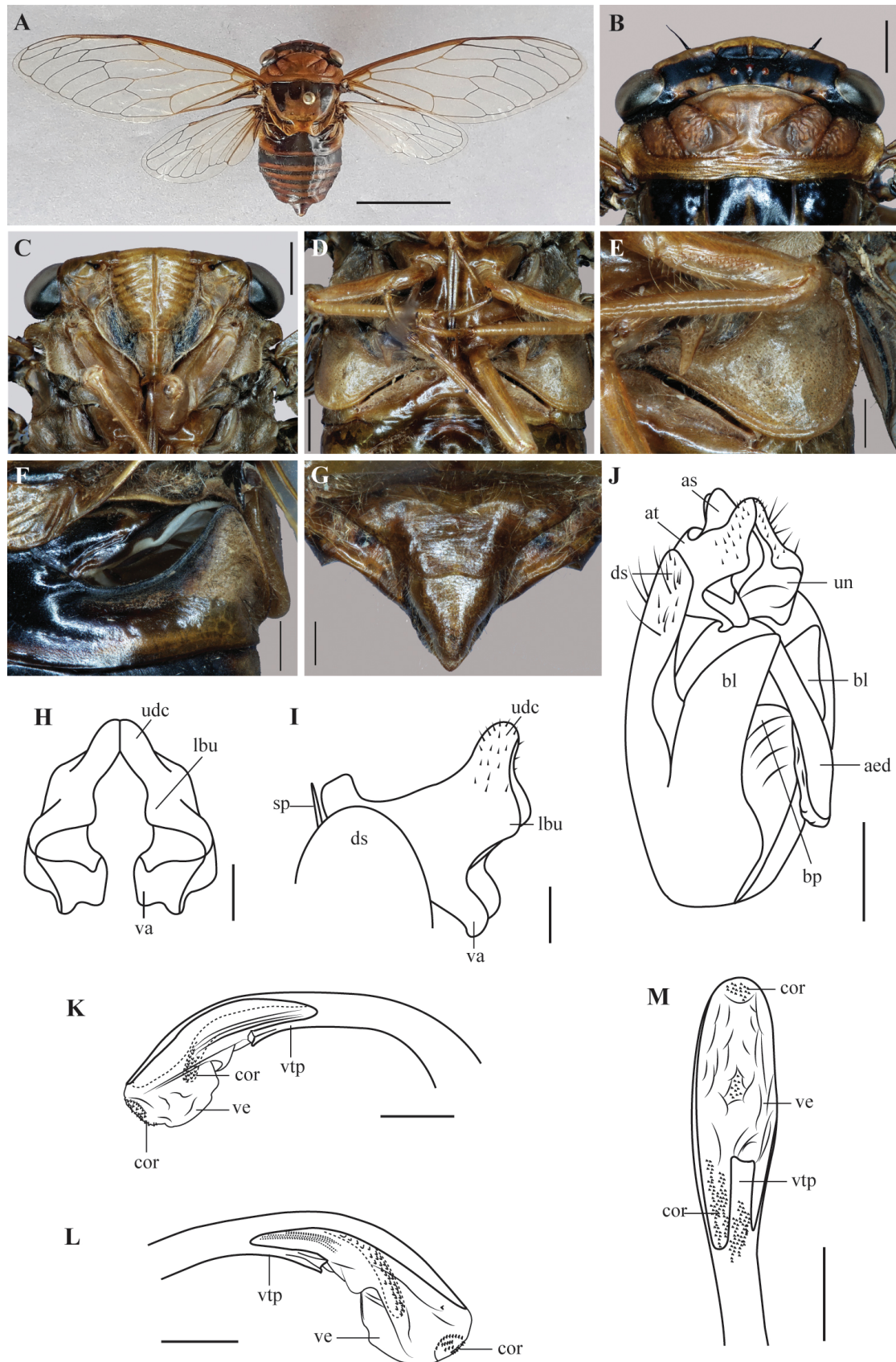


Figure 6. *Acanthoventris charrua* sp. nov., holotype male. **A** Habitus in dorsal view; **B** Head and pronotum in dorsal view; **C** Head and pronotum in ventral view; **D** Thorax in ventral view; **E** Operculum in latero-ventral view; **F** Timbal cover in dorso-lateral view; **G** Sternite VII in ventral view; **H** Uncus in ventral view; **I** Uncus in lateral view; **J** Pygofer in latero-ventral view; **K** Aedeagus in left lateral view; **L** Aedeagus in right lateral view; **M** Aedeagus in ventral view. Scale bars: A = 1 cm; B–D = 2 mm; E–G, J = 1 mm; H, I, K–M = 0.5 mm. Abbreviations: (aed) aedeagus; (as) anal styles; (at) anal tube; (bl) basal lobe of pygofer; (bp) basal plate; (cor) cornuti; (ds) distal shoulder; (lbu) lateral branch of uncus; (udc) uncal dorsal crest; (un) uncus; (va) ventral apophysis; (ve) vesica; (vtp) ventral thecal process.

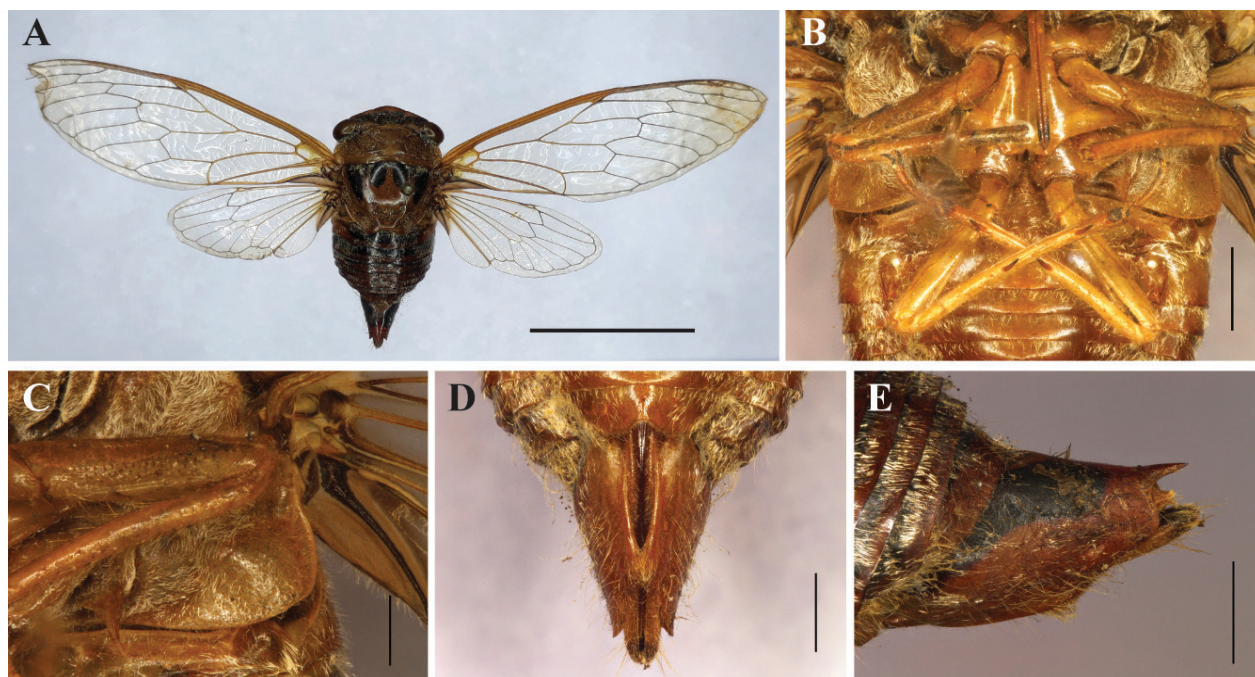


Figure 7. *Acanthoventris charrua* sp. nov., paratype female. **A** Habitus in dorsal view; **B** Thorax in ventral view; **C** Operculum in latero-ventral view; **D** Sternite VII, abdominal segment 9 and ovipositor sheath in ventral view; **E** Tergites and abdominal segment 9 in lateral view. Scale bars: A = 1 cm; B, D, E = 2 mm; C = 1 mm.

E): The female presents the same somatic characteristics as the male (Fig. 7A) except the operculum (Fig. 7C) is smaller; sternite VII (Fig. 7D) longer with a straight lateral margin and a concave posterior margin with an obtuse middle groove; dorsal beak of segment 9 with the same length as the ovipositor sheath (Fig. 7E). The ovipositor bears six teeth.

Measurements (in millimeters). $N = 5$ males and 5 females mean (range). Length of body: male 21.64 (20.39–23.09), female 21.44 (20.02–23.38); width of head including eyes: male 9.58 (9.07–10.13); female 9.46 (8.25–10.11); length of the head: male 2.42 (2.17–2.61), female 2.47 (2.26–2.67); width of pronotum including pronotal collar: male 9.38 (8.83–10.03), female 9.22 (8.04–9.80); length of pronotum including pronotal collar: male 3.36 (3.63–3.20), female 3.49 (3.40–3.56); width of mesonotum: male 7.93 (7.50–8.56), female 7.78 (6.41–8.46); length of mesonotum: male 6.01 (5.53–6.77); female 5.97 (4.89–6.65); length of forewing: male 28.72 (27.00–31.04), female 28.66 (25.72–30.39); width of forewing: male 9.82 (9.10–10.75), female 9.87 (9.56–10.55); length of hind wings: male 15.52 (14.38–16.63), female 15.55 (13.84–16.70).

Distribution. Brazil (Rio Grande do Sul).

Acanthoventris claudiae Ruschel sp. nov.

<http://zoobank.org/821FBA0D-78A1-4854-9BD6-8625BA43B35B>

Figs 8, 9

Type locality. Pelotas, Rio Grande do Sul (Brazil).

Type material. Holotype: male (MCTP) (Fig. 8A), Brazil, Rio Grande do Sul, Pelotas, V.1963, Ribeiro, A.S. col., cod. 32698. — **Paratypes** (8 males, 2 females): male (MCTP), same data as holotype except III.1963, Pedroso, P. col., cod. 32700; male (MCTP), IV.1963, Striagari, S. col., cod. 32699; male (MCTP), 01.V.1964, Goulart col., cod. 31746; male (MCTP), 28.IV.1965, Da Silva col., cod. 32697; male (NHMUK), 05.V.1967, Elmar col., cod. 32702; male (MCTP), X.1974, Senna col., cod. 32696; male (MCTP), 29.IV.1982, Cunha col., cod. 32701; male (MCTP), 12.III.1986, Augusto col., cod. 32703; female (MCTP), (Fig. 9A) IV.1982, Peres col., cod. 32704; female (NHMUK), 24.IV.1968, Bueno, A. col., cod. 32751.

Etymology. The species is named in honor to the mother of the first author, Claudia Petersen Ruschel.

Diagnosis. The species can be distinguished from all other species of *Acanthoventris* gen. nov. by the following combination of features: body yellowish; anterior margin of head slightly convex; basisternum 3 with little developed protuberances relative to the median insertion, closely spaced, and the posterior margin straight; basal vein of the second apical cell straight; timbal cover short, not reaching the lateral metascutellar plate; lateral margin of uncus straight becoming slightly convex in the ventral apophyses; basal lobe almost reaching the apex of ventral apophyses; the ventral thecal process is shorter than that of the other species of the genus, with the apex convex.

Color. Body yellowish with the head, mesonotum and abdomen marked with black.

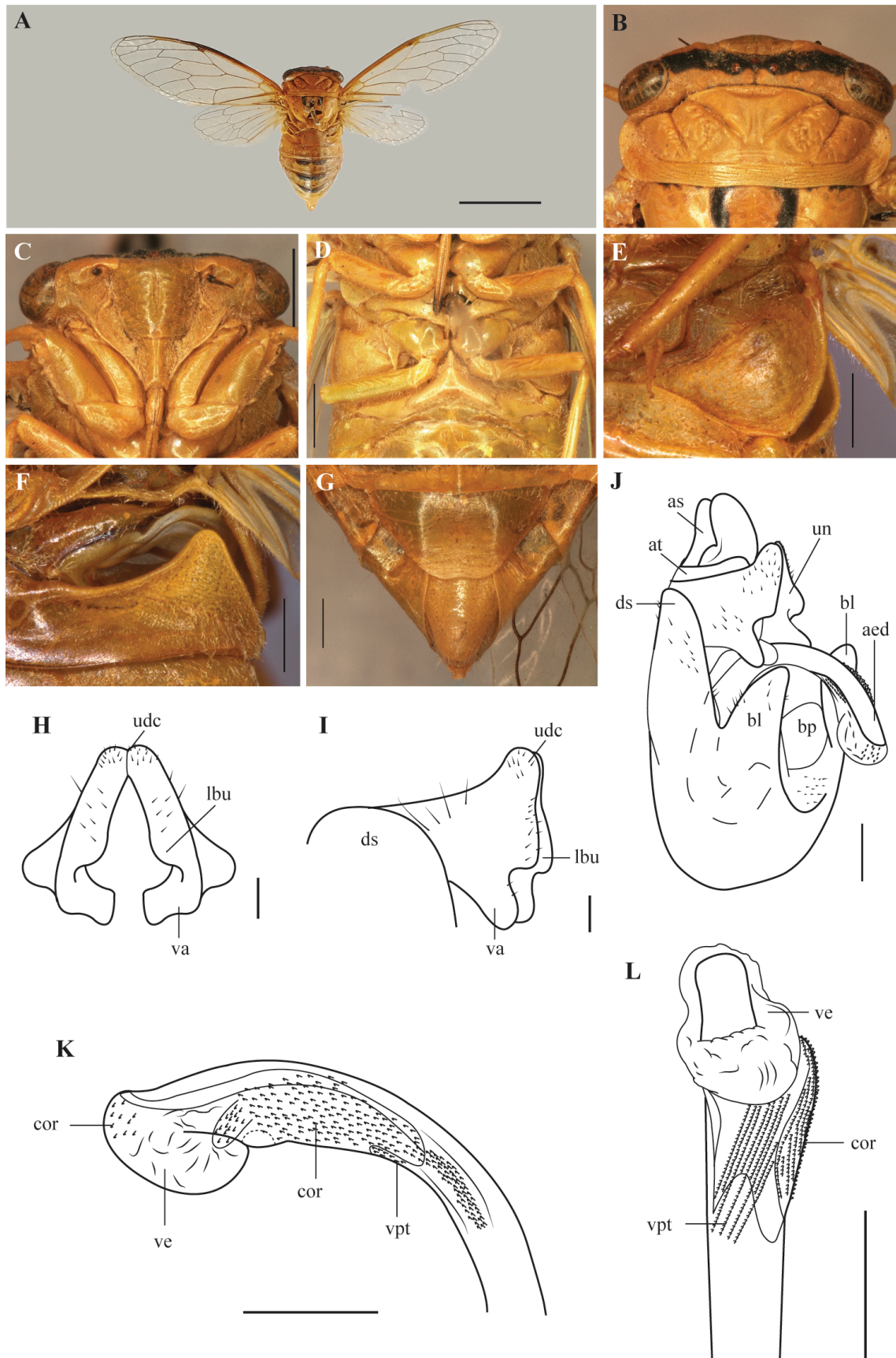


Figure 8. *Acanthoventris claudiae* sp. nov., holotype male. **A** Habitus in dorsal view; **B** Head and pronotum in dorsal view; **C** Head and pronotum in ventral view; **D** Thorax in ventral view; **E** Operculum in latero-ventral view; **F** Timbal cover in dorso-lateral view; **G** Sternite VII in ventral view; **H** Uncus in ventral view; **I** Uncus in lateral view; **J** Pygofer in latero-ventral view; **K** Aedeagus in left lateral view; **L** Aedeagus in ventral view. Scale bars: A = 1 cm; B–D = 2 mm; E–G, J = 1 mm; H, I, K, L = 0.5 mm. Abbreviations: (aed) aedeagus; (as) anal styles; (at) anal tube; (bl) basal lobe of pygofer; (bp) basal plate; (cor) cornuti; (ds) distal shoulder; (lbu) lateral branch of uncus; (udc) uncal dorsal crest; (un) uncus; (va) ventral apophysis; (ve) vesica; (vpt) ventral thecal process.

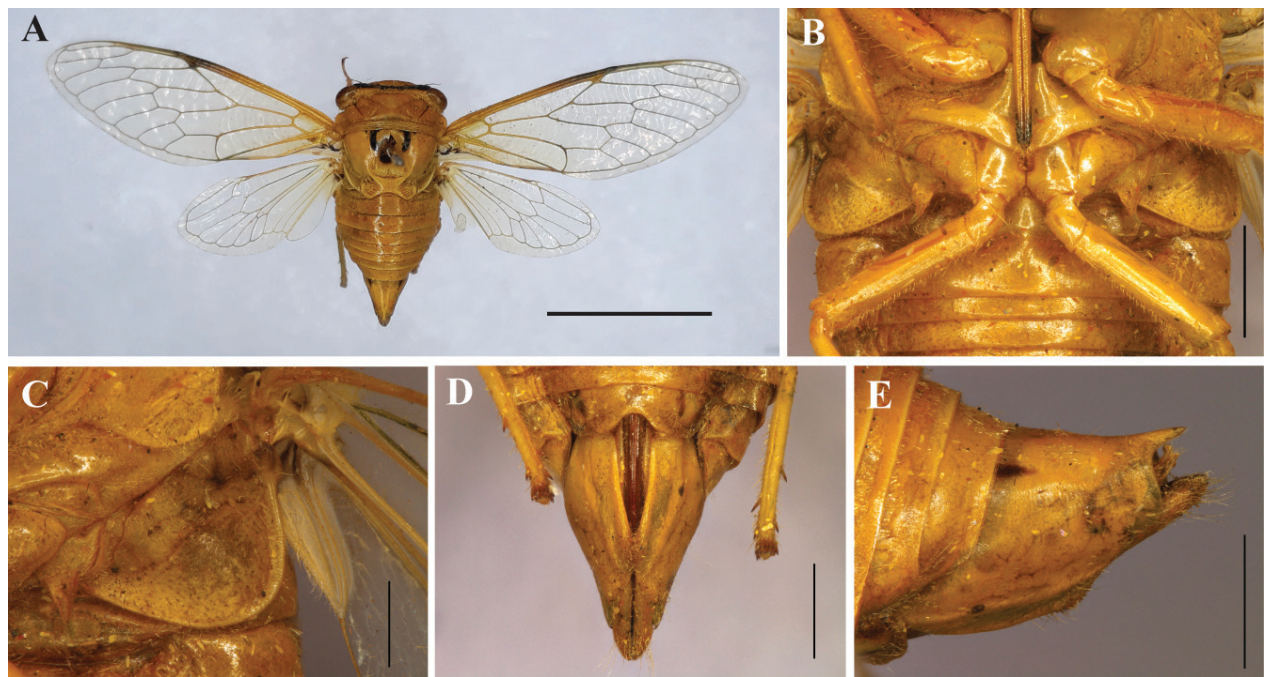


Figure 9. *Acanthoventris claudiae* sp. nov., paratype female. **A** Habitus in dorsal view; **B** Thorax in ventral view; **C** Operculum in latero-ventral view; **D** Sternite VII, abdominal segment 9 and ovipositor sheath in ventral view; **E** Tergites and abdominal segment 9 in lateral view. Scale bars: A = 1 cm; B, D, E = 2 mm; C = 1 mm.

Description. Head (Fig. 8B): with a transverse wide black band departing from each eye, extending through the area of the ocelli to the limit between the vertex and front; base of the eyes unmarked; anterior margin of head slightly convex; antennae with a yellowish scape, and the pedicel yellowish posteriorly and dark castaneous anteriorly, flagellum dark castaneous; postclypeus (Fig. 8C) unmarked, semi-rectangular in ventral view, and flat in lateral view, the apex not prominent in dorsal view relative to the supra-antennal plate; longitudinal groove slender and shallow; anteclypeus, carina, lorum, and rostrum yellowish; labium short, reaching the hind coxae, black at the apex. Pronotum: unmarked; paranota visible in dorsal view, wide and straight in lateral view. Mesonotum: submedian sigillae marked with black (in allotype and some paratypes, the parapsidal suture marked with black); scutal depression unmarked; basisternum 3 (Fig. 8D) with little developed protuberances relative to the median insertion, closely spaced; posterior margin straight; cruciform elevation not covering tergite 1; apex of the posterior projections of the cruciform elevation obtuse; operculum (Fig. 8E) not marked (inconspicuous central band in some paratypes), obtuse, the apex reaching the auditory capsule but not fully covering the timbal cavity, the internal angles very short, the apex obtuse and widely spaced, anteromedian margin concave anteriorly to the internal angles, the lateral margin concave, posterior margin slightly linear; meracanthus reaches the posterior margin, gutter present in all margins; legs yellowish becoming darker distally; wings hyaline; forewings: basal cell opaque, and the basal vein of the second apical cell oblique; basal vein of the second apical cell straight; apical cell 2 half of length of apical cell 1; hindwings: radius vein straight. Abdomen subcylindrical, the length equivalent to the

combined length of the head and thorax in dorsal view (Fig. 8A); timbal cover (Fig. 8F) flat and short, the apex acute, not reaching the lateral metascutellar plate, middle third of anteromedial margin concave, ventral anterior margin slightly concave (near the posterior margin of the operculum); tergites 4 to 6 with a medial anterior bande extending posteriorly (in allotypes and some paratypes, the band are weak or inconspicuous); sternite VII (Fig. 8G) sub-triangular, the lateral margin concave, the posterior margin concave and slightly emarginate. Uncus (Fig. 8H, I): lateral margin straight becoming slightly convex in the ventral apophyses; lateral branches of uncus undeveloped, convex bud-like, the internal margin slightly straight; ventral apophyses ventrally developed originating from below the lateral branches of uncus; internal margin forming a sub-rectangular distally directed, posterior margin sinuous. Pygofer (Fig. 8J) sub-cylindrical; the basal lobe almost reaching the apex of ventral apophyses. Theca (Fig. 8K, L) dorsally developed with a short ventral thecal process; apex of ventral thecal process convex; vesica originates in a fissure at the distal third of the theca extruded and adorned with cornuti in the inner and outer surfaces. — **Female (Fig. 9A–E):** The female presents the same somatic characteristics as the male (Fig. 9A) except the operculum (Fig. 9C) is smaller, and sternite VII (Fig. 9D) longer with a straight lateral margin convergent towards the apex, the posterior margin straight, directed anteromedially to a wide and truncated middle groove; dorsal beak of segment 9 with the same length as the ovipositor sheath (Fig. 9E); ovipositor bears nine teeth.

Measurements (in millimeters). Holotype male. Length of body: 16.01; width of head including eyes: 6.90; length of the head: 1.60; width of pronotum including pronotal

collar: 6.80; length of pronotum including pronotal collar: 2.20; width of mesonotum: male 5.70; length of mesonotum: 3.50; length of forewing: 19.90; width of forewing: male 6.5; length of hind wings: male 11.20. Paratypes 8 males and 2 females, mean (range). Length of body: male 15.05 (14.40–15.80), female 15.00 (16.10–13.90); width of head including eyes: male 6.93 (6.70–7.00); female 7.25 (7.60–6.90); length of the head: male 1.60 (1.60–1.60), female 1.65 (1.60–1.70); width of pronotum including pronotal collar: male 6.73 (6.40–7.00), female 7.20 (7.50–6.90); length of pronotum including pronotal collar: male 2.38 (2.40–2.50), female 2.65 (2.70–2.60); width of mesonotum: male 5.58 (5.40–5.70), female 5.80 (5.70–5.90); length of mesonotum: male 3.68 (3.30–3.90); female 3.95 (4.10–3.80); length of forewing: male 19.50 (18.00–21.00), female 21.50 (21.80–21.20); width of forewing: male 6.80 (6.50–7.00), female 6.90 (7.00–6.80); length of hindwings: male 10.93 (10.20–11.80), female 11.55 (11.70–11.40).

Distribution. Brazil (Rio Grande do Sul).

Acanthoventris densus (Boulard & Martinelli, 2011) comb. nov.

Figs 10, 11

Guyala densus Boulard & Martinelli, 2011: 224–225.

Type locality. Espírito Santo, Brazil.

Type material. Holotype male, allotype female, and paratype male (MNHN), Brésil, État d'Espírito Santo, route de Vitoria à Belo Horizonte, Km 118, 850 m, le 05/03/1981, D. Bertrand réc. Don de M. Hervé de Toulgoëti. Muséum National d'Histoire Naturelle, Entomologie, Paris. (Boulard & Martinelli 2011).

Diagnosis. The species can be distinguished from all other species of *Acanthoventris* **gen. nov.** by the following combination of features: anterior margin of head slightly convex; abdomen dark castaneous with the tergites marked with black dorsally with pilus silver setae in both lateral margins of tergites 2 and 3 and in the anterior margin of tergite 6; ventral apophyses grooved with internal margin straight and posterior margin straight forming a sub-rectangular posteriorly directed. This species has a similar morphology to *A. phoenix* **sp. nov.** due the pilus silver setae in both lateral margins of tergites. *A. densus* comb. nov. can be distinguished by the head, pronotum and mesonotum olive-green, the posterior margin of ventral apophyses without an acute-angled laterally and posteriorly developed; the anterior margin of the ventral thecal process without a slender projection.

Color. Body yellowish ventrally; head, pronotum, and mesonotum olive-green marked with black; abdomen dark castaneous with the tergites marked with black dorsally.

Description. Head (Fig. 10B): with a transverse wide black band departing from each eye, covering the posterior margin of eyes and the ocelli, reaching the apex of the postclypeus; silver setae in the posterior margin of eyes; anterior margin of head slightly convex; antenna with a yellowish scape, the pedicel and flagellum dark castaneous; postclypeus (Fig. 10C) rounded and unmarked in ventral view and flat in lateral view, the apex not prominent in dorsal view relative to the supra-antennal plate, longitudinal groove slender and shallow; anteclypeus and carina tawny; lorum black; mentum yellowish; labium short, reaching the metacoxae and black at the apex (Fig. 10D). Pronotum (Fig. 10B): pronotal collar olive-green with pilus silver setae. Mesonotum (Fig. 10A): submedian sigillae marked with black, lateral sigillae marked with black at the anterior margin; scutal depression unmarked; basisternum 3 (Fig. 10D) with well-developed protuberances relative to the median insertion, both protuberances approximate forming an acute angle; posterior margin angled; cruciform elevation not covering tergite 1; apex of the posterior projections obtuse; operculum (Fig. 10E) obtuse, covering the timbal cavity and the apex reaching the auditory capsule, the internal angles very short, the apex obtuse and widely spaced, anteromedian margin concave anteriorly to the internal angle and marked with black, lateral margin convex and marked with black, the posterior margin straight; meracanthus reaches the posterior margin; gutter slender present in all margins; legs yellowish, becoming tawny distally; wings hyaline; forewings: the anterior portion of the basal cell opaque, second apical cell with half the size of the first apical cell or a little more than half, basal vein of the second apical cell oblique; hindwings: radius vein straight. Abdomen subcylindrical and almost oblong in some specimens, the length equivalent to the combined length of the head and thorax in dorsal view (Fig. 10A); timbal cover (Fig. 10F) flat, apex obtuse almost reaching the lateral metascutellar plate; middle third of anteromedial margin concave with pilus silver setae, ventral anterior margin slightly concave (near the posterior margin of the operculum); tergites 2 to 8 with the anterior margin marked with black; pilus silver setae in both lateral margins of tergites 2 and 3 and in the anterior margin of tergite 6; sternite VII (Fig. 10G) sub-triangular, the lateral margin concave, becoming convex toward the apex, the posterior margin slightly emarginate. Uncus (Fig. 10H, I): lateral margin straight becoming convex in the ventral apophyses; uncal dorsal crest fused and dorsally projected; lateral branches of uncus undeveloped, convex bud-like, the internal margin slightly concave; ventral apophyses grooved, ventrally developed originating from below the lateral branches of uncus, internal margin straight; posterior margin straight forming a sub-rectangular posteriorly directed. Pygofer (Fig. 10J) sub-cylindrical; the basal lobe long reaching the lateral branches of the uncus. Theca (Fig. 10K, L) dorsally developed with a ventral thecal process; vesica originates in a fissure at the distal third of the theca, extruded and ornamented with cornuti in both the inner and outer surfaces. — **Female (Fig. 11A–E):** The female presents the same somatic characteristics as the male (Fig. 11A)

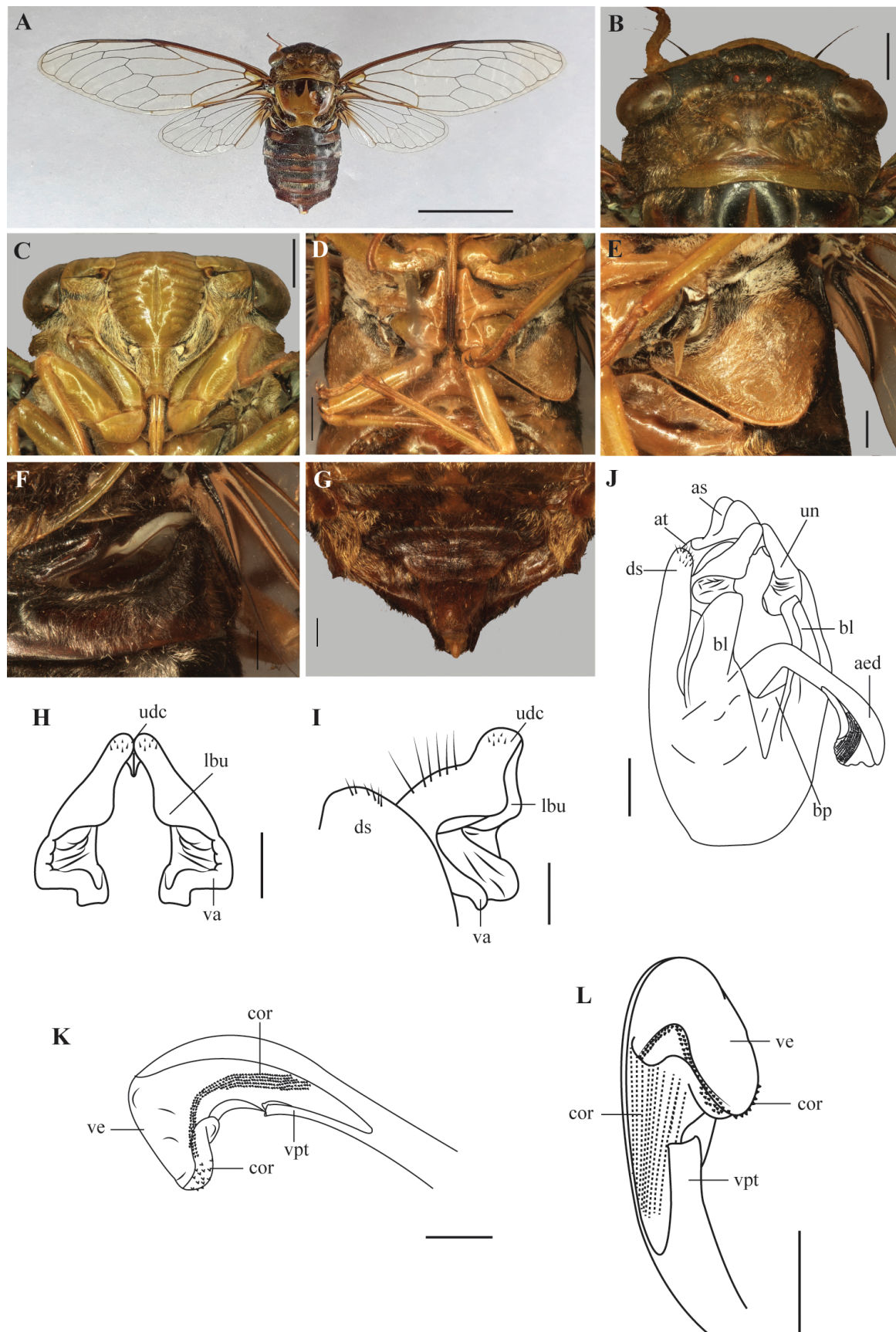


Figure 10. *Acanthoventris densus* **comb. nov.**, male. **A** Habitus in dorsal view; **B** Head and pronotum in dorsal view; **C** Head and pronotum in ventral view; **D** Thorax in ventral view; **E** Operculum in latero-ventral view; **F** Timbal cover in dorso-lateral view; **G** Sternite VII in ventral view; **H** Uncus in ventral view; **I** Uncus in lateral view; **J** Pygofer in latero-ventral view; **K** Aedeagus in left lateral view; **L** Aedeagus in latero-ventral view. Scale bars: A = 1 cm; B–D = 2 mm; E–G, J = 1 mm; H, I, K, L = 0.5 mm. Abbreviations: (aed) aedeagus; (as) anal styles; (at) anal tube; (bl) basal lobe of pygofer; (bp) basal plate; (cor) cornuti; (ds) distal shoulder; (lbu) lateral branch of uncus; (udc) uncal dorsal crest; (un) uncus; (va) ventral apophysis; (ve) vesica; (vpt) ventral thecal process.



Figure 11. *Acanthoventris densus* **comb. nov.**, female. **A** Habitus in dorsal view; **B** Thorax in ventral view; **C** Operculum in latero-ventral view; **D** Sternite VII, abdominal segment 9 and ovipositor sheath in ventral view; **E** Tergites and abdominal segment 9 in lateral view. Scale bars: A = 1 cm; B, D, E = 2 mm; C = 1 mm.

except the operculum smaller (Fig. 11C) and the sternite VII (Fig. 11D) longer with straight lateral and posterior margins, the posterior with a sub-triangular groove in the middle portion. Dorsal beak of segment 9 a little longer than the ovipositor sheath (Fig. 11E), the ovipositor bears eight teeth.

Measurements (in millimeters). N = 5 males and 5 females, mean (range). Length of body: male 26.79 (24.64–28.24), female 23.56 (22.49–24.34); width of head including eyes: male 10.83 (9.87–11.51); female 10.60 (10.11–11.06); length of the head: male 2.71 (2.58–2.82), female 2.79 (2.45–3.58); width of pronotum including pronotal collar: male 10.48 (9.36–11.09), female 10.28 (9.68–10.79); length of pronotum including pronotal collar: male 4.14 (3.63–4.41), female 3.91 (3.71–4.16); width of mesonotum: male 8.99 (8.29–9.39), female 8.83 (8.18–9.18); length of mesonotum: male 7.25 (6.74–7.69); female 7.02 (6.45–7.34); length of forewing: male 34.45 (32.77–36.84), female 34.89 (33.84–35.57); width of forewing: male 11.46 (10.51–12.53), female 11.14 (10.68–11.57); length of hind wings: male 17.44 (16.31–18.36), female 17.39 (16.85–18.07).

Material examined. 2 females (DZUP), BRAZIL, Espírito Santo: Santa Teresa, 12.II.1966, C.T. & C. Elias; female (DZUP), idem, 27.II.1964, C. Elias leg.; male (DZUP), Minas Gerais: Viçosa, 21.II.1987, Pe. Moure col.; 2 males (INPA), São Paulo: Restinga, 20°43'31"S, 47°30'60"W, 21.III.2008, J.A. Rafael, F.F. Xavier F^o & D.S. Amorim, 650 m; male (DZUP), Paraná: Curitiba, I.1982, A.M.S. e R.R.C.); male (DZUP), idem, Cavichioli leg.; male (DZUP), idem, Sakakibara leg.; 2 males, female (DZUP), idem, 29.I.1966, Dept. Zoo leg.; male, female (DZUP), idem, 16.II.1966, C. Ext. D.Z.UF.P.; male (ZMUC), no data collect,

Mus. Western; male (DZUP), Santa Catarina: Joinville, 23.I.1972, Ex. Zoologia; male (MAPA), Rio Grande do Sul: Porto Alegre, 26.III.1951, Pe. Buck leg.; female (MAPA), Pelotas, I.1962.

Distribution. Brazil (Espírito Santo, Minas Gerais*, São Paulo*, Paraná*, Santa Catarina*, Rio Grande do Sul*).

Acanthoventris drewseni (Stål, 1854) **comb. nov.**

Fig. 12

Cicada drewseni Stål, 1854: 242

Fidicina gastracanthophora Berg, 1879: 138 (syn. apud Distant, 1906: 92)

Fidicina drewseni; Distant, 1906: 92

Dorisia drewseni; Delétang, 1919: 85

Dorisiana drewseni; Metcalf, 1963: 405

Type locality. Minas Gerais, Brazil.

Type material. **Syntype:** male (NHRS) (Fig. 12A), Minas Gerais, Dreweni Stål, NHRS-GULI, 29414, Typus. (examined by photographs).

Diagnosis. The species can be distinguished from all other species of *Acanthoventris* **gen. nov.** by the following combination of features: anterior margin of head convex; postclypeus with a dark castaneous band covering the longitudinal groove and the transverse grooves; labium long, reaching the sternite III; lateral margin of operculum convex and marked with black becoming concave

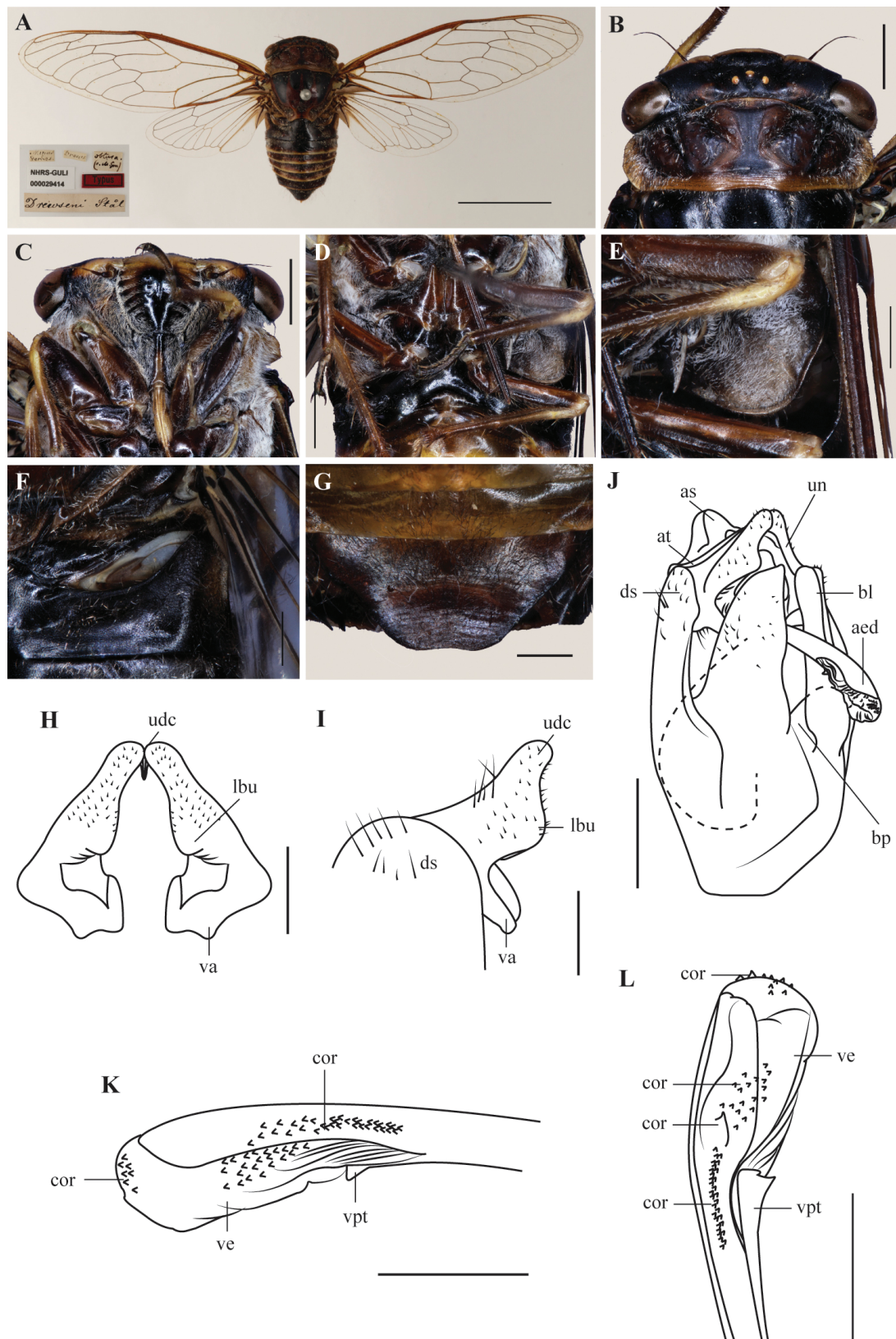


Figure 12. *Acanthoventris drewseni* **comb. nov.**, male. **A** Habitus of syntype in dorsal view; **B** Head and pronotum in dorsal view; **C** Head and pronotum in ventral view; **D** Thorax in ventral view; **E** Operculum in latero-ventral view; **F** Timbal cover in dorso-lateral view; **G** Sternite VII in ventral view; **H** Uncus in ventral view; **I** Uncus in lateral view; **J** Pygofer in latero-ventral view; **K** Aedeagus in left lateral view; **L** Aedeagus in latero-ventral view. Scale bars: A = 1 cm; B–D = 2 mm; E–G, J = 1 mm; H, I, K, L = 0.5 mm. Obs. Only the photograph A is from holotype: photographed by Gunvi Lindberg (© 2016 Naturhistoriska riksmuseet). Original photos cropped, light levels and contrast adjusted. Made available by the Swedish Museum of Natural History under Creative Commons Attribution 4.0 International Public License, CC-BY 4.0 [<https://creativecommons.org/licenses/by/4.0/legalcode>]. Abbreviations: (aed) aedeagus; (as) anal styles; (at) anal tube; (bl) basal lobe of pygofer; (bp) basal plate; (cor) cornuti; (ds) distal shoulder; (lbu) lateral branch of uncus; (udc) uncal dorsal crest; (un) uncus; (va) ventral apophysis; (ve) vesica; (vpt) ventral thecal process.

toward the apex; lateral margin of uncus slightly convex becoming tightly convex in the ventral apophyses; and a spine present on the vesica. This species has a similar morphology to *A. charrua* **sp. nov.** but can be distinguished by the small body size, dark castaneous color and the operculum short, not covering the timbal cavity and the apex does not reach the auditory capsule.

Color. Body dark castaneous, marked with black and tawny.

Description. Head (Fig. 12B): with a transverse wide black band departing from each eye, covering the posterior margin of eyes and the ocelli, reaching the apex of the postclypeus; silver setae in the posterior margin of eyes; antenna with a dark castaneous scape, pedicel and flagellum; anterior margin of head slightly convex; postclypeus (Fig. 12C) oval in ventral view and with a dark castaneous band covering the longitudinal groove and the transverse grooves; postclypeus flat in lateral view, the apex not prominent in dorsal view relative to the supra-antennal plate, longitudinal groove slender and shallow; anteclypeus dark castaneous and carina tawny marked with dark castaneous; lorum black; mentum tawny; labium dark castaneous and long, reaching the sternite III (Fig. 12D). Pronotum (Fig. 12B): with a longitudinal black band at middle; pronotal collar tawny with pilus silver setae. Mesonotum (Fig. 12A): submedian, lateral sigillae and scutal depression marked with black; basisternum 3 (Fig. 12D) with well-developed protuberances relative to the median insertion, both protuberances approximate forming an acute angle; posterior margin angled; cruciform elevation not covering tergite 1; apex of the posterior projections obtuse; operculum (Fig. 12E) obtuse and short, not covering the timbal cavity and the apex does not reach the auditory capsule, the internal angles very short, the apex obtuse and widely spaced, anteromedian margin concave anteriorly to the internal angle and marked with black, lateral margin convex and marked with black becoming concave toward the apex, the posterior margin slightly straight; meracanthus reaches the posterior margin; gutter present in all margins; legs tawny marked with castaneous, and tawny between the femur and tibia; wings hyaline; forewings: anterior portion of the basal cell opaque; hindwings: radius vein straight. Abdomen (Fig. 12A) subcylindrical and almost oblong in some specimens, the length equivalent to the combined length of the head and thorax in dorsal view; timbal cover (Fig. 12F) flat, apex obtuse reaching the lateral metascutellar plate; middle third of anteromedial margin concave, ventral anterior margin tightly concave (away from the posterior margin of operculum); tergites 3 to 7 tawny with the anterior margin marked with dark castaneous; sternite VII (Fig. 12G) sub-triangular, the lateral margin concave, becoming straight toward the apex, the posterior margin slightly emarginate. Uncus (Fig. 12H, I): lateral margin slightly convex becoming tightly convex in the ventral apophyses; uncal dorsal crest fused and dorsally projected; lateral branches of uncus undeveloped, convex bud-like, the internal margin slightly concave; ventral

apophyses with internal margin forming a sub-rectangular lobe distally directed; posterior margin forming an obtuse angle posteriorly directed. Pygofer (Fig. 12J) sub-cylindrical; the basal lobe long, almost reaches the uncal dorsal crest. Theca (Fig. 12K, L) dorsally developed with a ventral thecal process; vesica originates in a fissure at the distal third of the theca, extruded and ornamented with cornuti in both the inner and outer surfaces; spine present on the vesica. — **Female.** Unknown.

Measurements (in millimeters). Syntype male (NHRS) and specimen male (INPA). Length of body: 17.54, 16.05; width of head including eyes: 8.07, 7.24; length of the head: 1.25, 1.35; width of pronotum including pronotal collar: 7.92, 7.29; length of pronotum including pronotal collar: 2.59, 2.61; width of mesonotum: 6.75, 6.39; length of mesonotum: 5.66, 4.68; length of forewing: 27.46, 24.42; width of forewing: 8.59, 7.60; length of hind wings: 14.11, 12.42.

Material examined. Male (INPA), BRAZIL, Goiás: Caldas Novas, Parque Est. Serra, de caldas novas, 1.000 m, 17°46'13"S, 48°39'22"W, 22–23.II.2008 Luz, J. A. Rafael & F. F. Xavier F°.

Distribution. Brazil (Goiás, Minas Gerais).

Acanthoventris faustopsaltrius Ruschel **sp. nov.**

<http://zoobank.org/DBCF040B-4A4F-473B-9DD7-A2CA256CB604>

Fig. 13

Type locality. Itatiaia, Rio de Janeiro, Brazil.

Type material. Holotype: male (Fig. 13A) (DZRJ), RJ, Itatiaia, Penedo, Três Bacias, Rio das Pedras, 22°24'33.0"S 44°33'08.0"W, 706 m de altitude, Luz Branca, 6.III.2008, JL Nessimian, RB Braga, MR Souza, LL Dumas.

Etymology. This was the last species included in this study. Latin: faustus, lucky; psaltria, female harpist.

Diagnosis. The species can be distinguished from all other species of *Acanthoventris* **gen. nov.** by the following combination of features: apex of postclypeus in m-shaped with a black band in m-shaped; anterior margin of head convex; labium long, reaching the apex of the sternite II; operculum covered by golden setae, obtuse and long, covering the timbal cavity, the apex reaching the auditory capsule; sternites VII sub-triangular covered by golden setae; lateral branches of uncus convex bud-like with grooves. This species has a similar morphology to *A. charrua* **sp. nov.** but can be distinguished by the lateral margin of the timbal cover slightly concave (near of the posterior margin of operculum), the presence of golden setae, the uncus shape and the theca with the apex of the ventral thecal process in a half-moon shaped.

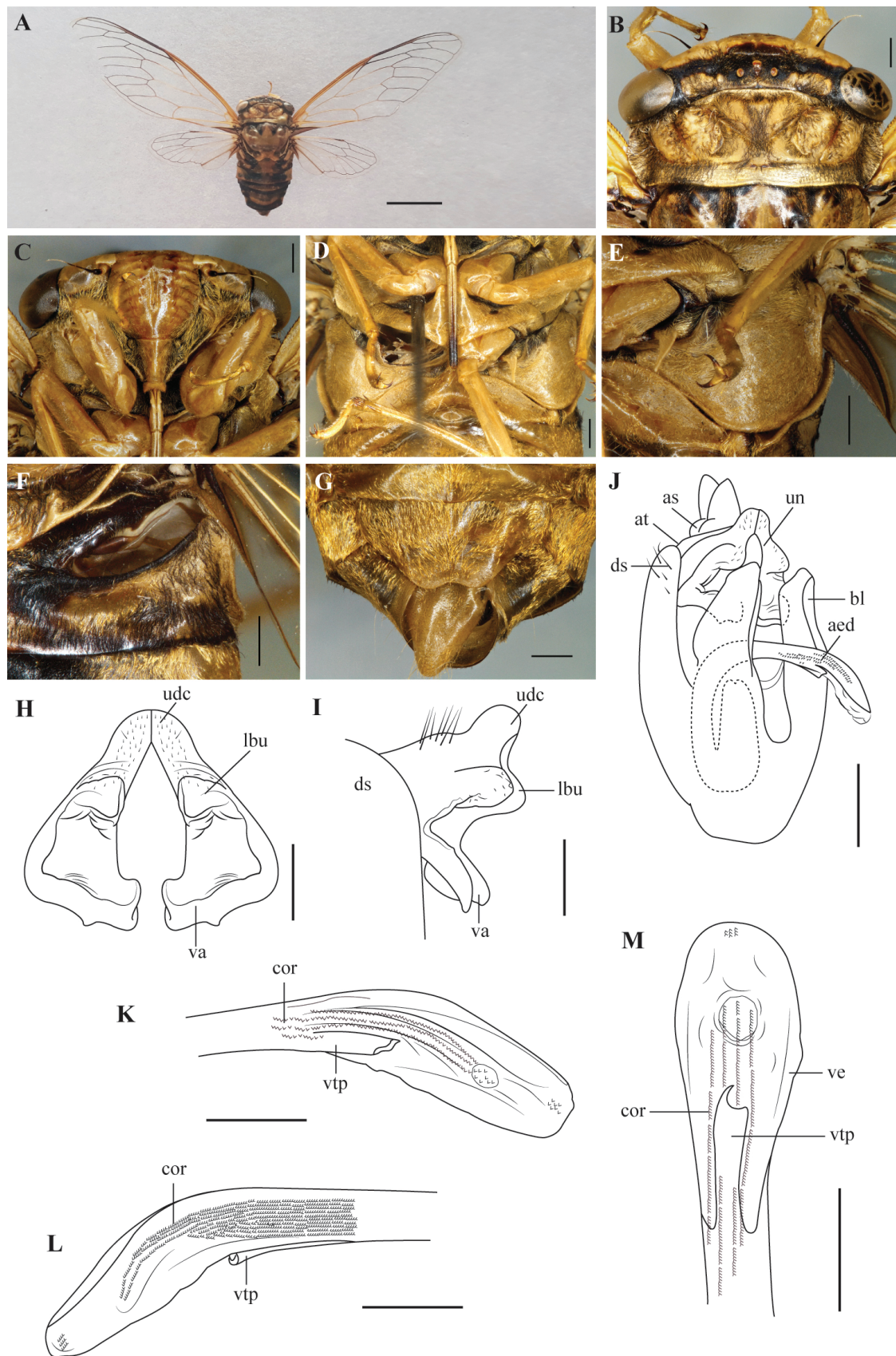


Figure 13. *Acanthoventris faustopsaltrius* sp. nov., holotype male. **A** Habitus in dorsal view; **B** Head and pronotum in dorsal view; **C** Head and pronotum in ventral view; **D** Thorax in ventral view; **E** Operculum in latero-ventral view; **F** Timbal cover in dorso-lateral view; **G** Sternite VII in ventral view; **H** Uncus in ventral view; **I** Uncus in lateral view; **J** Pygofer in latero-ventral view; **K** Aedeagus in right lateral view; **L** Aedeagus in left lateral view; **M** Aedeagus in ventral view. Scale bars: A = 1 cm; B–G, J = 1 mm; H, I, K–M = 0.5 mm. Abbreviations: (aed) aedeagus; (as) anal styles; (at) anal tube; (bl) basal lobe of pygofer; (bp) basal plate; (cor) cornuti; (ds) distal shoulder; (lbu) lateral branch of uncus; (udc) uncal dorsal crest; (un) uncus; (va) ventral apophysis; (ve) vesica; (vtp) ventral thecal process.

Color. Body tawny with the head, thorax and abdomen marked with black, covered by golden setae.

Description. Head (Fig. 13B): black setae over the head; head with a transverse slender black band departing from each eye, extending through the area of the ocelli, the base of the eyes and the apex of postclypeus in m-shaped; anterior margin of head convex; antennae with a marked with black scape and pedicel, and flagellum lighter at apex; postclypeus (Fig. 13C) unmarked, oval in ventral view, flat in lateral view, the apex not prominent in dorsal view relative to the supra-antennal plate; longitudinal groove inconspicuous; anteclypeus and carina tawny, lorum black; mentum and labium tawny; labium long, reaching the apex of the sternite II, black at the apex. Pronotum (Fig. 13B): covered by black setae; lateral and sub-lateral lobes with wrinkles; lateral part of pronotal collar slightly surpassing the eyes. Mesonotum (Fig. 13A): submedian sigillae marked with black, lateral sigillae marked with black at anterior margin; scutal depression marked with castaneous; basisternum 3 (Fig. 13D) with well developed and narrow protuberances relative to the median insertion, closely spaced; posterior margin in an obtuse angle; cruciform elevation covering the tergite 1; apex of the posterior projections of the cruciform elevation obtuse; operculum (Fig. 13E) covered by golden setae, obtuse and long, covering the timbal cavity, the apex reaching the auditory capsule, the internal angles short and narrow, the apex obtuse and widely spaced, anteromedian margin concave anteriorly to the internal angles, the lateral margin convex, posterior margin slightly straight; meracanthus surpassing the posterior margin, gutter present in all margins; legs and tarsus tawny; pretarsal claw black at apex; wings hyaline (Fig. 13A); forewings: basal cell opaque anteriorly, and the basal vein of the second apical cell oblique; apical cell 2 half of length of apical cell 1; hindwings: radius vein straight. Abdomen subcylindrical, the length equivalent to the combined length of the head and thorax in dorsal view (Fig. 13A); timbal cover (Fig. 13F) flat, the apex acute not reaching the lateral metascutellar plate, middle third of anteromedial margin concave, ventral anterior margin slightly concave (near of the posterior margin of operculum); anterior margin of tergites 2 to 8 marked with black; sternites II to VIII covered by golden setae; sternite VII (Fig. 13G) sub-triangular, the lateral margin convex becoming slightly straight toward the apex, the posterior margin emarginate. Uncus (Fig. 13H, I): lateral margin slightly straight becoming tightly convex in the ventral apophyses; lateral branches of uncus convex bud-like with grooves, the internal margin slightly rectangular; ventral apophyses with internal margin forming a sub-rectangular lobe distally directed; posterior margin forming sinuous with an obtuse angle posteriorly directed. Pygofer (Fig. 13J) sub-cylindrical, the basal lobe reaching the lateral branches of uncus. Theca (Fig. 13K–M) with the apex of the ventral thecal process in a half-moon shaped; vesica tightly extruded and adorned with cornuti in the inner and outer surfaces. — **Female:** Unknown.

Measurements (in millimeters). Holotype male. Length of body: 26.28; width of head including eyes: 9.13; length of the head: 1.84; width of pronotum including pronotal collar: 8.54; length of pronotum including pronotal collar: 3.27; width of mesonotum: 7.37; length of mesonotum: 7.94; length of forewing: 40.67; width of forewing: 14.62; length of hind wings: 20.39.

Distribution. Brazil (Rio de Janeiro).

Acanthoventris iara Ruschel sp. nov.

<http://zoobank.org/7E375109-F8A0-40DA-BD97-7403F1FB1758>

Figs 14, 15

Type locality. Amazonas, Brazil.

Type material. Holotype: Male (INPA) (Fig. 14A), Brasil, Amazonas, Manaus, BR-174 Km 50, ZF-2 Km21, 02°38'16"S, 60°09'26"W, 13–27.XII.2012, F.F. Xavier F; G.Z. Lopes, A.L. Aguiar; A.L. Rodrigues, J.R. de Oliveira, Armadilha de Luz, Mista. **Paratypes, 4 males and 2 females:** female (Fig. 15A), same data as holotype (INPA); female (INPA), Brasil, AM, Presidente Figueiredo, AM-240, Km 24, 02 35 21 S 60 06 55 W, 13–17.VII.2009, F.F. Xavier F; R. Machado, S. Oliveira; C. Schwertner, R.A.P. Freitas Silva, Armadilha de luz mista de mercúrio Lençol; 2 males (INPA), Brasil, RR, Amajari, Serra, Tepequém 03°44'45.5"N, -61°43'39"W, 09–10.VII.2010, 21-00:00, J.A. Rafael, F.F. Xavier F°, R. Machado, R.Freitas, luminosa dossel; male (INPA), Brasil, AM, Manaus, Rod. AM010, km 50, ZF-2, km 14, próximo à torre, 02°35'S, 60°06"W 6.III.2011, 00–03:00h. Armadilha luminosa móvel. J.T. Camara; P. Dias, J.A. Rafael leg.; male (DZRJ), Nascente Rio Pimenta divisa Vilhena – Colorado d'Oeste – RO, 13.XI.1988, J. Becker col., Dorisiana drewseni (Stål, 1854) A. Sanborn det. V/2009.

Etymology. The specific name refers to the distribution of the species. Iara is a mermaid from Brazilian folklore who lives in the Amazon River, who lures men singing with their enchanting music.

Diagnosis. The species can be distinguished from all other species of *Acanthoventris* **gen. nov.** by the following combination of features: anterior margin of head tightly convex; posterior margin of basisternum 3 tightly acute; lateral margin of operculum marked with black and convex, becoming slightly straight toward the apex; the internal margin slightly concave; lateral margin of uncus straight becoming slightly convex in the middle and straight toward the apex of ventral apophyses. This species has a similar morphology to *A. igneus* **sp. nov.** due the anterior margin of head tightly concave and lateral margin of operculum marked with black and convex. *A. iara* **sp. nov.** can be distinguished from *A. igneus* **sp. nov.** by the pronotal collar and wing groove olive-green, the ab-

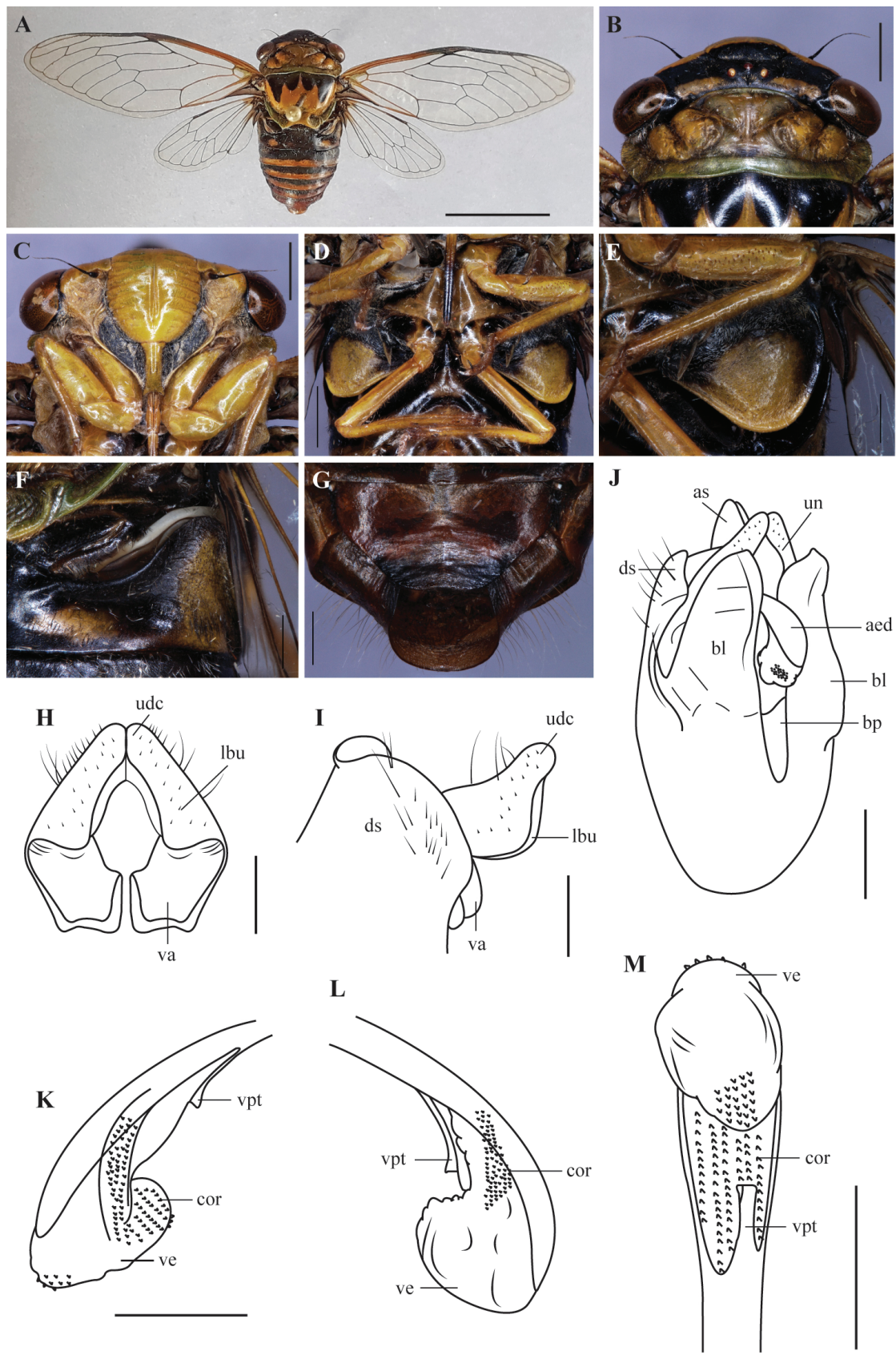


Figure 14. *Acanthoventris iara* sp. nov., holotype male. **A** Habitus in dorsal view; **B** Head and pronotum in dorsal view; **C** Head and pronotum in ventral view; **D** Thorax in ventral view; **E** Operculum in latero-ventral view; **F** Timbal cover in dorso-lateral view; **G** Sternite VII in ventral view; **H** Uncus in ventral view; **I** Uncus in lateral view; **J** Pygofer in latero-ventral view; **K** Aedeagus in left lateral view; **L** Aedeagus in right lateral view; **M** Aedeagus in ventral view. Scale bars: A = 1 cm; B–D = 2 mm; E–G, J = 1 mm; H, I, K–M = 0.5 mm. Abbreviations: (aed) aedeagus; (as) anal styles; (at) anal tube; (bl) basal lobe of pygofer; (bp) basal plate; (cor) cornuti; (ds) distal shoulder; (lbu) lateral branch of uncus; (udc) uncal dorsal crest; (un) uncus; (va) ventral apophysis; (ve) vesica; (vtp) ventral thecal process.

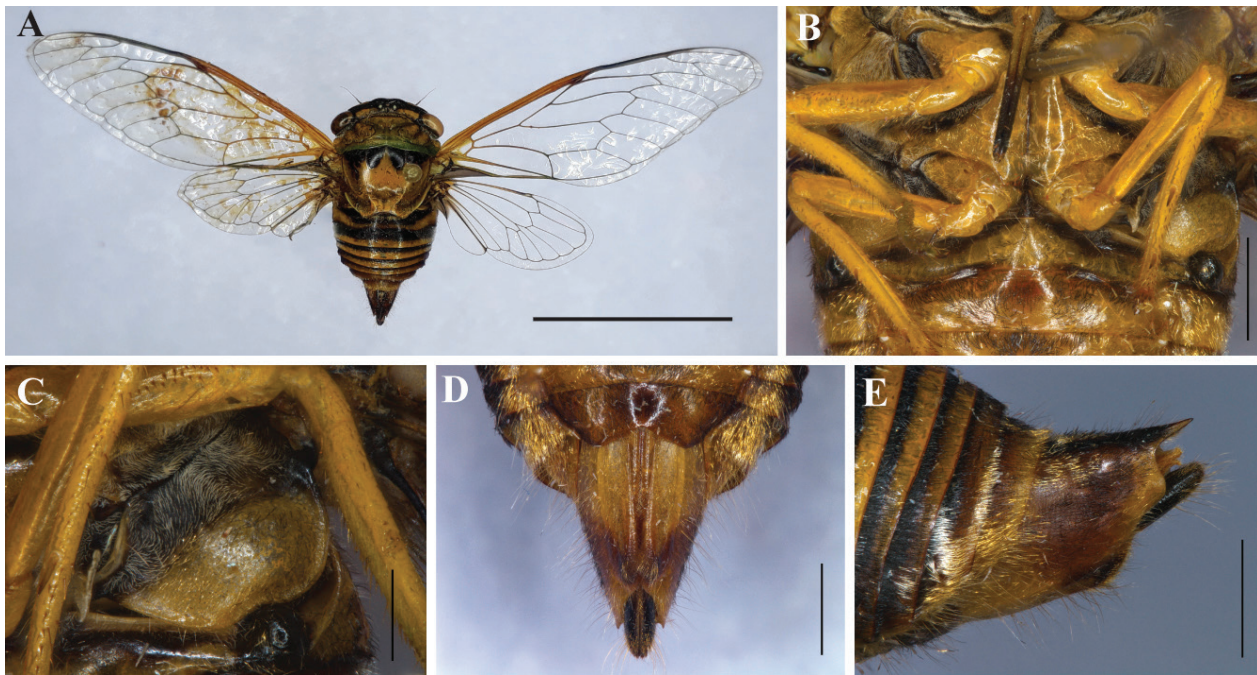


Figure 15. *Acanthoventris iara* sp. nov., paratype female. **A** Habitus in dorsal view; **B** Thorax in ventral view; **C** Operculum in latero-ventral view; **D** Sternite VII, abdominal segment 9 and ovipositor sheath in ventral view; **E** Tergites and abdominal segment 9 in lateral view. Scale bars: A = 1 cm; B, D, E = 2 mm; C = 1 mm.

sence of a black band departing the eyes in ventral view, and the lateral branches of uncus wider.

Color. Body tawny with head, thorax and abdomen marked with black; pronotal collar and wing groove olive-green.

Description. Head (Fig. 14B): with a transverse wide black band departing from each eye, covering the ocelli region and reaching the apex of postclypeus; anterior margin of head tightly concave; base of the eyes marked with black and with silver setae; antennae with a tawny scape, and the pedicel and flagellum dark castaneous; postclypeus (Fig. 14C) rounded in ventral view unmarked and with the longitudinal groove shallow; slightly salient in lateral view; apex slightly prominent in dorsal view relative to the supra-antennal plates; anteclypeus (Fig. 14C) black with a tawny carina; lorum black; rostrum with a tawny mentum; labium short, extending to the base of basisternum 3, marked with castaneous (Fig. 14D). Pronotum (Fig. 14B): pronotal collar olive-green. Mesonotum (Fig. 14A): submedian sigillae and lateral sigillae marked with black; scutal depression unmarked; wing groove olive-green; basisternum 3 (Fig. 14D) marked with dark castaneous anteriorly, with well-developed protuberances relative to the median insertion, posterior margin forming an acute angle; cruciform elevation not covering tergite 1; apex of the posterior projections obtuse; operculum (Fig. 14E) short, not covering the timbal cavity and the apex not reaching the auditory capsule; anteromedian margin marked with dark castaneous; lateral margin marked with black and convex, becoming slightly straight toward the apex; posterior margin slightly straight; gutter present from the lateral to the posterior margin; wings

hyaline (Fig. 14A). Abdomen (Fig. 14A) subcylindrical, the length equivalent to the combined length of the head and thorax; timbal cover (Fig. 14F) flat and broad (almost as wide as the base), the apex obtuse anteriorly directed, almost reaching the lateral metascutellar plates; middle third of anteromedial margin concave; ventral anterior margin tightly concave (away from the posterior margin of operculum); tergites: 1 totally marked with black, 2 almost totally marked with black, except the timbal covers; tergites 3 to 8 with the anterior margin marked with black; median projection marked with castaneous, only the middle tawny; edge of sternite II castaneous (Fig. 14D); sternite VII sub-rectangular, with the lateral margins convex becoming slightly straight toward the apex, posterior margin slightly emarginate. Uncus (Fig. 14H, I): lateral margin slightly emarginate. Uncus (Fig. 14H, I): lateral margin straight becoming slightly convex in the middle and straight toward the apex of ventral apophyses; uncal dorsal crest fused and dorsally projected; lateral branches of uncus undeveloped, convex bud-like, the internal margin slightly concave; ventral apophyses with the internal margin sub-rectangular; posterior margin sinuous forming an acute angle posteriorly directed. Pygofer (Fig. 14J) sub-cylindrical, the basal lobe very long nearly reaches the uncal dorsal crest. Theca (Fig. 14K–M) dorsally developed with a ventral thecal process; vesica internally and externally bearing the cornuti. — **Female (Fig. 15A–E):** The female presents the same somatic characteristics as the male (Fig. 15A) except the operculum (Fig. 15C) is smaller, sternite VII (Fig. 15D) longer with a slightly concave lateral margin and a sinuous posterior margin with an obtuse middle groove; the tip of the ovipositor with the same length of the dorsal beak of segment 9 (Fig. 15E); the ovipositor bears eight teeth.

Measurements (in millimeters). N = Holotype and paratypes (5 males and 2 females), mean (range). Length of body: male 19.22 (22.75–17.50), female 17.635 (17.64–17.63); width of head including eyes: male 8.698 (9.09–8.26); female 8.54 (8.64–8.44); length of the head: male 1.85 (1.62–1.97), female 1.575 (1.71–1.44); width of pronotum including pronotal collar: male 8.52 (8.90–7.82), female 8.28 (8.28–8.28); length of pronotum including pronotal collar: male 3.00 (2.72–3.26); female 2.835 (2.79–2.88); width of mesonotum: male 7.47 (6.80–7.88), female 7.065 (7.20–6.93); length of mesonotum: male 5.64 (5.94–5.10); female 5.49 (5.58–5.40); length of forewing: male 27.31 (28.80–25.38), female 26.385 (26.60–26.17); width of forewing: male 8.96 (9.73–8.00), female 9.095 (9.25–8.94); length of hindwings: male 12.98 (14.19–11.25), female 12.58 (12.90–12.26).

Distribution. Brazil (Roraima, Amazonas, Rondônia).

Acanthoventris igneus Ruschel sp. nov.

<http://zoobank.org/E80DAAD6-9B19-4ADB-88A9-1C9D3C-C4B077>

Fig. 16

Type locality. Alto Paraíso de Goiás, Goiás, Brazil.

Type material. Holotype: male (DZRJ) (Fig. 16A), Brasil, Goiás, Alto Paraíso de Goiás, córrego Rodoviarinha, S 14°10'04.2" W47° 49'15.9", el. 970 m, 26.iii.2013, colecta diurna, APM Santos & DM Takiya.

Genbank access number. OM937995 (COI); OP548616 (EF1-alpha).

Etymology. The specific name refers to the reddish color of species. Latin: ignis + arius, of fire.

Diagnosis. The species can be distinguished from all other species of *Acanthoventris* **gen. nov.** by the following combination of features: anterior margin of head tightly concave; labium long, reaching the sternite II; operculum slightly reddish, long, the apex reaching the auditory capsule but not covering fully the timbal cavity; the basal vein of the second apical cell of forewings straight; apical cell 2 of forewings half of length of apical cell 1; sternite VII sub-rectangular; the uncus lateral margin slightly sinuous becoming tightly convex in the line of lateral branches; the lateral branches of uncus undeveloped, convex bud-like and slender, with the internal margin tightly convex. This species has a similar morphology to *A. iara* **sp. nov.** due the anterior margin of head tightly concave and lateral margin of operculum marked with black and convex. *Acanthoventris igneus* **sp. nov.** can be distinguished by the presence of a black band departing the eyes in ventral view, and the lateral branches of uncus slender.

Color. Body castaneous marked with black and with pronotal collar and sternum tawny, operculum slightly reddish.

Description. Head (Fig. 16B): with a transverse black band departing from each eye, extending through the area of the ocelli to the ambient fissure and the apex of postclypeus; base of the eyes marked with black and with pilus setae; anterior margin of head tightly concave; antennae with a tawny scape, and the pedicel black (flagellum is missing); postclypeus (Fig. 16C) unmarked, oval in ventral view, and flat in lateral view, the apex slightly prominent in dorsal view relative to the supra-antennal plate; longitudinal groove slender and shallow; anteclypeus black and carina tawny, lorum black; mentum and labium tawny; labium long, reaching the sternite II, black at the apex. Pronotum (Fig. 16B): with lateral and sub-lateral lobes with wrinkles black setae; ambient fissure with a black band in the middle; pronotal collar tawny with black setae. Mesonotum (Fig. 16A): submedian and lateral sigillae and scutal depression marked with black; a rhomb black band present between the sigillae; basisternum 3 (Fig. 16D) with well developed protuberances relative to the median insertion, closely spaced; posterior margin forming an obtuse angle; cruciform elevation not covering tergite 1; apex of the posterior projections of the cruciform elevation obtuse; operculum (Fig. 16E) slightly reddish, obtuse and long, the apex reaching the auditory capsule but not covering the timbal cavity, the internal angles very short, the apex obtuse and widely spaced, anteromedian margin concave anteriorly to the internal angles, the lateral margin convex and marked with black, posterior margin slightly straight; meracanthus reaches the posterior margin, gutter present in all margins; legs tawny; wings hyaline (Fig. 16A); forewings: basal cell opaque anteriorly, and the basal vein of the second apical cell straight; apical cell 2 half of length of apical cell 1; hindwings: radius vein straight. Abdomen subcylindrical, the length equivalent to the combined length of the head and thorax in dorsal view (Fig. 16A); timbal cover (Fig. 16F) flat and short, the apex obtuse almost reaching the lateral metascutellar plate, middle third of anteromedial margin concave, ventral anterior margin tightly concave (away from the posterior margin of operculum); tergites 2 to 7 with setae and marked with black in anterior margins; sternite VII (Fig. 16G) sub-rectangular, the lateral margin convex becoming slightly straight toward the apex, the posterior margin slightly emarginate. Uncus (Fig. 16H, I): lateral margin slightly sinuous becoming tightly convex in the line of lateral branches; lateral branches of uncus undeveloped, convex bud-like and slender, the internal margin tightly convex; ventral apophyses with the internal margin forming a sub-rectangular lobe distally directed, posterior margin slightly straight forming an acute angled laterally. Pygofer (Fig. 16J) sub-cylindrical; the basal lobe reaching the lateral branches of uncus. Theca (Fig. 16K–M) dorsally developed with a ventral thecal process; vesica originates in a fissure at the distal third of the theca extruded and adorned with cornuti in the inner and outer surfaces. — **Female:** Unknown.

Measurements (in millimeters). Holotype male. Length of body: 16.90; width of head including eyes: 7.62; length of the head: 1.89; width of pronotum including pronotal collar: 7.65; length of pronotum including pronotal collar: 2.61; width of mesonotum: 6.66; length of mesonotum: 4.95; length of forewing: 24.21; width of forewing: 8.43; length of hind wings: 11.82.

Distribution. Brazil (Goiás).

***Acanthoventris jauffreti* (Boulard & Martinelli, 2011) comb. nov.**

Guyalna jauffreti Boulard & Martinelli, 2011: 225–226.

Type locality. French Guiana.

Type material. Holotype male, allotype female, paratypes 1 male and 1 female (MNHN). Guyane française, Territoire de l'Itani, île fluviale de Touenké, le 19–21/XI/1975, Mission Michel Boulard, Pierre Jauffret et Pierre Pompanon. Muséum National d'Histoire Naturelle, Entomologie, Paris. (Boulard & Martinelli, 2001).

Diagnosis. The species can be distinguished from all other species of *Acanthoventris* **gen. nov.** by the following combination of features: anterior margin of head slightly convex; labium short, reaching the base of basisternum 3; tumid timbal cover. This species has a similar morphology to *A. tumidus* **sp. nov.** comb. nov. due the tumid timbal cover, but *A. jauffreti* comb. nov. can be distinguished by the concave medial margin of the timbal cover, and the apex of the basal lobe reaching the uncal dorsal crest.

Color. Body ochre marked with green and black.

Description complement. Head: with a transverse wide black band extended over the vertex, covering the region of ocellus and reaches the apex of the postclypeus; base of eyes marked with black; anterior margin of head slightly convex; postclypeus unmarked, oval in ventral view, the apex not prominent in dorsal view relative to the supra-antennal plates; anteclypeus and carina tawny; lorum black; rostrum with a tawny mentum and labium; labium short, reaching the base of basisternum 3, black at the apex. Pronotum: paranota visible in dorsal view, wide, not reaching the eyes in dorsal view, and straight in lateral view. Mesonotum: submedian sigillae marked with black laterally; basisternum 3 with very developed protuberances relative to the median insertion, closely spaced forming an acute angle; posterior margin angled; cruciform elevation not covering tergite 1; apex of the posterior projections of the cruciform elevation obtuse; operculum obtuse; wings hyaline; forewings: basal vein of the second apical cell oblique; hindwings: radius vein straight. Abdomen subcylindrical, the length is equivalent to the combined length of the head and thorax in dorsal view; timbal cover tumid, middle third of anteromedial margin concave; tergites 2 to 8 marked with black ante-

riorly; sternite VII sub-rectangular. Pygofer sub-cylindrical; the basal lobe long, reaching the uncal dorsal crest.

Female. The female presents the same somatic characteristics as the male.

Measurements (in millimeters). Holotype male and allotype female. Length of body: 24.3 and (missing); fore body length: 10.12 and 9.75; abdomen length: 11.5 and 10; width of head including eyes: 9 and 9.37; width of mesonotum: 7.5 and 7.5; wingspan: 63 and 64; total length including wings: 32 and 33; length of forewings: 28 and 28.5; width of forewings: 9 and 9.1 (Boulard and Martinelli 2011).

Material examined. Photographs of original manuscript.

Distribution. French Guiana.

***Acanthoventris olivarius* Ruschel sp. nov.**

<http://zoobank.org/90D76BA0-4B18-4893-ACF1-0CDD4DC40007>

Fig. 17

Type locality. Londrina, Paraná, Brazil.

Type material. Holotype: Male (DZUP) (Fig. 17A), Londrina-PR, Café – campo, 14.I.00, Menequim, A.M., DZUP 362268. — **Paratypes** (4 males): Male (DZUP), Mandaguari-PR, Café-campo, 24.II.00, Menequim, A.M., DZUP 362269; 2 males (DZUP) Rib. do Pinhal-PR, Café-campo, 08.II.00, Menequim, A.M., DZUP / 362270, 362271"; male (DZUP) Paranavaí-PR, Café-campo, 30.III.00, Menequim, A.M., DZUP 362272.

Genbank access number. OP548610 (EF1-alpha).

Etymology. The specific name refers to the olive green color of the species. Latin: oliva, olive.

Diagnosis. The species can be distinguished from all other species of *Acanthoventris* **gen. nov.** by the following combination of features: body green; anterior margin of head tightly concave; apex of postclypeus slightly prominent in dorsal view relative to the anterior margin of head; timbal cover wide, almost covering the timbal cavity; sternite VII sub-rectangular; posterior margin of ventral apophyses forming a turned-back rim sclerotized and an acute angle posteriorly directed. This species has a similar morphology to *A. iara* **sp. nov.** due the anterior margin of head tightly concave, but can be distinguished by the operculum covering the timbal cavity and the apex reaching the auditory capsule, and by the diagnostic characters referred above.

Color. Body green with head, thorax and abdomen marked with black.

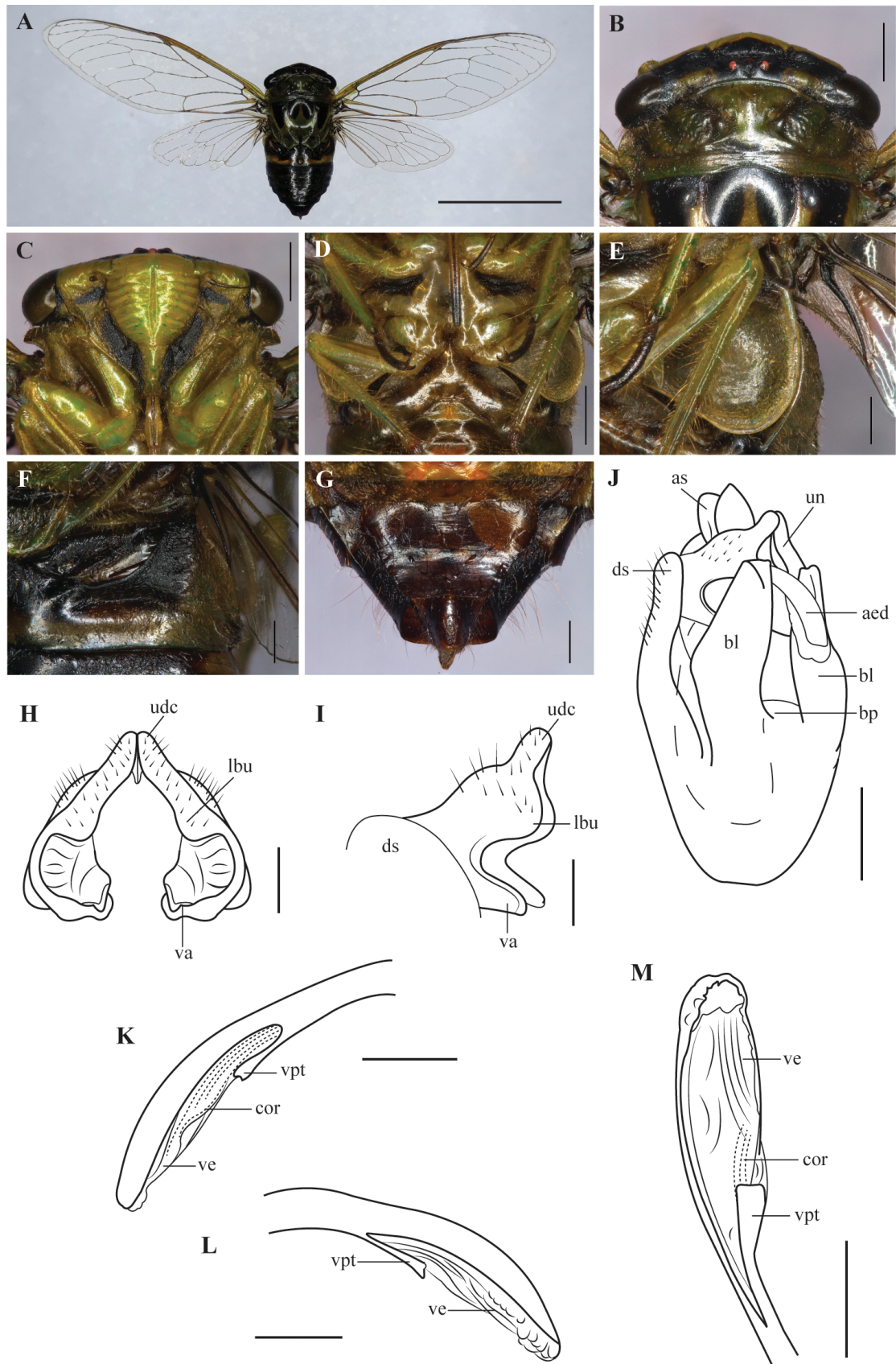


Figure 17. *Acanthoventris olivarius* sp. nov., holotype male. **A** Habitus in dorsal view; **B** Head and pronotum in dorsal view; **C** Head and pronotum in ventral view; **D** Thorax in ventral view; **E** Operculum in latero-ventral view; **F** Timbal cover in dorso-lateral view; **G** Sternite VII in ventral view; **H** Uncus in ventral view; **I** Uncus in lateral view; **J** Pygofer in latero-ventral view; **K** Aedeagus in left lateral view; **L** Aedeagus in right lateral view; **M** Aedeagus in latero-ventral view. Scale bars: A = 1 cm; B–D = 2 mm; E–G, J = 1 mm; H, I, K–M = 0.5 mm. Abbreviations: (aed) aedeagus; (as) anal styles; (at) anal tube; (bl) basal lobe of pygofer; (bp) basal plate; (cor) cornuti; (ds) distal shoulder; (lbu) lateral branch of uncus; (udc) uncal dorsal crest; (un) uncus; (va) ventral apophysis; (ve) vesica; (vpt) ventral thecal process.

Description. Head (Fig. 17B): with a transverse wide black band departing from each eye, covering the posterior margin of eyes and the ocelli, reaching the apex of the postclypeus; silver setae in the posterior margin of eyes; anterior margin of head tightly concave; antenna with a green scape, pedicel and flagellum dark castaneous; anterior margin of head slightly convex; postclypeus (Fig. 17C) unmarked and oval in ventral view, flat in lateral view, the apex slightly prominent in dorsal view relative to the anterior margin of head, longitudinal groove slender and shallow; anteclypeus black and carina green; lorum black; mentum green; labium short, reaching the base of basisternum 3 (Fig. 17D). Pronotum (Fig. 17B): pronotal collar green with pilus silver setae. Mesonotum (Fig. 18A): submedian, lateral sigillae and scutal depression marked with black; basisternum 3 (Fig. 17D) with well-developed protuberances relative to the median insertion, slightly salient; posterior margin tightly angled; cruciform elevation not covering tergite 1; apex of the posterior projections obtuse; operculum (Fig. 17E) obtuse and long, covering the timbal cavity and the apex reaching the auditory capsule, the internal angles very short, the apex obtuse and widely spaced, anteromedian margin concave anteriorly to the internal angle and marked with black, lateral margin convex, the posterior margin slightly straight; meracanthus reaches the posterior margin; gutter present in all margins; legs green marked with olive-green; wings hyaline; forewings: anterior portion of the basal cell slightly opaque; hindwings: radius vein straight. Abdomen (Fig. 17A) subcylindrical, the length equivalent to the combined length of the head and thorax in dorsal view; timbal cover (Fig. 17F) flat and wide, almost covering the timbal cavity, apex obtuse reaching the lateral metascutellar plate; middle third of anteromedial margin concave, ventral anterior margin tightly concave (away from the posterior margin of operculum); tergites 3 to 7 green with the anterior margin marked with black; sternite VII (Fig. 17G) sub-rectangular, the lateral margin convex becoming straight toward the apex, the posterior margin slightly emarginate. Uncus (Fig. 17H, I): lateral margin slightly sinuous becoming convex in the ventral apophyses; uncal dorsal crest fused and dorsally projected; lateral branches of uncus undeveloped, convex bud-like, the internal margin slightly straight; ventral apophyses grooved, ventrally developed originating from below the lateral branches of uncus, internal margin forming a sub-rectangular distally directed; posterior margin forming a turned-back rim sclerotized and an acute angle posteriorly directed. Pygofer (Fig. 17J) sub-cylindrical; the basal lobe long, reaching the lateral branches of uncus. Theca (Fig. 17K–M) dorsally developed with a ventral thecal process; vesica originates in a fissure at the distal third of the theca, extruded and ornamented with cornuti in both the inner and outer surfaces; spine present on the vesica. — **Female:** Unknown.

Measurements (in millimeters). Holotype male: Length of body: 19.25; width of head including eyes: 8.84; length of the head: 2.00; width of pronotum including pronotal collar: 8.70 length of pronotum including pronotal collar: 3.20; width of mesonotum: 7.44; length of mesonotum:

5.68; length of forewing: 28.28; width of forewing: 9.80; length of hind wings: 14.10. Paratypes (4 males): Length of body: 19.53 (20.78–18.73); width of head including eyes: 8.83 (9.12–8.56); length of the head: 1.76 (2.00–1.60); width of pronotum including pronotal collar: 8.62 (9.00–8.30); length of pronotum including pronotal collar: 3.18 (3.36–3.04); width of mesonotum: 7.26 (7.44–7.04); length of mesonotum: 5.70 (6.00–5.36); length of forewing: 26.27 (three paratypes are without the forewings); width of forewing: 9.43; length of hind wings: 14.92 (16.87–13.12).

Distribution. Brazil (Paraná).

Acanthoventris phoenix Ruschel sp. nov.

<http://zoobank.org/5EC1785C-FF4E-49E6-8495-DA3330A9F-6CA>

Fig. 18

Type locality. Magé, Rio de Janeiro, Brazil.

Type material. Holotype: Male (MNRJ) (Fig. 18A), Barreiras, Magé, E. do Rio, 24-I-58, D.Z. 67/60, J. Oiticica e R. Barros cols. — **Paratype:** Male (MNRJ) same data as holotype.

Etymology. The specific name refers to the immortal bird of Greek mythology which obtains new life by arising from the ashes. The specimens designated as holotype and paratype were received by the first author before the Museu Nacional (Rio de Janeiro, Brazil) fire in 2018. The name is in honor of this important museum that we hope arises from the ashes like a phoenix. Latin: phoenix, symbolic of resurrection and immortality.

Diagnosis. The species can be distinguished from all other species of *Acanthoventris* **gen. nov.** by the following combination of features: body orange; anterior margin of head slightly convex; labium short, almost reaching the base of basisternum 3; operculum obtuse and long, covering the timbal cavity and the auditory capsule; timbal cover flat and long, the apex acute, almost reaching the lateral metascutellar plate; tergites 2 to 7 with pilus setae in both lateral margins; the anterior margin of ventral thecal process with a slender projection. This species has a similar morphology to *A. densus* comb. nov. due the tergites with pilus setae in both lateral margins, and *A. charrua* sp. nov. due the body color and bands. *A. phoenix* sp. nov. can be distinguished by the posterior margin of ventral apophyses convex with an acute-angled laterally and posteriorly developed.

Color. Body orange with head, thorax and abdomen marked with black.

Description. Head (Fig. 18B): with a transverse black band departing from each eye, extending through the

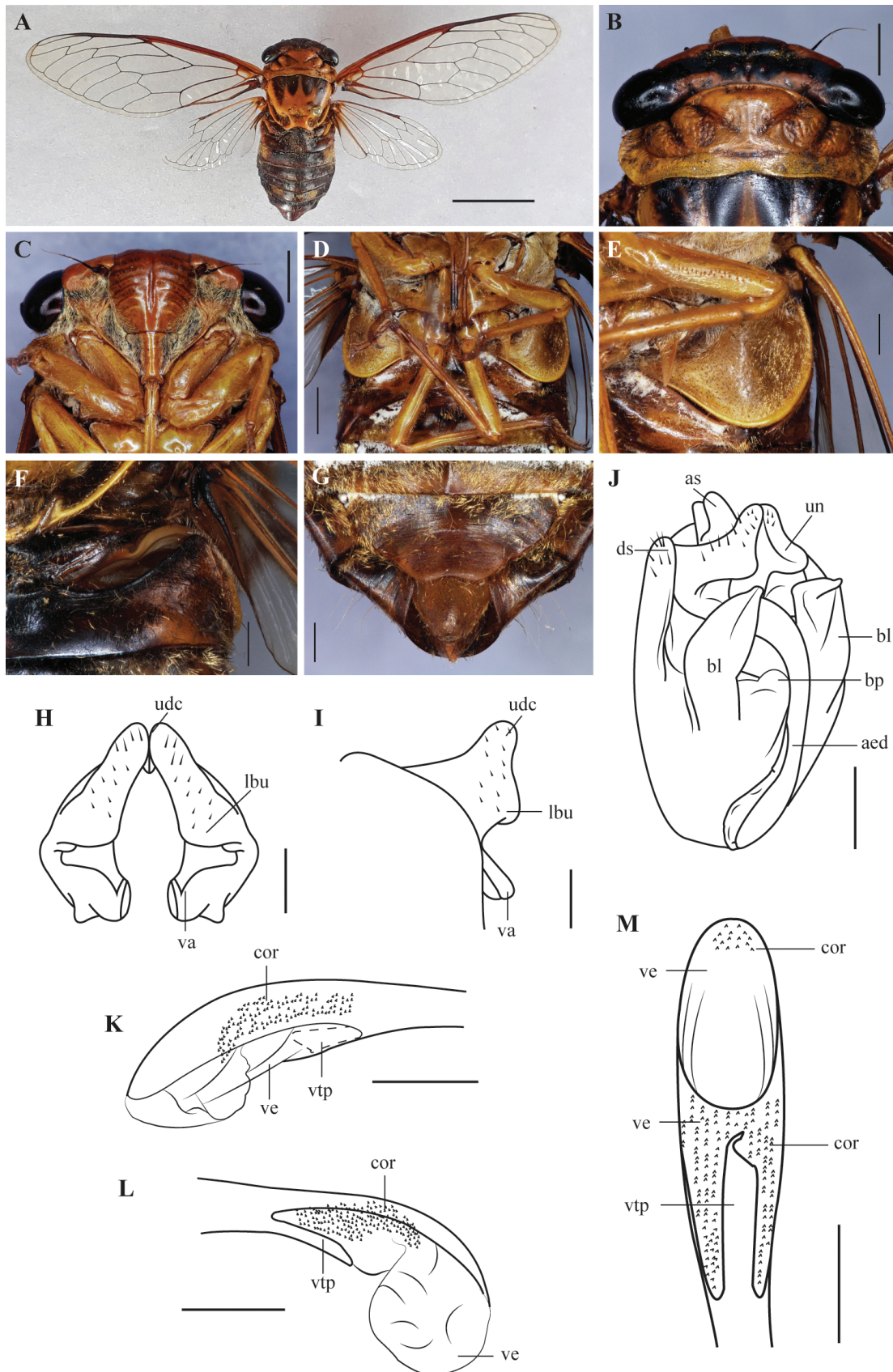


Figure 18. *Acanthoventris phoenix* sp. nov., holotype male. **A** Habitus in dorsal view; **B** Head and pronotum in dorsal view; **C** Head and pronotum in ventral view; **D** Thorax in ventral view; **E** Operculum in latero-ventral view; **F** Timbal cover in dorso-lateral view; **G** Sternite VII in ventral view; **H** Uncus in ventral view; **I** Uncus in lateral view; **J** Pygofer in latero-ventral view; **K** Aedeagus in left lateral view; **L** Aedeagus in right lateral view; **M** Aedeagus in ventral view. Scale bars: A = 1 cm; B–D = 2 mm; E–G, J = 1 mm; H, I, K–M = 0.5 mm. Abbreviations: (aed) aedeagus; (as) anal styles; (at) anal tube; (bl) basal lobe of pygofer; (bp) basal plate; (cor) cornuti; (ds) distal shoulder; (lbu) lateral branch of uncus; (udc) uncal dorsal crest; (un) uncus; (va) ventral apophysis; (ve) vesica; (vtp) ventral thecal process.

area of the ocelli to the limit between the vertex and front; base of the eyes marked with black; anterior margin of head slightly convex; antennae with a orange scape, and the pedicel and flagellum black; postclypeus (Fig. 18C) unmarked, oval in ventral view, and flat in lateral view, the apex not prominent in dorsal view relative to the supra-antennal plate; longitudinal groove slender and shallow; anteclypeus black and carina tawny, lorum black; mentum tawny; labium short, almost reaching the base of basisternum 3, black at the apex. Pronotum (Fig. 18B): slightly marked with black in lateral fissures with setae; paranota tawny with black setae. Mesonotum (Fig. 18B): submedian and lateral sigillae and scutal depression marked with black; basisternum 3 (Fig. 18D) with developed protuberances relative to the median insertion, closely spaced; posterior margin forming an obtuse angle; cruciform elevation not covering tergite 1; apex of the posterior projections of the cruciform elevation obtuse; operculum (Fig. 18E) obtuse and long, covering the timbal cavity and the auditory capsule, the internal angles very short, the apex obtuse and widely spaced, anteromedian margin concave anteriorly to the internal angles and marked with black, the lateral margin concave, posterior margin slightly straight; meracanthus reaches the posterior margin, gutter present in all margins; legs tawny becoming castaneus distally; wings hyaline (Fig. 18A); forewings: basal cell opaque anteriorly, and the basal vein of the second apical cell oblique; apical cell 2 almost half of length of apical cell 1; hindwings: radius vein straight. Abdomen subcylindrical, the length equivalent to the combined length of the head and thorax in dorsal view (Fig. 18A); timbal cover (Fig. 18F) flat and long, the apex acute, almost reaching the lateral metascutellar plate, middle third of anteromedial margin concave, ventral anterior margin slightly concave (near the posterior margin of the operculum); tergites 2 to 7 with pilus setae in both lateral margins; sternite VII (Fig. 18G) sub-triangular, the lateral margin convex becoming slightly concave toward the apex, the posterior margin slightly emarginate. Uncus (Fig. 18H, I): lateral margin slightly sinuous becoming tightly convex in the ventral apophyses; lateral branches of uncus undeveloped, convex bud-like, the internal margin slightly straight; ventral apophyses ventrally developed originating from below the lateral branches of uncus; internal margin forming a sub-rectangular distally directed, posterior margin convex with an acute-angled laterally and posteriorly developed. Pygofer (Fig. 18J) sub-cylindrical; the basal lobe almost reaches the lateral branches of the uncus. Theca (Fig. 18K–M) dorsally developed with a ventral thecal process; anterior margin of ventral thecal process with a slender projection; vesica originates in a fissure at the distal third of the theca extruded and adorned with cornuti in the inner and outer surfaces. — **Female.** Unknown.

Measurements (in millimeters). Holotype male. Length of body: 22.60; width of head including eyes: 9.90; length of the head: 2.07; width of pronotum including pronotal collar: 9.72; length of pronotum including pronotal collar:

3.15; width of mesonotum: 8.28; length of mesonotum: 6.48; length of forewing: 29.62; width of forewing: 9.86; length of hind wings: 14.07. Paratype male. Length of body: 22.13; width of head including eyes: 10.41; length of the head: 2.25; width of pronotum including pronotal collar: 10.12; length of pronotum including pronotal collar: 3.37; width of mesonotum: 8.37; length of mesonotum: 6.61; length of forewing: 31.44; width of forewing: 11.04; length of hind wings: 15.15.

Distribution. Brazil (Rio de Janeiro).

Acanthoventris rubemi Ruschel sp. nov.

<http://zoobank.org/D743933F-FD02-4D5F-AEF2-B60465E9EE54>

Fig. 19

Type locality. Serro, Minas Geras, Brazil.

Type material. Holotype: male (MCTP) (Fig. 19A), Serro – MG – Brasil, III-26-1976, Col. D. Kneip, *Dorisiana drewseni*. — **Paratypes** (2 males): (MCTP) same data as holotype.

Etymology. The species is named in honor to the father of the first author, Claudio Rubem Sassen Ruschel.

Diagnosis. The species can be distinguished from all other species of *Acanthoventris* **gen. nov.** by the following combination of features: anterior margin of head slightly convex; lateral and sub-lateral lobes of pronotum with wrinkles and black setae; posterior margin of basisternum 3 tightly acute; apex of operculum reaching the auditory capsule but not covering the timbal cavity; gutter of operculum broad present in all margins; apical cell 2 half of length of apical cell 1; timbal cover short, the apex acute not reaching the lateral metascutellar plate; sternite VII sub-triangular. This species has a similar morphology to *A. charrua* **sp. nov.** due the body color and bands. *A. rubemi* **sp. nov.** can be distinguished by the timbal cover shorter, the operculum slightly shorter, not covering the auditory capsule, the gutter at apex of the operculum broad, and the basal lobe of pygofer longer.

Color. Body tawny with the head, thorax and abdomen marked with black.

Description. Head (Fig. 19B): with a transverse black band departing from each eye, extending through the area of the ocelli to the apex of postclypeus; base of the eyes marked with black with silver setae; anterior margin of head slightly convex; antennae with a tawny scape, and the pedicel and flagellum black; postclypeus (Fig. 19C) unmarked, oval in ventral view, and flat in lateral view, the apex slightly prominent in dorsal view relative to the supra-antennal plate; longitudinal groove slender and shallow; anteclypeus and carina tawny, lorum black;

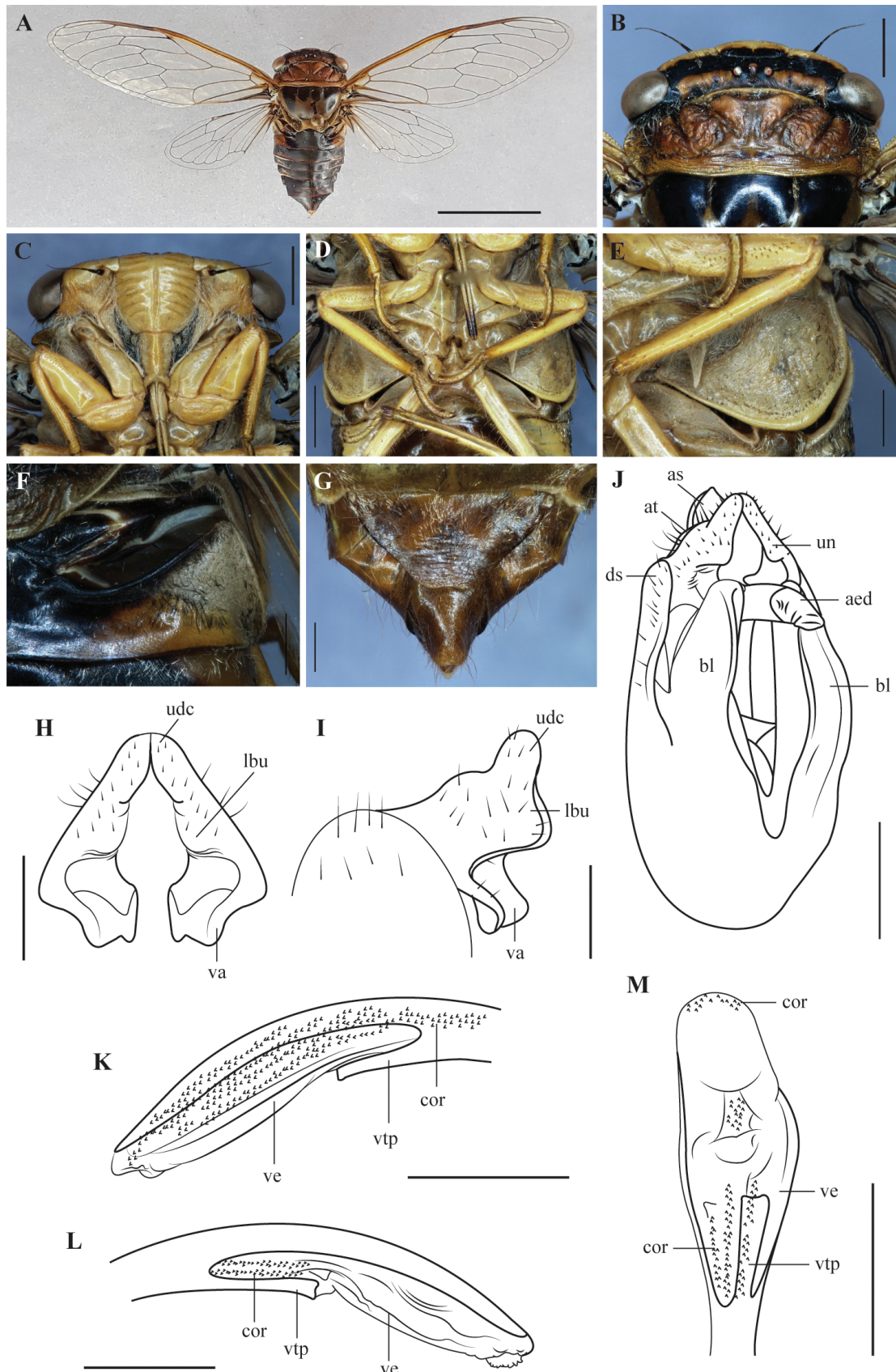


Figure 19. *Acanthoventris rubemi* sp. nov., holotype male. **A** Habitus in dorsal view; **B** Head and pronotum in dorsal view; **C** Head and pronotum in ventral view; **D** Thorax in ventral view; **E** Operculum in latero-ventral view; **F** Timbal cover in dorso-lateral view; **G** Sternite VII in ventral view; **H** Uncus in ventral view; **I** Uncus in lateral view; **J** Pygofer in latero-ventral view; **K** Aedeagus in left lateral view; **L** Aedeagus in right lateral view; **M** Aedeagus in ventral view. Scale bars: A = 1 cm; B–D = 2 mm; E–G, J = 1 mm; H, I, K–M = 0.5 mm. Abbreviations: (aed) aedeagus; (as) anal styles; (at) anal tube; (bl) basal lobe of pygofer; (bp) basal plate; (cor) cornuti; (ds) distal shoulder; (lbu) lateral branch of uncus; (udc) uncal dorsal crest; (un) uncus; (va) ventral apophysis; (ve) vesica; (vtp) ventral thecal process.

mentum and labium tawny; labium short, reaching the base of basisternum 3, black at the apex. Pronotum (Fig. 19B): with lateral and sub-lateral lobes with wrinkles and black setae; slightly marked with black in lateral fissures; paranota tawny with black setae. Mesonotum (Fig. 19A): submedian and lateral sigillae marked with black; scutal depression unmarked; basisternum 3 (Fig. 19D) with well developed protuberances relative to the median insertion, closely spaced; posterior margin tightly angled; cruciform elevation not covering tergite 1; apex of the posterior projections of the cruciform elevation obtuse; operculum (Fig. 19E) unmarked, obtuse, the apex reaching the auditory capsule but not covering the timbal cavity, the internal angles very short, the apex obtuse and widely spaced, anteromedian margin concave anteriorly to the internal angles, the lateral margin convex, posterior margin slightly straight; meracanthus reaches the posterior margin, gutter broad present in all margins; legs tawny becoming castaneus distally; wings hyaline (Fig. 19A); forewings: basal cell opaque anteriorly, and the basal vein of the second apical cell oblique; apical cell 2 half of length of apical cell 1; hindwings: radius vein straight. Abdomen subcylindrical, the length equivalent to the combined length of the head and thorax in dorsal view (Fig. 19A); timbal cover (Fig. 19F) flat and short, the apex acute not reaching the lateral metascutellar plate, middle third of anteromedial margin concave, ventral anterior margin tightly concave (away from the posterior margin of operculum); tergites 2 marked with black at middle, 3 to 8 marked with black anteriorly; sternite VII (Fig. 19G) sub-triangular, the lateral margin slightly convex becoming slightly straight toward the apex, the posterior margin slightly emarginate. Uncus (Fig. 19H, I): lateral margin of uncus slightly straight becoming tightly convex in the ventral apophyses; lateral branches of uncus undeveloped, convex bud-like, the internal margin sinuous; ventral apophyses ventrally developed originating from below the lateral branches of uncus; internal margin forming a sub-rectangular distally directed, posterior margin convex with an acute angled distally, and posteriorly developed. Pygofer (Fig. 19J) sub-cylindrical; the basal lobe reaching the ventral apophyses. Theca (Fig. 19K–M) dorsally developed with a ventral thecal process; anterior margin of ventral sclerotized expansion with a slender projection; vesica originates in a fissure at the distal third of the theca extruded and adorned with cornuti in the inner and outer surfaces. — **Female:** Unknown.

Measurements (in millimeters). Holotype male. Length of body: 17.06; width of head including eyes: 7.46; length of the head: 2.00; width of pronotum including pronotal collar: 7.76; length of pronotum including pronotal collar: 2.56; width of mesonotum: 6.72; length of mesonotum: 4.88; length of forewing: 23.35; width of forewing: 8.31; length of hind wings: 12.57. Paratypes (2 males). Length of body: 16.05 (15.36–16.75); width of head including eyes: 7.65, 7.71; length of the head: 1.60, 1.84; width of pronotum including pronotal collar: 7.655 (7.12–7.52); length of pronotum including pronotal collar: 3.23 (3.90–

2.56); width of mesonotum: 6.00 (5.60–6.40); length of mesonotum: 4.36 (4.16–4.56); length of forewing: 22.55 (22.00–23.11); width of forewing: 7.39 (7.22–7.56); length of hind wings: 11.78 (11.10–12.46).

Distribution. Brazil (Minas Gerais).

Acanthoventris tumidus Ruschel sp. nov.

<http://zoobank.org/805360B3-970A-4889-8AC2-1C9B-C90D0269>

Figs 20, 21

Type locality. Cusco, Peru.

Type material. Holotype: Male (Fig. 20A) (MUSM), Peru, Cusco, 3 rd km E Quincemil, 13°13'03"S, 70°43'40"W, 633 m, 20.VIII.2012, Santos, A.P.M. & Takiya, D.M. — **Paratypes** (male and female): male same data as holotype (DZRJ); female (Fig. 21A), (MUSM) Peru, Madre de Dios, 12 rd km E Mazuko, pte. Amanapu, 13°02'51 1"S 70°20'45 9"W, 382 m, 18.VIII.2012, Santos, A.P.M. & Takiya, D.M.

Genbank access number. OP548617 (EF1-alpha).

Etymology. The specific name refers to the timbal cover tumid. Latin: tumidus, swollen.

Diagnosis. The species can be distinguished from all other species of *Acanthoventris* **gen. nov.** by the following combination of features: longitudinal groove of the postclypeus very shallow; posterior margin of basisternum 3 angled with a pair of posterior projections present near the insertion; operculum triangular, very short (not completely covering the timbal cavity), the anteromedian margin inclined; tumid timbal cover. This species has a similar morphology to *A. jauffreti* comb. nov. due the tumid timbal cover, but *A. tumidus* **sp. nov.** can be distinguished by the convex medial margin of timbal cover, and the apex of the basal lobe reaching the apex of ventral apophyses.

Color. Body green and castaneous marked with black.

Description. Head (Fig. 20B) with a wide black band through to the supra-antennal plates extending to the margin between the vertex and the apex of the postclypeus; anterior margin of head slightly convex; posterior margin of eyes marked with black; antennae with a tawny scape, and the pedicel tawny basally, becoming dark castaneous apically, flagellum dark castaneous; postclypeus (Fig. 20C) unmarked, oval in ventral view and flat in lateral view, the apex not prominent in dorsal view relative to the supra-antennal plates; longitudinal groove very shallow; anteclypeus and carina tawny; lorum tawny with a black band in the proximal margin; rostrum tawny; labium short, reaching the base of basisternum 3, black at

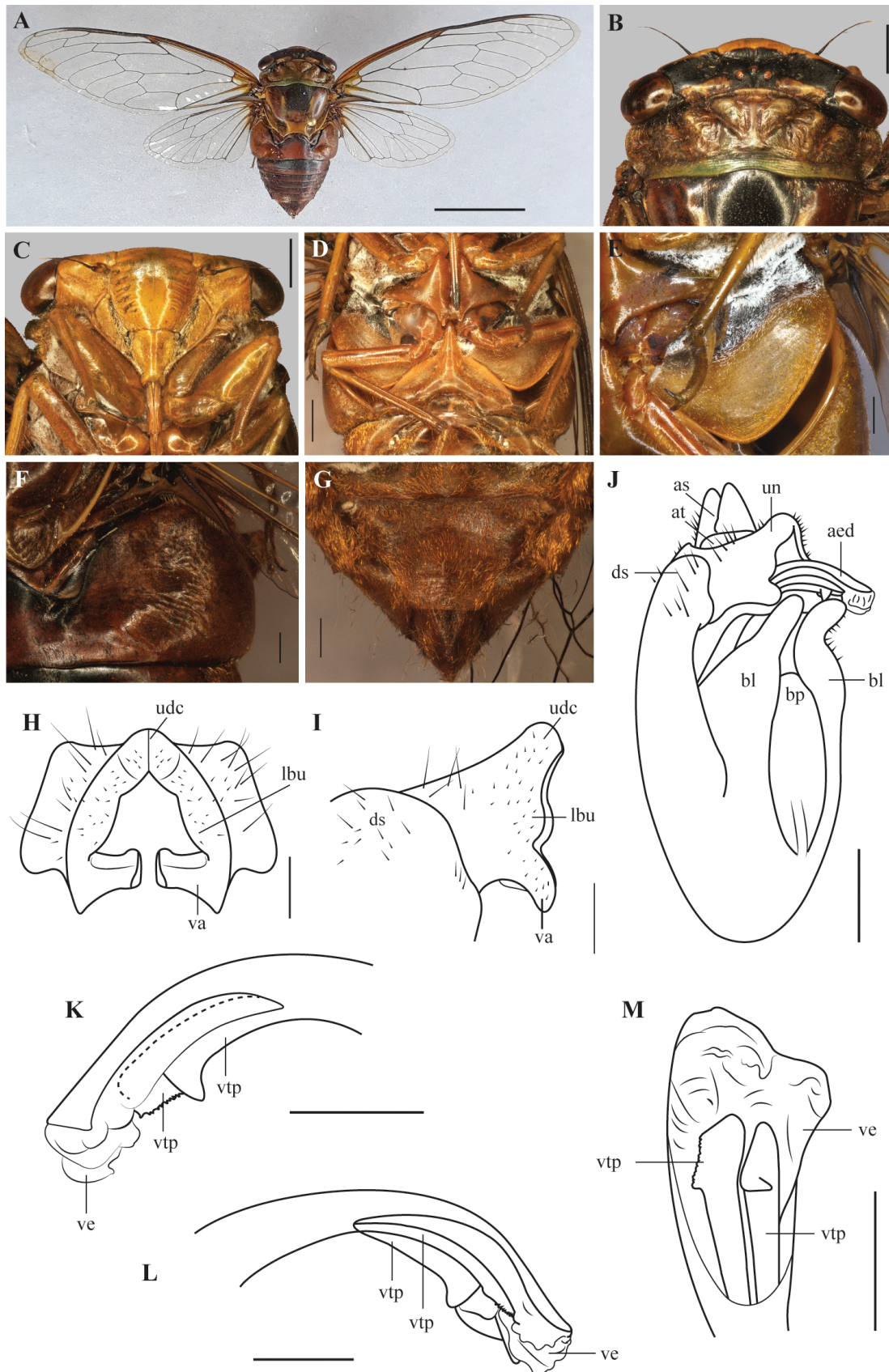


Figure 20. *Acanthoventris tumidus* sp. nov., holotype male. **A** Habitus in dorsal view; **B** Head and pronotum in dorsal view; **C** Head and pronotum in ventral view; **D** Thorax in ventral view; **E** Operculum in latero-ventral view; **F** Timbal cover in dorso-lateral view; **G** Sternite VII in ventral view; **H** Uncus in ventral view; **I** Uncus in lateral view; **J** Pygofer in latero-ventral view; **K** Aedeagus in left lateral view; **L** Aedeagus in right lateral view; **M** Aedeagus in ventral view. Scale bars: A = 1 cm; B–D = 2 mm; E–G, J = 1 mm; H, I, K–M = 0.5 mm. Abbreviations: (aed) aedeagus; (as) anal styles; (at) anal tube; (bl) basal lobe of pygofer; (bp) basal plate; (cor) cornuti; (ds) distal shoulder; (lbu) lateral branch of uncus; (udc) uncal dorsal crest; (un) uncus; (va) ventral apophysis; (ve) vesica; (vtp) ventral thecal process.

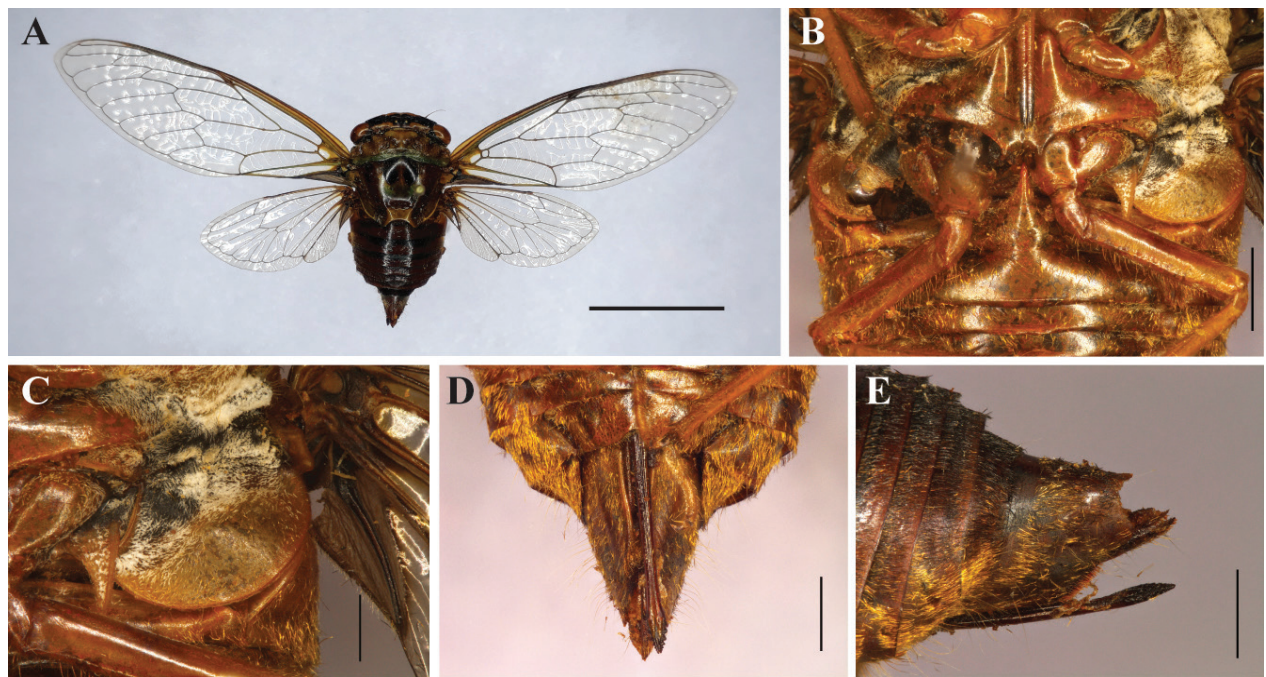


Figure 21. *Acanthoventris tumidus* sp. nov., paratype female. **A** Habitus in dorsal view; **B** Thorax in ventral view; **C** Operculum in latero-ventral view; **D** Sternite VII, abdominal segment 9 and ovipositor sheath in ventral view; **E** Tergites and abdominal segment 9 in lateral view. Scale bars: A = 1 cm; B, D, E = 2 mm; C = 1 mm.

the apex. Pronotum (Fig. 20B): fissure of the pronotum marked in black; ambient fissure with an inconspicuous black band in the middle; paranota visible and wide, not reaching the eyes in dorsal view. Mesonotum (Fig. 20A): submedian sigillae marked with black (in the holotype, the bands occupy the space between and posterior to the sigillae); lateral sigillae with a castaneous band; base of mesonotum with a castaneous band extending to the lateral area of the cruciform elevation; cruciform elevation not covering tergite 1; apex of the posterior projections of the cruciform elevation obtuse; scutal depression with a black band; basisternum 3 (Fig. 20D) with well-developed protuberances relative to the median insertion and with a black band laterally, the posterior margin angled, a pair of posterior projections present near the insertion; operculum (Fig. 20E) triangular, very short, not covering the timbal cavity and the apex does not reach the auditory capsule, the internal angles wide and short, the apices obtuse and widely spaced; anteromedian margin inclined with a black band extending to the anterior margin of the meracanthus, the lateral margin concave, becoming straight posteriorly and longer than the posterior margin, the posterior margin almost straight; meracanthus does not reach the posterior margin; gutter present in all margins; legs tawny; wings hyaline, forewings: basal vein of the second apical cell oblique; hindwings: radius vein arched. Abdomen (Fig. 20A) subcylindrical, the length equivalent to the combined length of the head and thorax in dorsal view; timbal cover (Fig. 20F) tumid, middle third of anteromedial margin convex; tergites 2 to 8 with a stain in black anteriorly; sternite VII (Fig. 20G) sub-rectangular, the lateral margin concave, becoming convex apically, the posterior margin linear, not emarginate. Uncus (Fig. 20H, I): lateral margin slightly convex;

lateral branches of uncus undeveloped, convex bud-like, the internal margin convex; ventral apophyses ventrally developed originating from below the lateral branches of uncus; internal margin forming a sub-rectangular distally directed, posterior margin tightly acute. Pygofer (Fig. 20J) sub-cylindrical; basal lobe long, reaching the apex of ventral apophyses, narrowing towards the rounded apex. Theca (Fig. 20K–M) dorsally developed with two ventral thecal processes: the right one serrated and the left one acute at the apex. Vesica originates in a fissure at the distal third of the theca, extruded and ornamented with cornuti in the inner surface. — **Female** (Fig. 21A–E): The female presents the same somatic characteristics as the male (Fig. 21A) except the operculum is smaller (Fig. 21C); sternite II (Fig. 21D) longer with a straight lateral margin that is convergent towards the apex, the posterior margin straight directed anteromedially to a concave middle groove; dorsal beak of segment 9 smaller than that of the ovipositor sheath (Fig. 21E). The ovipositor bears eight teeth.

Measurements (in millimeters). Holotype male. Length of body: 22.30; width of head including eyes: 10.27; length of the head: 2.52; width of pronotum including pronotal collar: 9.84; length of pronotum including pronotal collar: 3.50; width of mesonotum: 8.40; length of mesonotum: 6.76; length of forewing: 32.85; width of forewing: 11.00; length of hind wings: 15.82. Paratypes (male and female). Length of body: 22.71, 22.29; width of head including eyes: 10.85, 10.55; length of the head: 2.81, 2.74; width of pronotum including pronotal collar: 10.37, 10.34; length of pronotum including pronotal collar: 3.69, 3.58; width of mesonotum: 8.79, 8.55; length of mesonotum: 6.90, 7.08; length of forewing: 32.86, 33.17;

width of forewing: 11.35, 10.68; length of hind wings: 16.60, 16.96.

Distribution. Peru.

***Acanthoventris viridnotatus* Ruschel sp. nov.**

<http://zoobank.org/F8F3A980-0697-45A7-A15F-B7CED-D15065C>

Fig. 22

Type locality. Alto Caparaó, Minas Gerais, Brazil.

Type material. Holotype: male (DZRJ) (Fig. 22A), Brasil, MG, Alto Caparaó, PN do Caparaó Pano Branco 20°25'11.60"S, 41°50'44.80W, 1306 m, 17.I.2014, Nessiman et al.

Etymology. The specific name refers to the dorsal color of species (head, pronotum and mesonotum). Latin: viridis, green. Latin: nota, mark.

Diagnosis. The species can be distinguished from all other species of *Acanthoventris* **gen. nov.** by the following combination of features: head and thorax yellow greenish; anterior margin of head slightly convex; labium short, not reaching the base of basisternum 3; apex of timbal cover short and directed to the base of hindwings; middle third of anteromedial margin slightly concave, almost straight. This species has a similar morphology to *A. phoenix* **sp. nov.** due the body size, operculum shape and bands, but *A. viridnotatus* **sp. nov.** can be distinguished by the absence of pilus setae in both lateral margins of tergites 2 to 7, anteclypeus and carina tawny, labium shorter, the uncus shape. The ventral thecal process in *A. viridnotatus* **sp. nov.** has two sclerotized projections toward the anterior margin, but in *A. phoenix* **sp. nov.** the anterior margin presents an expansion with a slender projection.

Color. Head and thorax yellow greenish marked with black, and abdomen tawny marked with black.

Description. Head (Fig. 22B): with a transverse slender black band departing from each eye, extending through the area of the ocelli; base of the eyes marked with black with silver setae; anterior margin of head slightly convex; antennae with a green scape, and the pedicel and flagellum marked with black; postclypeus (Fig. 22C) unmarked, oval in ventral view, flat in lateral view, the apex not prominent in dorsal view relative to the supra-antennal plate; longitudinal groove slender and shallow; anteclypeus and carina tawny, lorum black; mentum and labium tawny; labium short, not reaching the base of basisternum 3, black at the apex. Pronotum (Fig. 22B): with lateral and sub-lateral lobes with wrinkles and black setae; slightly marked with green in the middle; paranota

yellowish marked with green with black setae. Mesonotum (Fig. 22A): submedian sigillae marked with black, lateral sigillae marked with black at anterior margin; scutal depression unmarked; basisternum 3 (Fig. 22D) with well developed protuberances relative to the median insertion, closely spaced; posterior margin in an obtuse angle; cruciform elevation covering the tergite 1; apex of the posterior projections of the cruciform elevation obtuse; operculum (Fig. 22E) obtuse and long, covering the timbal cavity, the apex reaching the auditory capsule, the internal angles very short, the apex obtuse and widely spaced, anteromedian margin concave anteriorly to the internal angles, the lateral margin convex, posterior margin slightly straight; meracanthus reaches the posterior margin, gutter present in all margins; legs tawny becoming greenish distally; tarsus black; wings hyaline (Fig. 22A); forewings: basal cell opaque anteriorly, and the basal vein of the second apical cell oblique; apical cell 2 half of length of apical cell 1; hindwings: radius vein straight. Abdomen subcylindrical, the length equivalent to the combined length of the head and thorax in dorsal view (Fig. 22A); timbal cover (Fig. 22F) flat and short, the apex acute not reaching the lateral metascutellar plate directed to the base of hindwings, middle third of anteromedial margin slightly concave, almost straight, ventral anterior margin tightly concave (away from the posterior margin of operculum); tergites 2 to 4 with two black band at middle, and tergites 5 to 7 marked with black anteriorly; sternite VII (Fig. 22G) sub-triangular, the lateral margin slightly convex becoming slightly straight toward the apex, the posterior margin slightly emarginate. Uncus (Fig. 22H, I): lateral margin slightly straight becoming tightly convex in the ventral apophyses; lateral branches of uncus undeveloped, convex bud-like, away from the midline; the internal margin slightly convex; ventral apophyses grooved with the apices strongly sclerotized; internal margin forming a sub-rectangular distally directed and with the posterior apex salient; posterior margin inclined and with an acute angled lateral and posteriorly developed. Pygofer (Fig. 22J) sub-cylindrical; the basal lobe reaching the apex of ventral apophyses. Theca (Fig. 22K–M) dorsally developed with the ventral thecal process with two sclerotized projections toward the anterior margin; vesica tightly extruded and adorned with cornuti in the inner and outer surfaces. — **Female:** Unknown.

Measurements (in millimeters). Holotype male. Length of body: 20.41; width of head including eyes: 9.14; length of the head: 1.71; width of pronotum including pronotal collar: 8.91; length of pronotum including pronotal collar: 1.89; width of mesonotum: 7.65; length of mesonotum: 5.67; length of forewing: 28.88; width of forewing: 9.97; length of hind wings: 13.60.

Distribution. Brazil (Minas Gerais).

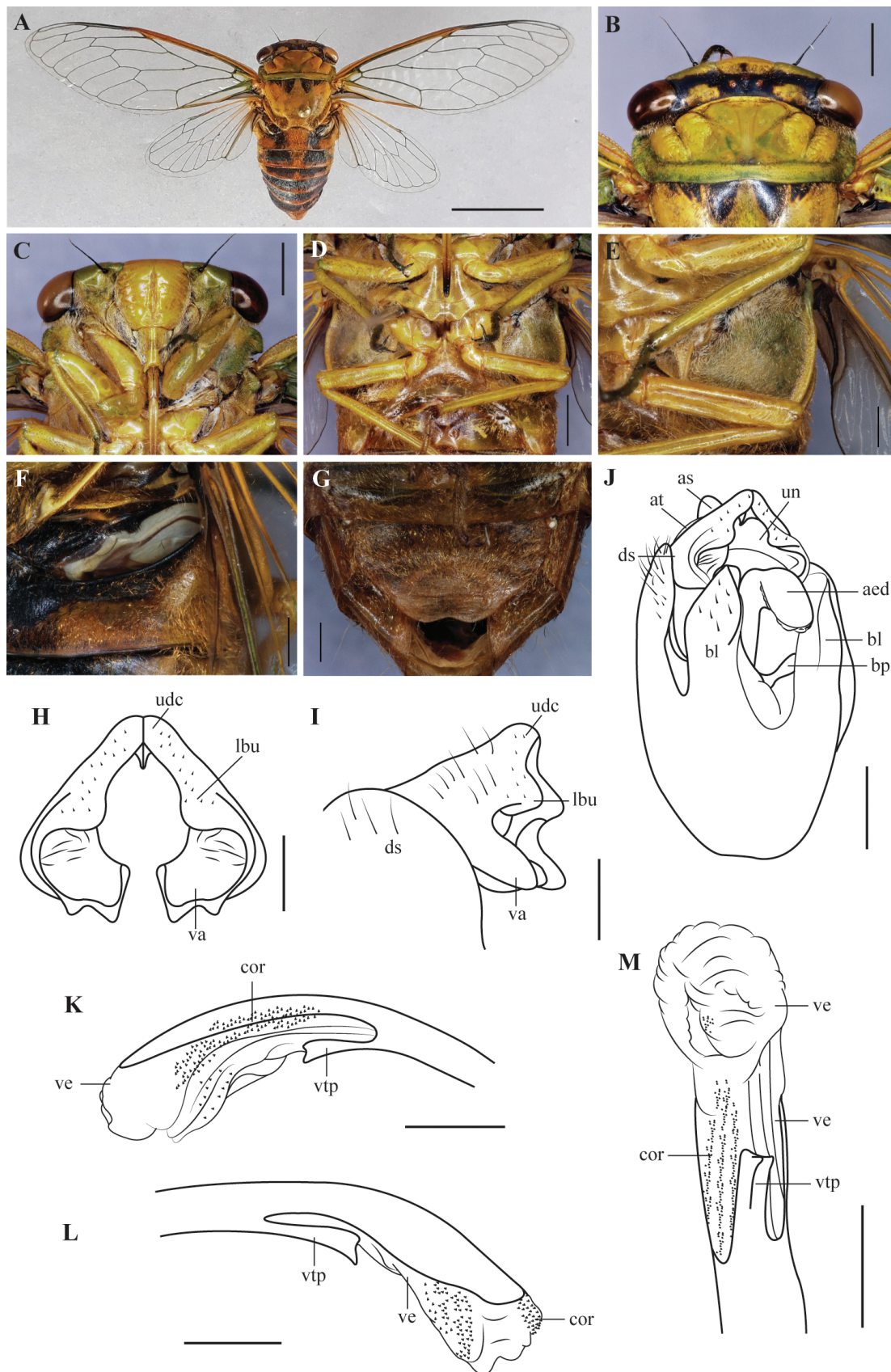


Figure 22. *Acanthoventris viridinotatus* sp. nov., holotype male **A** Habitus in dorsal view; **B** Head and pronotum in dorsal view; **C** Head and pronotum in ventral view; **D** Thorax in ventral view; **E** Operculum in latero-ventral view; **F** Timbal cover in dorso-lateral view; **G** Sternite VII in ventral view; **H** Uncus in ventral view; **I** Uncus in lateral view; **J** Pygofer in latero-ventral view; **K** Aedeagus in left lateral view; **L** Aedeagus in right lateral view; **M** Aedeagus in ventral view. Scale bars: A = 1 cm; B–D = 2 mm; E–G, J = 1 mm; H, I, K–M = 0.5 mm. Abbreviations: (aed) aedeagus; (as) anal styles; (at) anal tube; (bl) basal lobe of pygofer; (bp) basal plate; (cor) cornuti; (ds) distal shoulder; (lbu) lateral branch of uncus; (udc) uncal dorsal crest; (un) uncus; (va) ventral apophysis; (ve) vesica; (vtp) ventral thecal process.

4. Discussion

For the first time, we presented a phylogenetic hypothesis of Fidicinini under total evidence analysis encompassing a broad species sample representing most of the genera in the tribe. Based on a phylogenetic analysis, we described new species and proposed a reclassification along with the description of a new genus, *Acanthoventris* **gen. nov.** We also provide detailed distribution information of all species in the new genus. These results help lessen the Darwinian, Linnean, and Wallacean shortfalls in Fidicinini, indicating that the current classification of species within the tribe may not reflect their evolutionary history.

4.1. Phylogenetic implications and evolution of character states

Dorisiana and *Guyalna* were both recovered non-monophyletic. Although most of the sampled species of *Dorisiana* were recovered in the same clade (except *D. drewseni*) with moderate support, clade B lacks synapomorphies. The polyphyly of *Guyalna* reveals that none of the putative diagnostic characteristics as treated in the literature resulted in synapomorphies (Figs 3, 4).

The species currently classified in *Dorisiana* and *Guyalna* are morphologically similar and share a complex taxonomic history. Both genera were proposed in identification keys to sort them (Delétang 1919; Boulard and Martinelli 1996), and recently a diagnosis and complete description were presented for *Guyalna* (Sanborn 2016a). However, *Dorisiana* lacks formal diagnoses, and both genera have ambiguous species classification.

Recently, twelve species were transferred from *Dorisiana*, *Fidicinoides*, and *Fidicina* to *Guyalna*, primarily based on the number of tarsomeres and the shape of the timbal cover (Sanborn 2016a, b). Therefore, those structures have been considered primordial in classifying the genera in Fidicinina or Guyalnina (Distant 1889; Distant 1906; Moulds 2005; Boulard & Martinelli 1996; Sanborn 2016a, b).

The authorities of *Guyalna* and *Dorisiana* characterized the first by rounded timbal covers and the second by triangular ones (Boulard and Martinelli 1996, 2011). Sanborn (2016a) transferred species from *Dorisiana* to *Guyalna* based on the shape of the timbal cover; we followed the interpretation by this author for the putative diagnostic features to propose the characters 33–35. The optimizations showed that these characters present multiple transitions (Fig. 4). Even within clade B, which groups most of the sampled *Dorisiana* species, the character states related to the timbal cover are homoplastic.

The timbal cover surface (31) and its aperture (32) have at least two transitions within clade G, and the flat (31₁) and exposed (32₁) timbal cover are shared features between clades B and C. On the other hand, the same character states are spread out in the phylogeny. Thus, character states representing the putative diagnostic features of *Guyalna* (33₀ and 34₀) and *Dorisiana* (33₁ and

34₁) are not exclusive to these two genera (Fig. 4). Our results suggest that the characters describing the timbal cover shape are very homoplastic and liable to strong evolutionary convergence rather than resulting from common ancestry, a scenario similar to that recovered in a recent phylogeny of Cicadidae (Marshall et al. 2018).

Tympanoterpes was also recovered polyphyletic in our analyses. We included two of the six species currently classified in the genus (Sanborn 2013; Sanborn 2019), and the type species *T. serricosta* grouped with high support in clade C with five species of *Guyalna*. The species in clade C share a short vertex, triangular operculum, type G uncus (Figs 2–4), and the aedeagus lacking processes and with an almost non-expandable vesica bearing cornuti. We are aware that these features are present in some *Guyalna* species, such as *G. flavibasalis* (Distant), *G. innotabilis* (Walker), *G. panamensis* (Davis), *G. sublaqueata* (Uhler), and *G. viridifemur* (Walker) (not sampled in our analyses). However, we chose not to make any taxonomic decision about these species, considering the need for a phylogeny with a more extensive sampling of species, including those mentioned above.

Unlike the timbal cover, different works have proposed that the evolution of the uncus can be linked to phylogenetic relationships, at least at the genus and tribe level (Moulds 2005; Marshall et al. 2018; Lee and Hill 2010; Moulds and Hill 2015; Hill et al. 2015; Wang et al. 2018). Although the uncus is a single process (Moulds 2005), it has been regionalized, and its projections were named “lobes” (Marshall et al. 2018). The great morphological diversity of the uncus in Fidicinini causes difficulty in the delimitation of the lobes to determine primary homologies. Therefore, we chose to consider the shape of the uncus as a character, with each state corresponding to an overall group form (see character 44 in the character list, Fig. 2).

We recovered two clades with exclusive uncus states (type H in *Acanthoventris* **gen. nov.**, and type G in the *Tympanoterpes serricosta* clade); two monophyletic genera, each with a single, although not exclusive, uncus shape (type A in *Ariasa*, and type B in *Fidicina*); and a high diversity of types mainly between the *Guyalna* species. *Dorisiana* has one exclusive type of uncus (type E) within clade B. However, the other two uncus types (B and D) in clade B are also found elsewhere in the phylogeny, and the clade is only moderately supported and lacks exclusive synapomorphies, thus preventing us from proposing a new sensu for *Dorisiana*. In *Guyalna*, we observed all types of uncus, except the *Dorisiana*-exclusive type E. Our results are consistent with the phylogenetic study of *Tibicen* Latreille, 1825 (Hill et al. 2015), which is a large genus with unclear relationships to other genera in Cryptotympanini Handlirsch, 1925. The study established three new genera from *Tibicen* species using an uncus shape character, with an exclusive state in the clade of *Subsolanus* Moulds, 2015 (now a junior synonym of *Aurittibicen* Lee, 2015 apud Sanborn 2015) and two exclusive states in the clade of *Hadoa* Moulds, 2015 (Hill et al. 2015). In the same analysis, a single timbal cover character was used, with the recovered concave state

synapomorphic in the *Subsolanus* clade and the convex shape for the other species (Hill et al. 2015). However, unlike Fidicinini, the shape of the timbal cover is uniform across the genera of Cryptotympanini, demonstrating equally unreliable for the delimitation of genera or irrelevant in the evolutionary history of the group. Thus, the single most important diagnostic character given the formation of these genera is not very useful in distinguishing taxa.

5. Conclusion

We built the first phylogenetic hypothesis for Fidicinini testing the position of species classified in different genera but with similar somatic morphology and homogeneous unicus shape. At the same time, we optimized in the phylogeny the characters of the timbal cover shape, used in traditional taxonomy, and the unicus shape, a character that has been used in recent phylogenies for other groups of Cicadidae. Both the timbal cover and the unicus shape demonstrated high convergence in the evolutionary history of Fidicinini, but a homogeneous unicus shape (exclusive or not) was recovered in monophyletic genera. Our results corroborate other studies which associate the same unicus shape with natural groups.

The high variability of the timbal cover shape and the polyphyly of the included *Guyalna* species suggest that the genus is a tangle of evolutionarily unrelated species. Further investigations about *Guyalna* and *Dorisiana* are needed, using a broad sampling of species and exploring morphological and molecular data that can recover natural groups of species within these genera.

6. Acknowledgements

We are thankful to Conselho Nacional de Desenvolvimento Científico e Tecnológico – CNPq (L.A.C. 307204/2015–4) and to Coordenação de Aperfeiçoamento de Pessoal de Nível Superior – CAPES Finance Code 001, CAPES/CNPq PROTAX II [88882.156807/2017-01] (TPR). We would like to thank to the curators of the scientific collections for the loan of material, especially Dr Robin Thomson (UMSP), Dr Daniela Maeda Takiya (DZRJ), Dr Gabriel Mejdalani (MNRJ), Dr Rodney Cavichioli (DZUP), Dr Aline Barcellos (MCNZ), and Dr Henrik Enghoff (ZMUC); and Dr Gunvi Lindberg (NHRS), Ihor Shydlovskyy and Andriy Zatushevsky (ZMD), Ruth Salas (AMNH), and Jerome Sueur and Laurent Fauvre (MNHN) for sending the photographs of types and non-type species. We are also grateful to Dr David Marshall and Dr Chris Simon for the suggestions about the DNA markers, primers and PCR protocol used in this study; and to Dr Allen Sanborn for the suggestions that improved the manuscript.

7. References

Berg C (1879) Hemiptera Argentina (Continuacion) Hemiptera Homoptera Latr. Anales de la Sociedad científica Argentina 8: 135–144.

- Boulard M (1965) Notes sur la biologie larvaire des cigales (Homoptera: Cicadidae). Annales de la Société entomologique de France 1: 503–521.
- Boulard M, Martinelli NM (1996) Révision des Fidicinini, nouveau statut de la tribu, espèces connues et nouvelles espèces (Cicadomorpha, Cicadidae, Cicadinae) Première partie: Sous-tribu nouvelle des Fidicinina. Biologie et Evolution des Insectes Hemipteroidea 9: 11–81.
- Boulard M, Martinelli NM (2011) Nouvelles cigales néotropicales de la sous-tribu des Guyalnina (Rhynchota, Cicadidae, Cicadinae, Fidicinini). Lambillionea CXI 3: 219–232.
- Butchart SH, Walpole M, Collen B, Van Strien A, Scharlemann JP, Almond RE., ... , Watson, R (2010) Global biodiversity: indicators of recent declines. Science 328 (5982): 1164–1168. <https://www.science.org/doi/10.1126/science.1187512>
- Claridge MF (1985) Acoustic signals in the Homoptera: behavior, taxonomy, and evolution. Annual review of entomology 30(1) 297–317. <https://doi.org/10.1146/annurev.en.30.010185.001501>
- Delétang LF (1919) Contribución al estudio de los cicádidos (Cicadidae) argentinos, ensayo filogenético. Anales de la Sociedad Científica Argentina 88: 25–94.
- Diniz-Filho JAF, Loyola RD, Raia P, Mooers AO, Bini LM (2013) Darwinian shortfalls in biodiversity conservation. Trends in Ecology & Evolution 28 (12): 689–695. <https://doi.org/10.1016/j.tree.2013.09.003>
- Distant WL (1906) A synonymic catalog of Homoptera. Part I. Cicadidae. British Museum, London, 207 pp. <https://doi.org/10.5962/bhl.title.8554>
- Hill KB, Marshall DC, Moulds MS, Simon C (2015) Molecular phylogenetics, diversification, and systematics of *Tibicen* Latreille 1825 and allied cicadas of the tribe Cryptotympanini, with three new genera and emphasis on species from the USA and Canada (Hemiptera: Auchenorrhyncha: Cicadidae). Zootaxa 3985(2): 219–251. <https://doi.org/10.11646/zootaxa.3985.2.3>
- Hortal J, de Bello F, Diniz-Filho JAF, Lewinsohn TM, Lobo JM, Ladle RJ (2015) Seven shortfalls that beset large-scale knowledge of biodiversity. Annual Review of Ecology, Evolution, and Systematics 46: 523–549. <https://doi.org/10.1146/annurev-ecolsys-112414-054400>
- IC Measure v.1.2.0.265. 2016. The imaging source. <http://www.theimagingsource.com/support/downloadsfor-windows/end-user-software/icmeasure>
- Katoh K, Standley DM (2013) MAFFT multiple sequence alignment software version 7: improvements in performance and usability. Molecular biology and evolution 30(4): 772–780.
- Lee YJ, Hill KB (2010) Systematic revision of the genus *Psithyristris* Stål (Hemiptera: Cicadidae) with seven new species and a molecular phylogeny of the genus and higher taxa. Systematic Entomology 35(2): 277–305. <https://doi.org/10.1111/j.1365-3113.2009.00509.x>
- Lewis PO (2001) A likelihood approach to estimating phylogeny from discrete morphological character data. Systematic Biology (50): 913–925. <https://doi.org/10.1080/106351501753462876>
- Lomolino MV (2004) Conservation biogeography. Frontiers of Biogeography: new directions in the geography of nature. Sinauer Associates Inc, 293 pp.
- Maddison WP, Maddison DR. (2021) Mesquite: a modular system for evolutionary analysis. Version 3.70 <http://www.mesquiteproject.org>
- Marshall DC, Moulds M, Hill KB, Price BW, Wade EJ, Owen CL., ... , Simon C (2018) A molecular phylogeny of the cicadas (Hemiptera: Cicadidae) with a review of tribe and subfamily classification. Zootaxa 4424(1): 1–64. <https://doi.org/10.11646/zootaxa.4424.1.1>

- Martinelli NM, Zucchi RA (1989) Cigarras associadas ao cafeeiro. 3. Gênero *Dorisiana* Metcalf, 1952 (Homoptera, Cicadidae, Cicadinae). *Anais da Sociedade Entomologica do Brasil* 18: 5–12.
- Martinelli NM, Zucchi, RA (1997) Cigarras (Hemiptera: Cicadidae: Tibiniciidae) associadas ao cafeeiro: distribuição, hospedeiros e chave para as espécies. *Anais da Sociedade Entomológica do Brasil* 26: 133–143.
- Metcalf ZP (1963) General catalogue of the Homoptera, Cicadoidea. Part I, fascicle VIII. Raleigh, Waverly Press, North Carolina, USA, 585 pp.
- Miller MA, Pfeiffer W, Schwartz T (2011) The CIPRES science gateway: a community resource for phylogenetic analyses. In: Proceedings of the 2011 TeraGrid Conference: extreme digital discovery, 1–8.
- Morrone JJ, Escalante T, Rodríguez-Tapia G, Carmona A, Arana M, Mercado-Gómez JD (2022) Biogeographic regionalization of the Neotropical region: New map and shapefile. *Anais da Academia Brasileira de Ciências* 94(1): e20211167. <https://doi.org/10.1590/0001-376520220211167>
- Moulds MS (2005) An Appraisal of the Higher Classification of Cicadas (Hemiptera: Cicadoidea) with Special Reference to the Australian Fauna. *Records of the Australian Museum* 57: 375–446.
- Moulds MS (2012) A review of the genera of Australian cicadas (Hemiptera: Cicadoidea). *Zootaxa* 3287: 1–262.
- Moulds MS, Hill KB (2015) Phylogeny for the tribe Thophini (Cicadoidea: Cicadidae) with the description of a new subspecies of *Thopha sessiliba* Distant from Western Australia. *Records of the Australian Museum* 67: 55–66. <http://dx.doi.org/10.3853/j.2201-4349.67.2015.1634>
- Nixon KC, Carpenter JM (1993) On Outgroups. *Cladistics* 9: 413–426.
- Rambaut A, Suchard MA, Xie D, Drummond AJ (2014). Tracer v1. 6. Computer program and documentation distributed by the author. <http://beast.bio.ed.ac.uk/tracer>
- Ronquist F, Huelsenbeck JP (2003) MrBayes3: Bayesian phylogenetic inference under mixed models. *Bioinformatics* 19: 1572–1574. <https://doi.org/10.1093/bioinformatics/btg180>
- Ruschel TP, Bianchi FM, Campos LA (2019) Genital coupling, morphology and evolution of male holding structures in Cicadinae (Hemiptera: Cicadidae). *Biological Journal of the Linnean Society* 128(4): 838–853. <https://doi.org/10.1093/biolinnean/blz151>
- Ruschel TP, Campos LA (2019) Phylogeny and biogeography of the leaf-winged cicadas (Hemiptera: Auchenorrhyncha: Cicadidae). *Zoological Journal of the Linnean Society* 185 (4): 1150–1187. <https://doi.org/10.1093/zoolinnean/zly087>
- Sanborn AF (2013) Catalogue of the Cicadoidea (Hemiptera: Auchenorrhyncha). Academic Press/Elsevier, London, UK, 1001 pp.
- Sanborn, AF (2015) New combinations for six species belonging to Cryptotympanini Handlirsch (Hemiptera: Cicadidae), former members of the genus *Tibicen* Latreille, 1825. *Zootaxa* 4027 (3): 447–450. <https://doi.org/10.11646/zootaxa.4027.3.9>
- Sanborn AF (2016a) The cicada genus *Guyalna* Boulard & Martinelli, 1996 (Hemiptera: Cicadidae: Cicadinae: Fidicinini): generic description, twelve new combinations, and a key to species. *Zootaxa* 4105(5): 430–454. <https://doi.org/10.11646/zootaxa.4105.5.2>
- Sanborn AF (2016b) Five new species, a new genus and a new record of cicadas from French Guiana with four new combinations and three new synonymies (Insecta, Hemiptera, Cicadoidea, Cicadidae). *Zoosystema* 38(2): 177–199. <https://doi.org/10.5252/z2016n2a2>
- Sanborn AF (2019) The cicadas (Hemiptera: Cicadidae) of Bolivia including the descriptions of fifteen new species, the resurrection of one genus and two species, seven new combinations, six new synonymies, and twenty-eight new records. *Zootaxa* 4655(1): 1–104. <https://doi.org/10.11646/zootaxa.4655.1.1>
- Sanborn AF (2020) The cicadas (Hemiptera: Cicadidae) of Peru including the description of twenty-four new species, three new synonymies, and thirty-seven new records. *Zootaxa* 4785(1): 1–129. <https://doi.org/10.11646/zootaxa.4785.1.1>
- Sanborn AF (2020) The cicadas (Hemiptera: Cicadidae) of Suriname including the description of two new species, five new combinations, and three new records. *Zootaxa* 4881 (3): 453–481. <https://doi.org/10.11646/zootaxa.4881.3.2>
- Sanborn AF, Marshall DC, Moulds MS, Puissant S, Simon C (2020) Redefinition of the cicada tribe Hemidictyini Distant, 1905, status of the tribe Iruanini Boulard, 1993 rev. stat., and the establishment of Hovanini n. tribe and Sapantangini n. tribe (Hemiptera: Cicadidae). *Zootaxa* 4747(1): 133–155. <https://doi.org/10.11646/zootaxa.4747.1.5>
- Sereno PC (2007) Logical basis for morphological characters in phylogenetics. *Cladistics* 23: 565–587. <https://doi.org/10.1111/j.1096-0031.2007.00161.x>
- Simon C, Gordon ER, Moulds MS, Cole JA, Haji D, Lemmon AR, ..., Łukasik P (2019) Off-target capture data, endosymbiont genes and morphology reveal a relict lineage that is sister to all other singing cicadas. *Biological Journal of the Linnean Society* 128(4): 865–886. <https://doi.org/10.1093/biolinnean/blz120>
- Snodgrass RE (1957) A revised interpretation of the external reproductive organs of male insects. *Smithsonian Miscellaneous Collections* 135(6): 1–60.
- Song H, Bucheli SR (2010) Comparison of phylogenetic signal between male genitalia and non-genital characters in insect systematics. *Cladistics* 26: 23–35. <https://doi.org/10.1111/j.1096-0031.2009.00273.x>.
- Staden R, Beal KF, Bonfield JK (2000) The staden package, 1998. In: *Bioinformatics methods and protocols*. Humana Press, Totowa, NJ, 115–130.
- Stål C (1854) Nya Hemiptera. Öfversigt af Svenska Vetenskaps Akademiens Förhandlingar. 11 (8): 231–255.
- Vaidya G, Lohman DJ, Meier R (2011) SequenceMatrix: concatenation software for the fast assembly of multi-gene datasets with character set and codon information. *Cladistics* 27(2): 171–180.
- Wang X, Hayashi, M, Wei, C (2018) Revision, phylogeny and phylogeography of the cicada genus *Auritibicen* (Hemiptera: Cicadidae), with descriptions of ten new species. *European Journal of Entomology* 115: 53–103. <https://doi.org/10.14411/eje.2018.007>
- Wilson EO (1985) The biological diversity crisis. *BioScience* 35 (11) 700–706.

Supplementary material 1

File S1

Authors: Ruschel TP, Bianchi FM, Campos LA, Carvalho GS (2023)

Data type: .nex

Explanation note: File generated by the Mesquite software containing the list of sampled species and the coded morphological characters.

Copyright notice: This dataset is made available under the Open Database License (<http://opendatacommons.org/licenses/odbl/1.0>). The Open Database License (ODbL) is a license agreement intended to allow users to freely share, modify, and use this Dataset while maintaining this same freedom for others, provided that the original source and author(s) are credited.

Link: <https://doi.org/10.3897/asp.81.e85755.suppl1>

Supplementary material 2

Table S1

Authors: Ruschel TP, Bianchi FM, Campos LA, Carvalho GS (2023)

Data type: .xlsx

Explanation note: The table informs the type material examined and the literature used for species identification.

Copyright notice: This dataset is made available under the Open Database License (<http://opendatacommons.org/licenses/odbl/1.0>). The Open Database License (ODbL) is a license agreement intended to allow users to freely share, modify, and use this Dataset while maintaining this same freedom for others, provided that the original source and author(s) are credited.

Link: <https://doi.org/10.3897/asp.81.e85755.suppl2>

Supplementary material 3

Table S2

Authors: Ruschel TP, Bianchi FM, Campos LA, Carvalho GS (2023)

Data type: .xlsx

Explanation note: The table shows the list of species used in coding morphological characters. It contains the same information as Supplementary material 1 (File S1) but in a spreadsheet format.

Copyright notice: This dataset is made available under the Open Database License (<http://opendatacommons.org/licenses/odbl/1.0>). The Open Database License (ODbL) is a license agreement intended to allow users to freely share, modify, and use this Dataset while maintaining this same freedom for others, provided that the original source and author(s) are credited.

Link: <https://doi.org/10.3897/asp.81.e85755.suppl3>

Supplementary material 4

Table S3

Authors: Ruschel TP, Bianchi FM, Campos LA, Carvalho GS (2023)

Data type: .xlsx

Explanation note: The table shows the Primers and PCR conditions used in the DNA amplification.

Copyright notice: This dataset is made available under the Open Database License (<http://opendatacommons.org/licenses/odbl/1.0>). The Open Database License (ODbL) is a license agreement intended to allow users to freely share, modify, and use this Dataset while maintaining this same freedom for others, provided that the original source and author(s) are credited.

Link: <https://doi.org/10.3897/asp.81.e85755.suppl4>

Supplementary material 5

Table S4

Authors: Ruschel TP, Bianchi FM, Campos LA, Carvalho GS (2023)

Data type: .xlsx

Explanation note: The table shows the Genbank access numbers for the COI and EF1-alpha of species sampled.

Copyright notice: This dataset is made available under the Open Database License (<http://opendatacommons.org/licenses/odbl/1.0>). The Open Database License (ODbL) is a license agreement intended to allow users to freely share, modify, and use this Dataset while maintaining this same freedom for others, provided that the original source and author(s) are credited.

Link: <https://doi.org/10.3897/asp.81.e85755.suppl5>

Supplementary material 6

Table S5

Authors: Ruschel TP, Bianchi FM, Campos LA, Carvalho GS (2023)

Data type: .xlsx

Explanation note: Records and coordinates of Acanthoventris species used for compose the distribution map.

Copyright notice: This dataset is made available under the Open Database License (<http://opendatacommons.org/licenses/odbl/1.0>). The Open Database License (ODbL) is a license agreement intended to allow users to freely share, modify, and use this Dataset while maintaining this same freedom for others, provided that the original source and author(s) are credited.

Link: <https://doi.org/10.3897/asp.81.e85755.suppl6>